REMARKS

Claim Amendments

The claims have been amended to clarify the claim language, place some previously dependent claims into independent form, and to correct the multiple dependent claims accordingly. Support for the addition of "comprises an iron-sulfur cluster" to Claims 2, 5, 21, 36 and 69-71 is found in Claim 1 as previously presented All remaining amendments are clerical in nature.

Objection to the Specification and Rejection of Claims 1, 2, 4, 5, 7, 21, 24, 36,39, 44, 47, 48, 50-52, 54-56, 58-65, and 68-71 Under 35 U.S.C. § 112, First Paragraph (Written Description):

The Examiner has objected to the specification and rejected Claims 1, 2, 4, 5, 7, 21, 24, 36,39, 44, 47, 48, 50-52, 54-56, 58-65, and 68-71 under 35 U.S.C. § 112, first paragraph, on the basis of written description. Specifically, the Examiner states that Applicants' arguments regarding the various structural features of the claimed oxygenase (e.g., free iron-binding domains) that were known in the art at the time of the invention to be conserved among all oxygenases of this same type and to be required for function of the enzyme are not persuasive, because the Examiner contends that the presence of free iron-binding domains in a monoxygenase does not describe a dicamba-degrading oxygenase of the present invention, but rather describe a genus beyond dicamba-degrading oxygenases. The Examiner states that an invention may not be adequately described when it is described solely in terms of a method of making it coupled with its function and there is no described or art-recognized correlation or relationship between the structure of the invention and its function. With regard to Applicants' prior arguments that the art recognizes that within the Rieske non-heme iron-binding family of oxygenases, the location of the substrate binding region is known to be in proximity to the site of the free iron atom that is a catalyst for the reaction (with the binding site for the iron atom being conserved among this type of oxygenase), the Examiner argues that this is not persuasive because Applicant does not describe the substrate binding region of the claimed oxygenase. The Examiner further dismisses Applicants' arguments that sequence similarity with other monoxygenases of the same type that degrade substrates other than dicamba provides significant information regarding the structure-to-function relationship of the enzyme. With regard to the Weeks Declaration of 2004, the Examiner states that while this data might provide evidence

that one of skill in the art could isolate other dicamba-degrading oxygenases from other bacteria, it does not overcome the issue of written description.

Applicants traverse the Examiner's rejection. Based on the Examiner's comments in the May 28 Office Action, it appears to Applicants as though the Examiner's position rests on the contention that Applicants have not demonstrated where in the oxygenase sequence the substrate, dicamba, binds, and that there was insufficient knowledge in the art at the time of the invention for one of skill in the art to modify up to 35% of the amino acid sequence of the enzyme or produce a fragment without destroying the substrate specificity of the enzyme. The Examiner also appears to completely dismiss any other structure-to-function knowledge regarding this type of oxygenase that was known in the art at the time of the invention and concludes that there is "no described or art-recognized correlation or relationship between the structure of the invention and its function." Applicants strongly disagree with the Examiner's position for the following reasons.

First, contrary to the Examiner's conclusions, Applicants have clearly demonstrated that, at the time of the present invention, there was a *substantial* amount of art-recognized correlation and relationship between the structure of Rieske non-heme iron-binding oxygenases that transfer electrons through iron-sulfur clusters and free iron atoms and the function of such enzymes. As previously stated, the oxygenase of the present invention falls within this class of oxygenases. In particular, examination of the biochemical and physical properties of oxygenase$_{DIC}$, as well as its primary amino acid sequence, revealed that it contains two essential elements, a Rieske iron-sulfur cluster (see the specification at page 40, line 27 to page 41, line 1, wherein this iron-sulfur cluster is first identified) and a mononuclear iron binding site (page 52, lines 15-18, for example, discloses the requirement for iron (Fe^{2+}) for activity). These specific structural regions, which have been further illustrated and discussed in the Weeks December 2002 Declaration in comparison to other oxygenases of the same or similar class that were known at the time of the invention (see Figure A), account for the majority of the functional capability of the claimed oxygenase and the identifying motifs for such structures were known in the art at the time of the invention.

Indeed, at the time of the invention, numerous examples of multicomponent oxygenases were documented in the literature, including those containing terminal oxygenases of the Rieske non-heme iron oxygenase type of the present invention. The art knew the consensus binding sites for the

Rieske iron-sulfur clusters, and binding sites for the free iron in Rieske non-heme iron oxygenases were widely known (See, *e.g.*, Mason J.R, and Cammack R. (1992) *Annu Rev Microbiol.* 46:277-305 (full text article enclosed); or Butler, C. S. and Mason, J. R. (1997) *Advances in Microbial Physiology* **38**, 47-84 (full text article enclosed); Neidle et al. (1991) *J. Bacteriol.* 173(17):5385-5395 (full text article enclosed); Junker et al. (1997) *J. Bacteriol.* 179(3):919-927 (full text article enclosed); Gurbiel et al. (1996) *Biochemistry* 35:7834-7845 (abstract enclosed); Harayama et al. (1992) *Annu Rev Microbiol.* 46:565-601 (abstract enclosed)). Further, these binding sites in oxygenase$_{DIC}$ are illustrated in Figure A of the Weeks Declaration submitted December 2002, and could be readily identified by one of skill in the art. Again, these are significant portions of the structure of the oxygenase that are required for the functionality of the oxygenase$_{DIC}$, and it is information that one of skill in the art at the time of the invention would absolutely use to determine where in the protein modifications will be best tolerated. Therefore, this information is relevant to the issue of whether one knows what modifications to the claimed enzyme will affect biological activity.

Furthermore, at the time of the invention, it was widely known by biochemists, molecular biologists, and many other chemists and biologists that any class of enzymes catalyzing a specific reaction dealing with a specific substrate (or set of specific required substrates) can be carried out with members of this class of enzymes that have variable amino acid sequences. As previously argued by Applicants, it was known from a multitude of published results that scientists could readily alter the amino acid sequence at several sites within any given enzyme without causing lose of enzymatic activity. This was known to be true for amino acid residues near or even within the active site domain or substrate binding site(s) of an enzyme. In support of this position, Applicants refer to the prior discussion in the Weeks Declaration of December 2002 and the example referencing variants of cytochrome oxidases.

It was also widely known at the time of the invention that members of a specific class of enzymes frequently contained motifs (domains) for binding ligands required for the reaction (NADH, ATP, iron-sulfur clusters, free iron, etc.) or for the proper structure and/or function of the enzyme. Such motifs usually are defined not by a precise amino acid sequence, but rather by a consensus amino acid sequence in which certain key amino acid residues (or close homologs) are usually

present and often are located similar distances apart. An example is the consensus sequence for the binding of a [2Fe-2S] cluster that comprises a Rieske iron-sulfur cluster, found in the oxygenase of the present invention. Note that the consensus sequence is C-X-H-X_{16}-C-X_2-H, where X can be any amino acid. However, there are cases known in which the number of amino acids between the normally invariant cysteine and histidine residues are different than the consensus above (See *e.g.*, Mason J.R, and Cammack R. (1992) *Annu Rev Microbiol.* 46:277-305, article enclosed). That is to say, while consensus sequences for the known motifs can be easily recognized within an oxygenase of the type represented by the present invention, the exact amino acid sequence within a *bona fide* consensus sequence can be quite variable. It was also known at the time of the invention that there was a consensus binding site for free iron (i.e., a non-heme Fe(II) domain with the consensus sequence D/E-X_3-D-X_2-H-X_4-H). Thus, the same logic put forth for variability in the amino acid sequences comprising the Rieske non-heme iron consensus sequence pertains to the consensus sequence for iron binding sites. Similarly, and of particular importance to the Examiner's apparent focus on the substrate binding site of the enzyme, it also was known at the time of the invention that within a substrate-binding site, *there are only a few amino acids that form direct contacts with the substrate* (See *e.g.*, the chapter on Enzymes in: Nelson, D.L. and Cox, M.M. (2005) Lehninger Principles of Biochemistry, 4th Edition, W.H. Freeman and Co., NY). Other surrounding amino acids often can be changed without significantly affecting the ability of the enzyme to bind the substrate and to catalyze the usual reaction involving the substrate. This is especially true of oxygenases, where the range of substrates is often quite large, an indication that the substrate binding region lacks significant geometric specificity (See *e.g.*, ., Mason J.R, and Cammack R. (1992) *Annu Rev Microbiol.* 46:277-305; or Butler, C. S. and Mason, J. R. (1997) *Advances in Microbial Physiology* **38**, 47-84).

Therefore, Applicants submit that the Examiner simply can not discount these structural features and conclude that there is no art-recognized correlation or relationship between the structure of the invention and its function. Such a conclusion is, on its face, completely incorrect and unsubstantiated by the art at the time of the invention.

Second, Applicants submit that evidence has already been provided that, at the time of the present invention, one of skill in the art would have sufficient knowledge regarding where the

substrate for the oxygenase would bind, so that such person would easily be able to avoid disrupting this site, even without knowing *exactly* which residues contact substrate, and still modify up to 35% of the structure of the enzyme without destroying function. More specifically, as noted above and as previously stated, at the time of the invention, it was known that the binding site for free iron was situated in immediate proximity to the portion of the substrate that is modified in the chemical reaction catalyzed by the oxygenase$_{DIC}$ (i.e., the O-methyl group of dicamba) (see, *e.g.*, Mason J.R, and Cammack R. (1992) *Annu Rev Microbiol.* 46:277-305; Junker, F., Kiewitz, R., and Cook, A.M. (1997) 179:919-927).

The Examiner seems to assert in the May 28 Office Action that this argument is irrelevant because Applicants' specification did not specifically identify the sequence that binds dicamba. However, such an assertion is groundless, because Applicants have already demonstrated that, at the time of the invention, one can readily identify the free iron binding site in the claimed oxygenase (because the identifying consensus sequence or motif was well known) and therefore, one can certainly identify residues that are in close proximity to this binding site. The skilled in the art who wished to retain enzymatic activity while changing amino acid sequences of the enzyme would simply avoid residues in the immediate vicinity of the free iron-binding site. Importantly, because the essential free iron binding site residues and the substrate binding site comprise only *a limited portion* of any Rieske non-heme iron oxygenase molecule, there would easily be available to one skilled in the art a very large number of amino acid sequences (easily up to 35%) that could be altered without significantly affecting the enzymatic activity of the enzyme, and without knowing the exact sequence of the substrate binding site. Referring again to the sequence of the oxygenase shown in Figure A, which represents less than half of the 340 amino acids in the full sequence of the oxygenase, one can see that the active sites are just a small portion of the total sequence.

Applicants are not claiming *any sequence* of unrestricted structural features, but rather a sequence that is at least 65% identical to SEQ ID NO:4. Referring again to the December 2002 Declaration of Dr. Weeks and to the additional papers presented herein, it is clear that one of skill in the art had ample knowledge to predictably modify up to 35% of the protein and retain enzyme activity. Therefore, it is clear that the present inventors were in possession of the claimed invention at the time of filing.

Third, Applicants have provided an abundance of evidence generated post-filing that simply substantiates Applicants' position that one of skill in the art could, given the description in the specification and the knowledge in the art at the time of the invention, envision the full scope of the oxygenase sequences as claimed, and then readily make and use such enzymes. This evidence supports Applicants' position that the invention was sufficiently described or supported by the knowledge in the art at the time the invention was filed. Applicants will not reiterate these data again here, but will remind the Examiner that Applicants have demonstrated: the identification, isolation and sequencing of dicamba-degrading oxygenases from three additional bacterial strains (having 90.1-99% identity to the claimed SEQ ID NO:4); the mutation of sites within the oxygenase while retaining biological activity; the comparison of the modeled tertiary structure of the $oxygenase_{DIC}$ with the known structure of naphthalene dioxygenase.

Finally, the Examiner appears to acknowledge the post-filing evidence that one of skill in the art could isolate other dicamba-degrading oxygenases from other bacteria, and Applicants submit that, given that these sequences were obtained using the disclosed sequence of SEQ ID NO:3 and that the specification teaches that naturally occurring oxygenase sequences from other dicamba-degrading bacteria exist and will have structures similar to that of SEQ ID NO:3 and further taught methods to obtain and identify such sequences (e.g., see page 10, line 19 to page 11, line 4), this evidence demonstrates that Applicants were in possession of the invention as claimed in Claim 1 or 2 and related claims at the time of the invention.

In view of the foregoing remarks, Applicants respectfully request that the Examiner withdraw the rejection of Claims 1, 2, 4, 5, 7, 21, 24, 36,39, 44, 47, 48, 50-52, 54-56, 58-65, and 68-71 under 35 U.S.C. § 112, first paragraph.

Objection to the Specification and Rejection of Claims 1, 2, 4, 5, 7, 21, 24, 36,39, 44, 47, 48, 50-52, 54-56, 58-65, and 68-71 Under 35 U.S.C. § 112, First Paragraph (Enablement):

The Examiner has objected to the specification and rejected Claims 1, 2, 4, 5, 7, 21, 24, 36,39, 44, 47, 48, 50-52, 54-56, 58-65, and 68-71 under 35 U.S.C. § 112, first paragraph, on the basis of enablement. Specifically, in response to Applicants' last arguments, the Examiner contends that the structure of an enzyme is integral to its function, but that Applicants have only provided

guidance to make and use an isolated DNA molecule encoding SEQ ID NO:4. The Examiner states that the "art teaches the cytochrome P450 enzymes interact with other proteins, in particular reductases that donate an electron during the reaction, and are associated with membrane structures within the cell" and concludes that one must also take into consideration structures of a P450 enzyme that are critical to association with other proteins involved in the transfer of electrons and associations within the membrane. The Examiner does not find Applicants' data regarding other bacterial dicamba-degrading oxygenases to be persuasive because they are greater than 90% identical to SEQ ID NO:4. Finally, the Examiner contends that Applicants have not addressed the issue of fragments claimed in Claim 2.

Applicants traverse the Examiner's rejection. Initially, Applicants again note, as stated in the last response, the oxygenase of the present invention is not in the family of cytochrome P450 oxygenases that use a heme group to transfer electrons. Rather, the oxygenase described in the present invention is a member of the Rieske non-heme iron-binding oxygenases that transfer electrons through iron-sulfur clusters and free iron atoms (see specification, Examples, March 2004 response). Applicants have clearly demonstrated, referring to the discussion above under written description, that the specification teaches that both the iron-sulfur clusters and the free iron binding site are found in the claimed oxygenase and that at the time of the invention, one of skill in the art would readily identify both of these structures in the claimed oxygenase (see Weeks Declaration of December 2002 and Figure A). Therefore, contrary to the Examiner's contention, the specification and the guidance available in the art at the time of the invention provides sufficient guidance to one of skill in the art regarding the structures of the claimed Rieske non-heme iron-binding oxygenase that are required for enzyme activity. With regard to substrate binding, Applicants further note that it was known at the time of the invention that the binding site for free iron in a Rieske non-heme iron-binding oxygenase is situated in immediate proximity to the portion of the substrate that is modified in the chemical reaction catalyzed by the oxygenase$_{DIC}$ (i.e., the O-methyl group of dicamba). Therefore, one of skill in the art would also know where in the protein the substrate binding region will be located.

As discussed previously, the specification and the art teach one of skill in the art how to make modifications to a nucleotide sequence and/or protein sequence, and based on the discussion

provided above, one of skill in the art would clearly be able to modify up to 35% of the protein sequence without undue experimentation while predictably maintaining protein function. Moreover, the specification provides assays by which dicamba-degrading catalytic activity can easily be evaluated. Applicants' post-filing data have demonstrated that one of skill in the art can easily produce mutations that do not disrupt protein function. Furthermore, post-filing evidence regarding the established substrate binding sites for a few Rieske non-heme iron-binding oxygenases indicate that the art was correct regarding the location of the substrate binding site being proximal to the free iron binding site (e.g., see Karlsson et al., (2003) *Science* 299:1039-42 (cited in Weeks Declaration of 2004); see also Kauppi et al., (1998) *Structure* 6:571-586; and Carredano et al., (2000) *J. Mol. Biol.* 296:701-712).

Applicants have also established that, as predicted by the specification, one can use the sequence for the oxygenase of the present invention and readily identify, isolate and clone additional dicamba-degrading oxygenases that fall within the scope of Claim 1 or Claim 2. The fact that the identified dicamba-degrading oxygenases from other bacteria are greater than 90% identical to SEQ ID NO:4 does not discount their value in demonstrating the ease in obtaining an oxygenase within the scope of Claim 1, nor even an oxygenase within the scope of Claim 2. Applicants additional arguments provided above demonstrate additional enablement support for the full breath of the present claims.

With regard to biologically active fragments of SEQ ID NO:4, Applicants submit that the same arguments as set forth above apply to fragments of SEQ ID NO:4. Given the knowledge of where in the protein lie the structures required for function of the claimed oxygenase as described above, one of skill in the art would readily be able to produce truncated versions of the oxygenase that retain enzymatic activity. It is particularly noted that the iron-sulfur cluster and the free iron binding site (and by extrapolation, the substrate binding site) are not located at the C- or the N-terminus of the protein (see Figure A of the December 2002 Weeks Declaration). Therefore, one of skill in the art would be able to predictably produce fragments of SEQ ID NO:4 that would retain enzymatic activity.

In view of the foregoing remarks, Applicants respectfully request that the Examiner withdraw the rejection of Claims 1, 2, 4, 5, 7, 21, 24, 36,39, 44, 47, 48, 50-52, 54-56, 58-65, and 68-71 under 35 U.S.C. § 112, first paragraph.

Applicants have attempted to respond to all of the Examiner's concerns as set forth in the May 28 Office Action, and submit that the claims are in a condition for allowance. Any further concerns regarding these claims can be discussed with the below-named agent at (303) 863-9700.

Respectfully submitted,

SHERIDAN ROSS P.C.

By: Angela Sebor

Angela Dallas Sebor
Registration No. 42,460
1560 Broadway, Suite 1200
Denver, Colorado 80202-5141
(303) 863-9700

Date: November 29, 2004

Attachments:

Mason J.R, and Cammack R. (1992) *Annu Rev Microbiol.* 46:277-305
Butler, C. S. and Mason, J. R. (1997) *Advances in Microbial Physiology* **38**, 47-84
Neidle et al. (1991) *J. Bacteriol.* 173(17):5385-5395
Junker et al. (1997) *J. Bacteriol.* 179(3):919-927
Gurbiel et al. (1996) *Biochemistry* 35:7834-7845 (abstract)
Harayama et al. (1992) *Annu Rev Microbiol.* 46:565-601 (abstract)

Annu. Rev. Microbiol. 1992. 46:277–305

THE ELECTRON-TRANSPORT PROTEINS OF HYDROXYLATING BACTERIAL DIOXYGENASES

Jeremy R. Mason and Richard Cammack

Divisions of Biosphere Sciences and Biomolecular Sciences, King's College London, Campden Hill Road, London W8 7AH, United Kingdom

KEY WORDS: flavoprotein, ferredoxin, iron-sulfur protein, Rieske-type [2Fe-2S] cluster, nonheme iron

CONTENTS

Abstract

The degradation of aromatic compounds by aerobic bacteria frequently begins with the dihydroxylation of the substrate by nonheme iron-containing dioxygenases. These enzymes consist of two or three soluble proteins that interact to form an electron-transport chain that transfers electrons from reduced nucleotides (NADH) via flavin and [2Fe-2S] redox centers to a terminal dioxygenase. The dioxygenases may be classified in terms of the number of constituent components and the nature of the redox centers. Class I consists of two-component enzymes in which the first protein is a reductase

0066-4227/92/1001-0277$02.00

containing both a flavin and a [2Fe-2S] redox center and the second component is the oxygenase; Class II consists of three-component enzymes in which the flavin and [2Fe-2S] redox centers of the reductase are on a separate flavoprotein and ferredoxin, respectively; and Class III consists of three-component enzymes in which the reductase contains both a flavin and [2Fe-2S] redox center but also requires a second [2Fe-2S] center on a ferredoxin for electron transfer to the terminal oxygenase. Further subdivision is based on the the type of flavin (FMN or FAD) in the reductase, the coordination of the [2Fe-2S] center in the ferredoxin, and the number of terminal oxygenase subunits.

From the deduced amino acid sequence of several dioxygenases the ligands involved in the coordination of the nucleotides, iron-sulfur centers, and mononuclear nonheme iron active site are proposed. On the basis of their spectroscopic properties and unusually high redox potentials, the [2Fe-2S] clusters of the ferredoxins and terminal oxygenases have been assigned to the class of Rieske-type iron-sulfur proteins. The iron atoms in the Rieske iron-sulfur cluster are coordinated to the protein by two histidine nitrogens and two cysteine sulfurs.

INTRODUCTION

The benzene nucleus is one of the most abundant chemical structures in the biosphere, originating from both natural and anthropogenic sources. The biodegradation of compounds containing this structure is carried out almost exclusively by microorganisms (26), and with few exceptions, the initial step is the introduction of two hydroxyl groups into the benzene ring. This action is a prerequisite for further fission and catabolism of the aromatic compound. The enzymes that perform this specialized function of catalyzing the insertion of molecular oxygen into the organic substrate are termed *oxygenases*.

This review describes the properties and structure of a class of dioxygenases that convert aromatic rings to *cis*-diols. The enzymes generally comprise several protein subunits, an iron center, iron-sulfur clusters, and a flavin, arranged in an electron-transfer chain. The structures of these components vary in several ways. The structural evidence derives from very limited X-ray crystallographic results, extensive amino-acid sequence data and comparison with other electron-transfer proteins, and the application of spectroscopic methods.

Oxygenases

The most extensively investigated oxygenase enzymes are those isolated from *Pseudomonas* species (54). They activate molecular oxygen and incorporate it directly into the chemical structure of the organic molecule. Although the

reactions catalyzed by oxygenases are highly exergonic, the free energy released is not conserved by the formation of ATP. Thermodynamically, the effect of the oxygenase reaction is to destabilize the aromatic growth substrate and render the catabolism of the aromatic compounds irreversible (22).

The various oxygenases differ in structure, mechanism, and in coenzyme requirements. They can, however, be classified into two groups: the monooxygenases, which incorporate one atom of oxygen into one molecule of substrate, and the dioxygenases, which add both atoms of oxygen into the substrate. In monooxygenases, the other atom of oxygen is reduced to water so that these enzymes function as part oxygenase and part oxidase; hence, they are also termed *mixed-function oxidases* (73). The distinction between dioxygenase and monooxygenase activities is, however, not always absolute. For example, both toluene and naphthalene dioxygenases can catalyze monooxygenase reactions as in the oxidation of indene and indan to 1-indenol and 1-indanol, respectively (112), while 4-methoxy benzoate monooxygenase dihydroxylates the vinylic side chain of 4-methoxystyrene with both atoms derived from molecular oxygen (114, 115).

Dioxygenases are involved at several stages in the pathways for the catabolism of aromatic compounds and may be considered to fall into two groups:

1. Dioxygenases involved in ring hydroxylation. These all require reduced cofactors, either NADH or NADPH, in addition to oxygen. They dihydroxylate aromatic substrates to produce *cis*-diols, e.g. toluene dioxygenase:

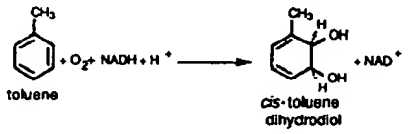

2. Dioxygenases involved in ring fission. These have no cofactor requirement and cleave the benzene ring of hydroxylated (di- or tri-) aromatic substrates, e.g. catechol 1,2-dioxygenase:

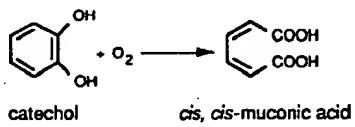

This review deals with the former group of dioxygenases, which are essential for the activation of aromatic compounds.

STRUCTURE OF RING-HYDROXYLATING DIOXYGENASES

Gibson and coworkers (40, 41) were the first to show that the dioxygenase system of *Pseudomonas putida* oxidized benzene to generate *cis*-1,2-dihydroxy-cyclohexa-3,5-diene. Several aromatic ring-hydroxylating dioxygenases have since been isolated and characterized (2, 30, 49, 50, 101, 102, 120, 123). The enzymes are nonheme dioxygenases that oxidize the aromatic substrates to give *cis*-dihydrodiols or *cis*-diol carboxylic acids. They require, in addition to molecular oxygen, cofactors, including reduced pyridine nucleotides and Fe(II), for the reactions they catalyze.

In the ring-hydroxylating oxygenases so far investigated, the preferred reductant is NADH. All are soluble, multicomponent enzymatic systems comprising the same types of redox components (Table 1). The details of the electron-transfer chains have not been elucidated in all cases; however, a typical arrangement is a short electron-transfer chain:

$$\underset{\text{Reductase site}}{\text{NADH} \rightarrow \text{Flavin}} \quad \underset{\text{Electron-transfer chain}}{\rightarrow \text{Fe-S}_{\text{Fd}} \rightarrow \text{Fe-S}_{\text{R}} \rightarrow} \quad \underset{\text{Oxygenase site}}{\text{Fe} \rightarrow \text{O}_2}$$

Here, Fe-S_{Fd} and Fe-S_{R} represent ferredoxin-type and Rieske-type [2Fe-2S] iron-sulfur clusters respectively, as defined below. Fe represents the iron-binding site proposed to be the terminal oxygenase center.

The distribution of the redox components, and the number and size of protein subunits, depend on the type of the ring-hydroxylating dioxygenases being considered (Table 1). All of the terminal dioxygenase proteins of this class consist of an iron-sulfur protein with a Rieske-type [2Fe-2S] cluster and an iron site, but the reductase chain, which transfers reducing equivalents from NADH to the terminal dioxygenase, may consist of either one or two separate proteins.

Reductase System

Table 1 shows that the reductase chains of different ring-hydroxylating dioxygenases occur in three different arrangements, depending on the number of subunits and the disposition of iron-sulfur clusters. They may be further subdivided on the basis of the types of iron-sulfur clusters and flavin present:

1. Two-component dioxygenases, in which the flavin and iron-sulfur cluster are combined in the same protein. Examples include benzoate 1,2-dioxygenase (EC 1.13.99.2) (119), phthalate dioxygenase (EC 1.14.12.7) (5), 4-chlorophenylacetate-3,4-dioxygenase (71, 95), and 4-sulfo-

Table 1 Multicomponent hydroxylating oxygenases

Enzyme System	Components		Prosthetic group(s)	Gene designation	Class[a]	References
Phthalate dioxygenase	Reductase	34,000	FMN, [2Fe-2S]		IA	3, 5
(*P. cepacia*)	Oxygenase	$\alpha(48,000)_4$	$4[2Fe\text{-}2S]_R$, 4Fe			3, 5
4-chlorophenylacetate 3,4-dioxygenase	Reductase				IA	71
(*P.* sp. CBS)	Oxygenase	$\alpha(46,000)_3$	3[2Fe-2S]			71, 72
4-sulfobenzoate 3,4-dioxygenase	Reductase				IA	69
(*Comamonas testosteroni* T-2)	Oxygenase	$\alpha(50,000)_2$				69
Benzoate dioxygenase	Reductase	37,500	FAD, 2Fe-2S	*benC* (*xylZ*)	IB	75, 79, 122
(*P. arvilla* C-1, *Acinetobacter calcoaceticus*)	Oxygenase	$\alpha(50,000)_3$ $\beta(20,000)_3$	3[2Fe-2S], 3Fe	*benAB* (*xylXY*)		79, 122
4-Methoxybenzoate O-demethylase	Reductase	42,000	FMN, [2Fe-2S]		IB	9, 91
(*P. putida* DSM No. 1868)	Putidamonooxin	$\alpha(41,000)_3$	[2Fe-2S], Fe			8, 9
Benzene, 1,2-dioxygenase	$Reductase_{BED}$	$\alpha(42,000)_2$	FAD	*bedA* (*bnzC*)	IIB	2, 38, 59, 105
(*P. putida* ML2 NCIB 12190)	$Ferredoxin_{BED}$	11,860	$[2Fe\text{-}2S]_R$	*bedB* (*bnzB*)		2, 38, 59, 105
	ISP_{BED}	$\alpha(54,500)_2$ $\beta(23,500)_2$	$2[2Fe\text{-}2S]_R$, Fe	*bedC1C2* (*bnzAB*)		2, 38, 59, 105, 126
Pyrazon dioxygenase	Reductase	67,000	FAD		IIA	93
(*Pseudomonas*)	Ferredoxin	12,000	[2Fe-2S]			93
	Oxygenase	180,000	[2Fe-2S]			93
Toluene dioxygenase	$Reductase_{TOL}$	46,000	FAD	*todA*	IIB	43, 101, 111
(*P. putida* F1)	$Ferredoxin_{TOL}$	11,900	$[2Fe\text{-}2S]_R$	*todB*		43, 101
	ISP_{TOL}	$\alpha(52,500)_2$ $\beta(20,800)_2$	$2[2Fe\text{-}2S]_R$, Fe	*todC1C2*		43, 93, 101
Naphthalene dioxygenase	$Reductase_{NAP}$	36,300	FAD, [2Fe-2S]		III	31, 50
(*P. putida* NCIB 9816)	$Ferredoxin_{NAP}$	15,300	[2Fe-2S]	*ndoA*		31, 49, 67
	ISP_{NAP}	$\alpha(55,000)_2$ $\beta(20,000)_2$	2[2Fe-2S], 2Fe	*ndoBC*		29, 31, 67

[a] The classes of dioxygenases are as defined by Batie et al (4).

benzoate-3,4-dioxygenase (69). These are Class I dioxygenases in the classification of Batie et al (4) and are subdivided into Class IA, containing FMN, and IB, containing FAD.

2. Three-component dioxygenases, in which the electron-transfer chain comprises a flavoprotein and a separate iron-sulfur protein (ferredoxin). Class IIA comprises pyrazon dioxygenase (EC 1.14.12), which has a plant-type ferredoxin as judged by its electron paramagnetic resonance (EPR) spectrum (93). Class IIB includes benzene dioxygenase (EC 1.14.12.3) (2, 39) and toluene dioxygenase (101, 102) which, as discussed later, appear to have Rieske-type iron-sulfur clusters in their ferredoxins.
3. Three-component dioxygenases, in which the electron-transfer chain comprises both an iron-sulfur flavoprotein and a ferredoxin. The sole representative, so far, of Class III is naphthalene dioxygenase (49, 50).

The differences between the dioxygenases may be related to function; the products of the three-component dioxygenases are all *cis*-dihydrodiols, whereas those of the two-component dioxygenases are either *cis*-diol carboxylic acids or catechols. In the latter case (e.g. 4-sulfobenzoate-3,4-dioxygenase), a hypothetical dihydrodiol intermediate represents a highly unstable configuration that spontaneously loses a group (sulfite or chloride) with the concomitant energetically favorable rearomatization.

RELATED SYSTEMS The electron-transfer chains of the aromatic dioxygenases may be considered in the wider context of mixed-function oxidases. This review refers to other oxygenases that have similar electron-transfer chains from NAD(P)H.

For example, 4-methoxybenzoate monooxygenase from *P. putida* (DSM No. 1868) is a closely related system that has a similar reductase chain. It does not catalyze dioxygenation of the aromatic ring (9), but as already noted, it has dioxygenase activity towards certain substrates (115). It comprises a nonheme iron-containing terminal oxygenase, which Bernhardt and coworkers (8, 109) named putidamonooxin, and a reductase that contains FMN and a [2Fe-2S] cluster. The vanillate demethylase of *Pseudomonas* strain ATCC 19151 catalyzes a similar monooxygenase reaction and consists of two similar components, the sequences of which were recently determined (16).

Another similar oxygenase is the cytochrome P-450 monooxygenase, in which the terminal oxygenase component is heme (83). All P-450 systems incorporate a pyridine nucleotide-linked flavoprotein, and some, but not all, involve ferredoxins with [2Fe-2S] clusters. They are typified by the well-studied camphor monooxygenase of *P. putida* (strain CIB), which comprises a flavoprotein (putidaredoxin reductase), a ferredoxin (trivial name putidaredoxin), and the terminal monooxygenase P-450_{CAM} (28, 98). Overall,

more is known about the mechanism of oxygen activation in the P-450 monooxygenases than in any other hydroxylase.

Finally, the third similar oxygenase is methane monooxygenase, in which the terminal oxygenase component is a dimeric nonheme iron cluster, probably with μ-oxo bridging ligands (34, 85, 118). This has a NADH-linked reductase comprising an iron-sulfur flavoprotein (70, 86).

We now consider the various components of the aromatic ring-hydroxylating dioxygenases, and what is known about their composition, catalytic activity and structure.

SIMPLE FLAVOPROTEINS In the three-component dioxygenase systems, the flavoprotein, the first component of the electron-transfer chain, acts as an oxidoreductase catalyzing the transfer of two electrons from NADH. The flavoprotein consists of a single polypeptide with relative molecular mass (M_r) ranging from 42 to 67 kilodaltons (kDa) (Table 2). The protein is reportedly monomeric for toluene and pyrazon dioxygenases (93, 101). It contains FAD as the only prosthetic group, which is readily lost during purification (50, 101). These flavoproteins belong to a large family of FAD-containing pyridine nucleotide oxidoreductases. They vary in size, substrate specificities, and preference for NADH or NADPH (51).

The reductase components of the benzene dioxygenase and toluene dioxygenase contain FAD as their prosthetic groups (2, 101). The flavoproteins show absorption spectra typical of FAD with maxima at around 375 and 450 nm. They function as oxidoreductases by transferring electrons from NADH to the ferredoxin components. Both enzymes are specific for NADH. By contrast, the flavoprotein of naphthalene dioxygenase (50) is significantly reduced when NADPH is substituted for NADH as the coenzyme.

The probable cofactor binding sites in the reductase proteins may be inferred from their amino acid sequences and comparison with other flavoproteins. NADH-dependent reductases of dioxygenases may be compared with the FMN-containing putidaredoxin reductase, which performs an analogous function in the cytochrome P-450–dependent camphor hydroxylase (63, 91). Other NADH-dependent flavoproteins found in *Pseudomonas* sp. include dihydrolipoamide dehydrogenase [*P. fluorescens* (7)] and the flavin-containing monooxygenases, *p*-hydroxyphenylacetate hydroxylase (87) and salicylate hydroxylase (61). Examples of NADPH-dependent flavoproteins include mercuric reductase [*P. aeruginosa* (15)], glutathione reductase [*P. aeruginosa* (N. L. Brown, cited in 96)], and *p*-hydroxybenzoate hydroxylase [*P. fluorescens* (56)]. (Note that the above-mentioned flavoprotein monooxygenases contain no metal centers.)

The proteins are each expected to contain two binding sites for ADP moieties, one in FAD and the other in NAD. For convenience, these sites are referred to as the FAD-binding and NAD-binding sites. Common to the

Table 2 Properties of the reductase component of aromatic dioxygenases

Dioxygenase	Component	Prosthetic group(s)	Absorption λ_{max} (nm)	EPR g_x, g_y, g_z	References
Benzene	A_2 (Ferredoxin $_{BED}$ reductase)	FAD	385, 425, 455		2
Toluene	Ferredoxin$_{TOL}$ reductase	FAD	372, 488, 475		101
Pyrazon	A2	FAD	450, 475		93
Naphthalene	Ferredoxin$_{NAP}$ reductase	FAD, [2Fe-2S]	278, 340, 420, 460, 540[a]		50
Benzoate	Reductase	FAD, [2Fe-2S]	273, 340, 402, 467		119
Phthalate	Reductase	FMN, [2Fe-2S]	330, 420, 462, 495[a], 530[a]	1.900, 1.949, 2.008, 2.041	4, 24
4-Chlorophenylacetate 3,4-dioxygenase	B	FMN, [2Fe-2S]	336, 394, 458	1.90, 1.94, 2.004, 2.03	71
4-Sulfobenzoate	B	FMN, [2Fe-2S]	~330, ~400, 465		69

[a] Shoulder.

FAD-binding (ADP-binding) site of the flavoprotein oxidoreductases is the highly conserved sequence

Gly-X-Gly-X-X-Gly-X-X-X-Ala-X-X-X-X-X-X-Gly,

where X represents any amino acid, situated near the amino terminus of the protein (7, 51, 99). The Gly-X-Gly-X-X-Gly sequence constitutes a tight turn between the first strand of a β-sheet and the succeeding α-helix (117). The NAD-binding (ADP-binding) domain of many enzymes has also been reported to be a $\beta\alpha\beta$-fold centered around a highly conserved Gly-X-Gly-X-X-Gly sequence (7, 96). A comparison of the primary structure of reductase$_{BED}$ and reductase$_{TOL}$ with the amino acid sequence of other flavoprotein oxidoreductases reveals two such regions as shown in Figure 1. The first sequence of Gly-X-Gly-X-X-Gly-X-X-X-Gly-X-X-X-X-X-X-Gly, which is conserved in the dioxygenase flavoproteins examined, is located close to the amino terminus of the protein and is most probably the FAD-binding site of the reductase component of the dioxygenase.

Some 140 residues along the protein from the first conserved Gly, one finds another dinucleotide-binding consensus sequence, although with significant differences (Figure 2). First, the conserved alanine residue in the dioxygenase reductase is replaced by a glycine in the other oxidoreductases. Second, a glutamate residue is always seven residues farther along the protein from the last conserved glycine. This negatively charged residue at the carboxy end of

Enzyme	Amino acid sequence
ReductaseBED	^{1}MANHVAIIGNGVAGFTTAQALRAEGYEGRISLIGEEQHLP
ReductaseTOL	^{1}MATHVAIIGNGVGGFTTAQALRAEGFEGRISLIGDEPHLP
LipoamideDH	^{2}QKFDVVVIGAGPGGYVAAIRAAQLGLKTACIEKYIGKEGK
PutidaredoxinR	^{3}ANDNVVIVGTGLAGVEVAFGLRASGWEGNIRLVGDAWVIP
p-OH benzoateH	^{2}MKTQVAIIGAGPSGLLLGQLLHKAGIDNVILERQTPDYVL
Consensus sequence	G G G A/G G
Secondary structure	βββββββTααααααααααααTTβββββββ

Figure 1 Alignment of the putative FAD-binding sites of reductase$_{BED}$ and reductase$_{TOL}$ with those of other *Pseudomonas* oxidoreductases. The numbers indicate the position of the amino acid in the protein sequence. In the secondary structure, α, β, and T indicate α-helix, β-sheet, and turn, respectively. The sequences presented are: reductase$_{TOL}$ (127); lipoamide dehydrogenase (7); putidaredoxin reductase (90), and *p*-hydroxybenzoate hydroxylase (113).

the second β-strand is involved in binding the 2'-OH of the ribose of NADH (96). In NADPH-dependent oxidoreductases, this residue is replaced by an uncharged amino acid, presumably to accommodate the 2'-phosphate group on the coenzyme. The other difference in the NADP-binding domain is the replacement of the third glycine residue of the conserved trio by alanine, with another alanine four residues farther along the helix. The substitution of alanine for glycine is thought to modify the local polypeptide conformation associated with the difference in coenzyme specificity (96). These differences in the amino acid sequence could explain why NADPH cannot replace NADH as the coenzyme in the benzene and toluene dioxygenase systems (2, 101). The other salient feature of the two conserved regions in all these enzymes is their similar distance from each other, which could indicate similar overall folding of the polypeptide.

IRON-SULFUR FLAVOPROTEINS In contrast to the two-component reductase chains in which the iron-sulfur cluster resides on a separate polypeptide, dioxygenases have been isolated in which this redox center is arranged on the same polypeptide as the flavoprotein. Table 2 lists the properties of these iron-sulfur flavoprotein reductases. There are two classes, depending on whether they contain FAD or FMN. They each contain a [2Fe-2S] cluster.

Although they fulfill the same role as the two-component electron-transfer

Enzyme	Amino acid sequence
Reductase$_{BED}$	^{141}TPNTRLLIVGGGLIGCEVATTARKLGLSVTILEAGDELLV
Reductase$_{TOL}$	^{141}TSATRLLIVGGGLIGVEVATTARKLGLSVTILEAGDELLV
Lipoamide dehydrogenase *P. fluorescens*	^{178}AVPKKLGVIGAGVIGLELGSVWARLGAEVTVLEALDKFLP
A. vinelandii	^{178}NVPGKLGVIGAGVIGLELGSVWARLGAEVTVLEAMDKFLP
E. coli	^{178}EVPERLLVMGGGIIGLEMGTVYHALGSQIDVVEMFDQVIP
Consensus sequence	G G G A/G G E
Secondary structure	βββββββTααααααααααααTTβββββββ

Figure 2 Alignment of the putative NAD-binding sites of reductase$_{BED}$ and reductase$_{TOL}$ with those of other oxidoreductases. The numbers indicate the position of the amino acid in the protein sequence. In the secondary structure, α, β, and T indicate α-helix, β-sheet, and turn, respectively. The sequences presented are: reductase$_{BED}$ (59), reductase$_{TOL}$ (127), and lipoamide dehydrogenase [*P. fluorescens* (7), *Azotobacter vinelandii* (116), *E. coli* (99)].

systems, these "true" reductases show little homology with the former. Thus, the reductase component of the benzoate 1,2-dioxygenase, although showing a high degree of immuno-cross-reactivity with the toluate dioxygenase, showed no such homology with the components of the benzene or naphthalene dioxygenases (75).

The recently determined structure of phthalate dioxygenase reductase (4) shows that the protein comprises three domains. The N-terminal domain, containing FMN, has the same structural topology as the plant ferredoxin: NADP reductase (62), consisting of a six-stranded β-barrel. The intermediate NAD-binding domain has the typical Rossman α/β fold of nucleotide-binding proteins. The C-terminal domain resembles the plant-type ferredoxins from cyanobacteria (35, 92, 108). The sequences of the iron-sulfur flavoproteins of the benzoate and toluate dioxygenases (79) show homologies with the plant-type ferredoxins, as do the reductases of vanillate demethylase (16), xylene monooxygenase (103), and methane monooxygenase (97).

The iron-sulfur flavoproteins can transfer electrons directly from NADH to an artificial electron acceptor. Thus, the reductase components of benzoate 1,2-dioxygenase, phthalate dioxygenase, and 4-chlorophenylacetate 3,4-dioxygenase reduce cytochrome *c* directly in the presence of NADH (5, 95, 119, 123). These proteins are monomeric with M_r of 34–38 kDa and contain a [2Fe-2S] cluster in addition to the flavin prosthetic group. Consequently, the absorption spectra of the oxidized proteins show absorption maxima at 340 and 460 nm. The EPR spectra of the reduced proteins show typical features of plant-type [2Fe-2S] clusters, together with a signal around $g = 2.004$ from the flavosemiquinone radical (5, 95).

Yamaguchi & Fujisawa (119) studied the iron-sulfur flavoprotein (designated NADH-cytochrome *c* reductase) of the benzoate 1,2-dioxygenase of *P. arvilla*. They succeeded in removing the [2Fe-2S] cluster by treatment with *p*-chloromercuriphenyl-sulfonate and in reconstituting it by incubation with iron, sulfide, and mercaptoethanol (121). This technique has been successfully applied to ferredoxins (e.g. 107a), but it is unusual to achieve reconstitution with an enzyme of this complexity. On removal of the [2Fe-2S] cluster, the protein retained some ability to transfer electrons from NADH to artificial acceptors such as ferricyanide (60%), but not to the dioxygenase protein (less than 1%). Full activity was restored when the [2Fe-2S] cluster was replaced.

Ferredoxin$_{NAP}$ reductase resembles the reductases described above in that it can catalyze the reduction of cytochrome *c* independently. The absorption spectrum is also similar to the spectra of the iron-sulfur flavoproteins with absorption maxima at 340, 420, and 460 nm, and a broad shoulder at 540 nm. Unlike these proteins, however, ferredoxin$_{NAP}$ reductase requires an additional protein, ferredoxin$_{NAP}$ to transfer electrons to the terminal dioxygenase component (49).

FERREDOXINS The intermediate electron-transfer carrier in the aromatic dioxygenases is a ferredoxin containing an iron-sulfur cluster of the [2Fe-2S] type. Ferredoxins are small proteins that contain iron-sulfur clusters, whose sole function is to transfer electrons (17).

Several different types of [2Fe-2S] clusters are known in proteins. The largest class consists of the plant-type ferredoxins, of which the first known example was spinach ferredoxin, found in chloroplast membranes. Similar proteins have been found in cyanobacteria, and the structures of three of these have been determined (35, 92, 108). Ferredoxins with similar properties are involved in electron transfer to certain cytochrome P-450–dependent monooxygenases; these include putidaredoxin from *P. putida* camphor monooxygenase, and adrenodoxin of the steroid monooxygenase of mammalian adrenal mitochondria. NMR studies indicate that the structures of these proteins have a similar fold (45, 82). All of these are small hydrophilic proteins containing one [2Fe-2S] cluster per molecule, serving as one-electron carriers. The [2Fe-2S] clusters contain two atoms of iron, bridged by two labile sulfide atoms, and coordinated to the protein by four sulfide ligands contributed by four cysteine residues. They are reddish in color; the visible absorption principally results from sulfur-to-Fe(III) charge-transfer transitions (81). Upon reduction, one of the iron ions is reduced to Fe(II), and the visible absorption decreases to about half.

^{57}Fe Mössbauer spectroscopy enables the investigator to distinguish the individual iron atoms in the iron-sulfur clusters. In reduced ferredoxins, the spectra of Fe(III) and Fe(II) ions can be clearly identified as quadrupole doublets with chemical shifts characteristic of their valence states (20, 27, 78). The electronic structure of the [2Fe-2S] clusters is such that the spins on the iron ions are antiferromagnetically coupled. As a result, the oxidized protein has a ground state with zero spin, and there is no electron paramagnetic resonance (EPR) spectrum. Upon reduction, one of the iron ions becomes high-spin Fe(II), and the net spin of the coupled Fe(III) and Fe(II) ions is $S = 1/2$. Thus, unlike most iron compounds, the [2Fe-2S] clusters give an EPR signal in the reduced state, when measured at low temperatures, which has an average g-factor of less than 2 (44). In the plant-type ferredoxins g_{av} is around 1.96.

Plant-type ferredoxin

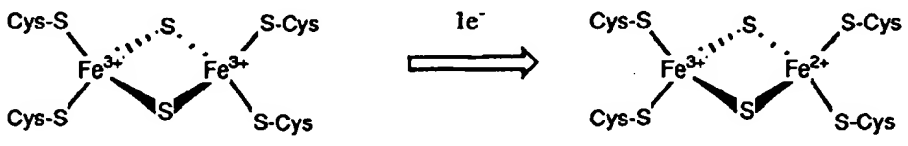

Oxidized Reduced

Another class of proteins that contain [2Fe-2S] clusters comprises the Rieske proteins. They are named after J. S. Rieske, who described a protein isolated from the cytochrome bc_1 complex of mitochondria (89). Similar proteins are associated with the b_6-f complex of the thylakoid membrane of chloroplasts (58, 88) and the plasma membrane of some aerobic and photosynthetic bacteria (32, 36); for a recent review on microbial *bc* complexes, see the report by Trumpower (106). Among the distinguishing properties of the Rieske iron-sulfur clusters are red-shifted visible spectra with maximum absorbance about two-thirds those of the plant-type ferredoxins and relatively positive midpoint redox potentials. In the EPR spectra of the reduced proteins, g_{av} is lower, around 1.91, with a characteristic sharp derivative peak at $g \simeq 2.02$ and a broad trough around $g \simeq 1.80$. The plant-type and Rieske-type [2Fe-2S] clusters can be distinguished using several different spectroscopic methods, including optical absorption, EPR, Mössbauer, resonance Raman, and X-ray absorption. As explained below, there is evidence that two of the ligands to the Rieske iron-sulfur cluster are the nitrogens of histidine residues (33, 48).

The ferredoxins of the ring-hydroxylase dioxygenase systems are small acidic proteins of M_r ranging from 12 to 15 kDa, containing 2 gram atoms of iron and acid-labile sulfide per mole (Table 3). The ferredoxins are one-electron acceptors (25, 102). In addition to transferring electrons from the flavoprotein to the terminal oxygenase component, the ferredoxin catalyzes a flavoprotein-dependent reduction of other electron acceptors such as cytochrome *c* (2, 102).

Gibson and coworkers found that analogous electron-transfer proteins, such as spinach ferredoxin, putidaredoxin, adrenodoxin, and the 2[4Fe-4S] ferredoxin from *Clostridium pasteurianum*, cannot replace ferredoxin_{TOL} in either cytochrome *c* reduction or toluene oxidation (43, 102). Similarly, ferredoxin_{TOL} could not substitute for ferredoxin_{NAP} in the naphthalene dioxygenase system (49). Thus, the ferredoxins are apparently rather specific for the dioxygenase system, in which they act as electron-transfer proteins. This specificity is reflected in the primary structure of the proteins.

The ferredoxins of the different ring-hydroxylating dioxygenases are similar in size: ferredoxin_{NAP} comprises 104 amino acids, while ferredoxin_{BED} and ferredoxin_{TOL} have three amino acids more. Ferredoxin_{BED} and ferredoxin_{TOL} are almost identical in sequence, but ferredoxin_{NAP} reportedly shares only 34% homology with ferredoxin_{BED} in amino acid composition (67). In all other [2Fe-2S] ferredoxins [with the exception of a [2Fe-2S] protein of *C. pasteurianum*, which appears to represent yet another family of iron-sulfur proteins (74)], the cysteine residues involved in binding the cluster are arranged as

Cys-X-X-X-Cys-X-X-Cys–29 amino acids–Cys

Table 3 Properties of the ferredoxin component of aromatic dioxygenases

Dioxygenase	Component	Prosthetic group	Absorption λ_{max} (nm)	EPR g_x,g_y,g_z	Redox potential (mV)	References
Benzene	B ($Ferredoxin_{BED}$)	[2Fe-2S]	280, 320, 456	1.834, 1.890, 2.026	−155	25, 77
Toluene	$Ferredoxin_{TOL}$	[2Fe-2S]	277, 327, 460	1.81, 1.86, 2.01	−109	102
Naphthalene	$Ferredoxin_{NAP}$	[2Fe-2S]	280, 325, 460			49
Pyrazon	B	[2Fe-2S]	411, 453	1.94, 2.02		93

where X denotes any amino acid (125). The arrangement of the cysteines in the dioxygenase ferredoxins is quite different, however. Figure 3 shows an alignment of the conserved regions in the four sequences determined so far. Because the ferredoxin serves as an intermediate electron carrier in these dioxygenases, it is conceivable that some of the conserved regions in the proteins represent domains involved in recognition of the flavoprotein and terminal oxygenase components. However, examination of the conserved regions shows that they include three cysteine and two histidine residues, suggesting that these include ligands involved in binding to the [2Fe-2S] cluster, in which case the ligation is different from that in the plant-type ferredoxins.

The EPR spectrum of the ferredoxin of the pyrazon dioxygenase resembles those of the P-450 monooxygenases such as putidaredoxin with *g*-factors of 2.02 and 1.94 (93), indicating that it is a typical [2Fe-2S] cluster with cysteine ligands. By contrast, the fact that ferredoxins of the toluene and benzene dioxygenases have unusual [2Fe-2S] clusters is shown by their spectroscopic

Ferredoxin homology

```
    45       53        63        77        87
----CTHG-  -SdGYLeG- -ECpLH-  -KALCAP- -IKtyPvKiE-        ND
    43       51        61        77        85
----CTHG-  -SeGYLdG- -ECtLH-  -KALPAC- -IKvyPiKiE-        BED1
    41       49        59        75        83
----CTHG-  -SdGYLdG- -ECtLH-  -KALPAC- -IKvfPiKvE-        BED2
    43       51        61        77        85
----CTHG-  -SdGYLdG- -ECtLH-  -KALPAC- -IKvfPiKvE-        TOD
```

Terminal oxygenase (ISP) α subunit homology

```
    81              101
----CRHRG-          -CSYHGW-                              ND
    96              116
----CRHRG-          -CSYHGW-                              BED1
    96              116
----CRHRG-          -CSYHGW-                              TOD
```

Rieske iron-sulfur protein homology

```
   108              126
----CTHLGCV-        -CPCHGS-                              CYPETC
   159              178
----CTHLGCV-        -CPCHGS-                              SCRIP1
   174              193
----CTHLGCV-        -CPCHGS-                              NCUCR
```

Figure 3 Conserved cysteines and histidines in the putative cluster-binding sequences of Rieske-type [2Fe-2S] clusters in ferredoxins, dioxygenases, and Rieske proteins. Ferredoxins: ND, naphthalene dioxygenase from *P. putida* 9816 (67); BED1, benzene dioxygenase from *P. putida* ML2 (77); BED2, benzene dioxygenase from *P. putida* BE81 (59); TOD, toluene dioxygenase from *P. putida* F1 (127); CYPETC, Rieske iron-sulfur protein (PetC) from the cyanobacterium *Nostoc* PCC 7906; SCRIP1, Rieske iron-sulfur protein 1 from *Saccharomyces cerevisiae* (6); NCUCR, ubiquinol-cytochrome *c* reductase from *Neurospora crassa* (55).

and redox properties (Table 3). Evidently, they have features that differ from the plant and other bacterial [2Fe-2S] ferredoxins. These include the absence of the typical doublet peak in the 410- to 463-nm region of the absorption spectrum exhibited by other well-studied [2Fe-2S] ferredoxins (81). The molar absorbance at λ_{max} = 460 nm is only about 70% of the value for plant-type ferredoxins at λ_{max} = 415 nm (102), and is nearly equivalent to those for Rieske iron-sulfur proteins (33). The midpoint redox potentials of the ferredoxins of benzene (ferredoxin$_{BED}$) and toluene dioxygenase (ferredoxin$_{TOL}$) are −155 mV and −105 mV, respectively (39, 102). This is significantly more positive than spinach ferredoxin [−420 mV (104)], adrenodoxin [−270 mV (57)], or putidaredoxin [−239 mV (46)], but more negative than the Rieske clusters, which range from −140 to +350 mV (19, 65). Furthermore, the EPR spectra of reduced ferredoxin$_{BED}$ and ferredoxin$_{TOL}$ have average g-factors of 1.92 and 1.84, respectively. These may be compared with g_{av} = 1.96 for most plant-type ferredoxins (11), and g_{av} = 1.91 for the Rieske-type proteins (32, 48). These properties appear more similar to those of the Rieske-type iron-sulfur proteins (32, 33) than the plant-type [2Fe-2S] ferredoxins.

The Catalytic Terminal Oxygenase Component

The terminal oxygenase, also an iron-sulfur protein, is the catalytic component of the dioxygenase enzyme. For hydroxylation of the aromatic substrate, both O_2 and Fe^{2+} must be present. Thus, in addition to a substrate binding site, the terminal dioxygenase component also contains an iron-binding site and a Rieske-type [2Fe-2S] cluster (5, 39, 73).

The terminal dioxygenase components are large oligomeric proteins of M_r 150–200 kDa (Table 4). The majority of them have two dissimilar subunits, α and β of about 50 and 20 kDa, respectively. They are organized either as $\alpha_2\beta_2$ for benzene, toluene, and naphthalene dioxygenases (42, 93, 126) or $\alpha_3\beta_3$ for benzoate dioxygenase (122). The exceptions are the terminal dioxygenase components of 4-sulfobenzoate 3,4-dioxygenase (69), 4-chlorophenylacetate 3,4-dioxygenase (72), and phthalate dioxygenase (5), which comprise two, three, and four identical monomers, respectively. All the terminal dioxygenase components have [2Fe-2S] clusters of the Rieske-type with one [2Fe-2S] cluster per $\alpha\beta$ dimer or α monomer. For the terminal dioxygenase components with an $\alpha\beta$ dimeric configuration, research has indicated that the α subunit contains the [2Fe-2S] cluster [benzoate 1,2-dioxygenase (122)], while the β subunit has been implicated as the subunit involved with substrate recognition [toluate 1,2-dioxygenase (53)].

IRON CENTER OF THE TERMINAL OXYGENASE Several aromatic dioxygenases require Fe(II) for activity. The iron is presumed to bind to a specific site in the protein, where it may be oxidized to Fe(III). The iron-

Table 4 Properties of the oxygenase component of aromatic dioxygenases

Dioxygenase	Component	Prosthetic group	Absorption λ_{max} (nm)	EPR g_x, g_y, g_z	Redox potential (mV)	References
Benzene	A_1 (ISP_{BED})	2[2Fe-2S]	326, 450, 550[a]	1.754, 1.917, 2.018	−115	25, 38, 126
Toluene	ISP_{TOL}	2[2Fe-2S]	326, 450, 550[a]			100
Naphthalene	ISP_{NAP}	2[2Fe-2S]	334, 462, 566[a]			29
Pyrazon	A_1	[2Fe-2S]	445, 545[a]	1.79, 1.91, 2.02		93
Benzoate	Oxygenase	3[2Fe-2S]	325, 464, 565[a]			120, 122
Phthalate	Oxygenase	4[2Fe-2S]	325, 460, 560[a]	1.73, 1.91, 2.01		5
4-Chlorophenylacetate	A	3[2Fe-2S]	325, 458, 564			72
4-Sulfobenzoate	A	2[2Fe-2S]	327, 467, 560			69

[a] Shoulder.

binding site is the least well understood component, so any discussion of its structure and function will necessarily be speculative. A center capable of single-electron transfer is required for efficient activation of the O_2, which has a triplet ground state. Although all the terminal dioxygenases contain Rieske-type clusters, there is no precedent for a [2Fe-2S] cluster serving as an oxygen-binding site; the sulfide is prone to oxidative damage. Analogy with other types of oxygenases indicates that oxygen activation occurs at the iron site. Several classes of oxygenase involve an iron site without an NADH-linked reductase chain. An example is protocatechuate dioxygenase from *P. aeruginosa;* the structure of this molecule has been determined using X-ray crystallography (80). The protein ligands to the iron were found to be two tyrosines and two histidines. Spectroscopy experiments revealed that tyrosine is a ligand in other nonheme iron-containing dioxygenases, including 4-hydroxyphenylpyruvate dioxygenase (14). If the iron represents the site at which O_2 reacts, it is presumed to be close to the substrate-binding site.

Amino acid sequences of the terminal oxidases of benzene, toluene, benzoate, toluate, and naphthalene dioxygenases all contain, in addition to the characteristic Rieske sequence near the N terminus (Figure 4), two conserved histidines and two conserved tyrosines near the middle of the sequence (59, 67, 79, 127). This site represents a likely binding domain for the iron center. Interestingly, the iron-containing monooxygenases for alkanes (64) and xylene (103) also have a homologous region rich in histidines and tyrosines, which is dissimilar from those of the dioxygenases. The iron-binding site presumably dictates the type of oxygenation reaction that takes place.

One should be able to observe this reaction using EPR, though for some types of ligand field, the reaction may become too broad to be detected. No EPR signals due to high-spin Fe(III) have yet been reported for the aromatic dioxygenases. The comparable iron site in 4-methoxybenzoate monooxygenase has been examined using EPR and Mössbauer spectroscopy (12, 13, 109). In the oxidized protein, the iron center is expected to be high-spin Fe(III). A distribution of a complex series of EPR signals was around $g = 6.0$ and 4.3, corresponding to high-spin Fe(III) in a tetragonal and rhombic symmetry, respectively. The $g = 6.0$ signals shifted upon addition of substrates; the $g = 4.3$ did not. A comparison of enzyme reoxidized by oxygen with enzyme oxidized anaerobically demonstrated that these signals do not correspond to Fe(III)·O_2·substrate complexes.

The mechanism of the dioxygenase reaction remains to be elucidated. A proposal by Twilfer et al (110) envisaged the activation of oxygen at the iron center by successive electron transfers from the reductase:

$$\text{Fe (III)} \xrightarrow{1\,e^-} \text{Fe (II)} \xrightarrow{O_2} \text{Fe (II)} \cdot O_2 \rightarrow \text{Fe (III)} \cdot O_2^- \xrightarrow{e^-} \text{Fe (II)} \cdot O_2^- \rightarrow \text{Fe (III)} \cdot O_2^{2-}$$

Figure 4 Comparison of the amino acid homology of the ISP α subunits from the Class IIB benzene (*bedC1*) (59), Class III, naphthalene (*ndoB*) (67), and Class IB benzoate (*benA*) (79) dioxygenases. The asterisks indicate conserved amino acids.

followed by reaction of the peroxo complex with the substrate. Twilfer et al (110) obtained a series of nitrosyl analogs of the oxo-derivatives by using nitric oxide. Since NO is an odd-electron species, it can convert Fe(II), which is normally undetectable by EPR, to an EPR-detectable species. EPR signals were observed for high-spin ($S = 3/2$) Fe(II)·NO (or Fe(III)·NO^-) species, with g-factors $g_\perp = 4$, $g_{||} = 2$. The g-factors of signals changed upon binding of several substrates (110).

COORDINATION OF THE IRON-SULFUR CLUSTERS The [2Fe-2S] clusters of the Rieske proteins of electron-transfer chains, and of the aromatic dioxygenases, appear to have similar chemical structures, as judged by the similarities in amino-acid sequences and spectroscopic properties (Figure 3). On this assumption, the results of the Rieske-protein studies, such as that

from *Thermus thermophilus* (32), have been extrapolated to those of the dioxygenases.

The sequences for the Rieske iron-sulfur protein from various organisms have been determined by amino acid sequencing [beef heart (94)] or deduced from their DNA sequence [spinach cytochrome b_6-f complex (94), *Neurospora crassa* (55), *Saccharomyces cerevisiae* (6), *Rhodobacter capsulatus* (36), and *Paracoccus denitrificans* (68)]. Analysis of these amino acid sequences reveals that the cysteine residues are conserved in two regions (94). From a comparison of these conserved regions with those observed in the terminal oxygenase and the ferredoxin components of the dioxygenases, shown in Figure 3, the following consensus sequence emerged:

Cys-X-His–15 to 17 amino acids–Cys-X-X-His

(where X is any amino acid). Because all the above-mentioned proteins contain an iron-sulfur cluster that has Rieske-type properties, we propose that this consensus sequence is the motif involved in binding to the Rieske-type [2Fe-2S] cluster.

In the conserved regions of sequences of the Rieske proteins, each histidine residue is flanked by a single glycine residue either next to it or one residue away. Glycine residues occur in the turns of protein secondary structure (51), and the [2Fe-2S] cluster may be situated in a cleft of the protein. One of the two conserved regions in these Rieske proteins is found in a hydrophobic part of the protein and the other in a more amphipathic environment [hydrophobicity plots (94)].

Mössbauer spectra of the dioxygenase protein of benzene dioxygenase from *P. putida* ML2 (37) indicated the presence of [2Fe-2S] clusters similar to those observed in the plant-type ferredoxins. The main difference was the isomer shift of one of the iron sites, which was greater than in the ferredoxins. This effect is similar to that observed in Rieske-type proteins such as that from *Thermus thermophilus* (32). The Mössbauer parameters were compared with those of the monooxygenase ferredoxin putidaredoxin, which has a [2Fe-2S] cluster with all-sulfur ligation (78). In the reduced state, the Fe(III) site of the dioxygenase Fe-S clusters was similar to the corresponding ion in the ferredoxin, but the Fe(II) sites were different, as shown by the electric-field gradient and hyperfine tensors. This difference between the two types of protein might be explained by different distortions of the cluster geometry, or alternatively by their having different ligands. The latter interpretation considered it likely that the Fe(II) iron site had nonsulfur ligands, because in the Rieske cluster, this iron atom had a larger Mössbauer isomer shift than that in putidaredoxin (78).

Electron-spin relaxation processes are characteristic of the iron-sulfur clust-

ers. In EPR spectra, the relaxation rate affects the temperature range over which the spectrum can be determined; in Mössbauer spectra it determines the highest temperature at which hyperfine structure is observed. It enables the reduced [2Fe-2S] clusters to be distinguished, for example, from the more rapidly relaxing [4Fe-4S] clusters. The electron-spin relaxation rate of the [2Fe-2S] clusters in the dioxygenases and the Rieske proteins is slower than in plant-type ferredoxins, but faster than in hydroxylase ferredoxins such as putidaredoxin and adrenodoxin. Bertrand et al (10) interpreted such effects in terms of differences in geometry of the [2Fe-2S] cluster.

Cline et al (23), by using electron nuclear double resonance (ENDOR) and electron spin-echo envelope modulation (ESEEM) spectroscopy, observed hyperfine interactions in the [2Fe-2S] clusters in the respiratory Rieske iron-sulfur protein of *Thermus thermophilus* and in the phthalate dioxygenase of *Pseudomonas cepacia*. All of the spectra showed resonances attributed to protons that were weakly coupled to the iron-sulfur clusters. Similar proton interactions have been found in all iron-sulfur proteins. However, in addition, unusually strong hyperfine resonances were observed, which were assigned to the ^{14}N of two histidines.

In a recent series of measurements of the phthalate dioxygenase of *P. cepacia*, Gurbiel et al (48) established the nature of the nitrogen-containing ligands to the [2Fe-2S] Rieske-type cluster. Cells of a histidine auxotroph were grown on ^{15}N-labeled histidine and ^{14}N background (using natural-abundance NH_4^+ as nitrogen source), and on ^{14}N histidine in a ^{15}N background. In spectra recorded at Q-band microwave frequency (35 GHz), the ENDOR lines due to nitrogen were clearly distinguished from those due to protons. The pairs of nitrogen hyperfine lines were assigned as resulting from two nitrogens with similar coupling constants. All of the ENDOR lines assigned to nitrogen behaved as expected for ^{15}N (nuclear spin $I = 1/2$) in the ^{15}N-histidine protein, and for ^{14}N (nuclear spin $I = 1$) in the ^{14}N-histidine protein. These results demonstrate the presence of two histidines in the first coordination sphere of iron. Furthermore, specific ^{15}N labeling showed that the δ-nitrogens of the imidazole ring bind the iron (47). Based on these results, the following structure is proposed as a model of the Rieske iron-sulfur cluster:

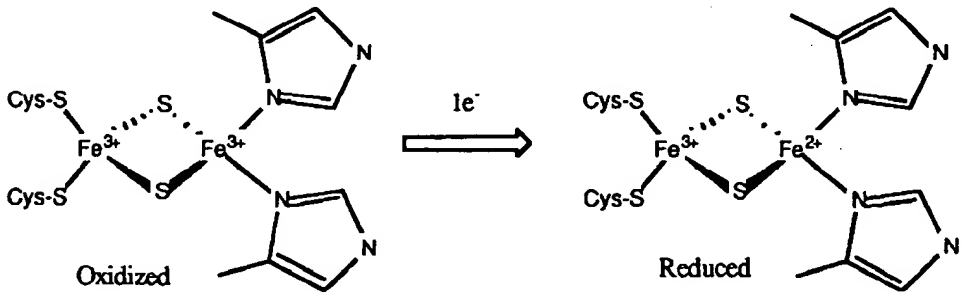

Kuila et al (66) determined the resonance Raman spectra of the Rieske protein of *T. thermophilus* and the phthalate dioxygenase of *P. cepacia*. Resonance Raman spectroscopy examines the vibrational modes of the chromophoric metal center. For the plant-type ferredoxin [2Fe-2S] cluster, the modes are as expected for a centrosymmetric cluster. For the dioxygenase cluster, the spectrum showed additional vibrational modes, indicating a major perturbation from centrosymmetry. The spectrum was analyzed in terms of the above model, with two sulfur and two nitrogen ligands in various relative positions. Of the three possible arrangements, the above, with both nitrogens on one iron atom, was considered to be the most likely.

X-ray absorption spectroscopy has been applied to the Rieske protein of heart mitochondria (84) and the terminal dioxygenase component of the phthalate dioxygenase of *P. cepacia* (107). In order to observe the Rieske cluster in the dioxygenase protein, without interference from the Fe center, the latter was eliminated by depletion of iron and replacement with cobalt or zinc. Extended X-ray absorption fine structure (EXAFS) spectra of an atom such as an iron site depend critically on distances of nearby atoms, particularly heavy atoms. They depend less on the number of atoms and the bond angles. Based on the above model, Tsang et al (107) estimated the following distances for the oxidized cluster: Fe-S (bridging), 0.22 nm; Fe-S (terminal), 0.231 nm; Fe-Fe, 0.268 nm. The Fe-Fe distance expanded slightly on reduction. Unfortunately, it was not possible to estimate the number or distances of any nitrogen ligands.

FACTORS INFLUENCING THE MIDPOINT REDOX POTENTIALS OF THE IRON-SULFUR CLUSTERS Apparently, two, or possibly three, classes of proteins contain Rieske-type [2Fe-2S] clusters. The first are the membrane-bound proteins involved in respiration and photosynthesis, which contain a single [2Fe-2S] cluster and are characterized by having an unusually high redox potential that varies with pH. The protein from *T. thermophilus* that has similar properties reportedly contains two [2Fe-2S] clusters per molecule (32) and might therefore represent another class of proteins; the sequence is not yet determined. The other group includes the NADH-dependent dioxygenase components and the 4-methoxybenzoate monooxygenase. By contrast, the negative redox potential of the [2Fe-2S] cluster in the dioxygenase components does not appear to be pH dependent (33, 66). Although the coordination environment is spectroscopically similar in all three classes of proteins, other differences must exist that modulate the properties of the iron-sulfur cluster in meeting the different functional needs.

The redox potentials of the [2Fe-2S] clusters in the aromatic dioxygenases are less negative, by 100–250 mV, than the ferredoxins of photosynthesis or P-450 systems, but not as positive as the Rieske clusters of respiratory chains. These differences should have a functional significance. In photosynthesis, a

strong reductant is required to reduce NADP, while in complexes of the bc_1 type, the Rieske clusters must be reducible by quinones. The dioxygenase systems apparently need not have as negative a potential as that in the P-450$_{CAM}$ system. This may be an advantage, as a higher-potential ferredoxin would be less likely to react with O_2 to generate superoxide.

Most iron-sulfur clusters are strong reducing agents. Their midpoint potentials are generally more negative than those of simple iron centers. This may be the consequence of the net negative charge on the clusters, which results from the charges on the cysteine ligands and bridging sulfides. However, in addition to the Rieske-type iron-sulfur proteins, other types of iron-sulfur clusters have less negative midpoint potentials, including the high-potential iron-sulfur proteins (HiPIPs), in which the cluster can take up a higher oxidation state with fewer electrons, and the [3Fe-4S] clusters. In addition, the midpoint potentials of iron-sulfur clusters of a particular type differ considerably depending on their protein environment (19).

The most important factors determining the midpoint potential are probably the electrostatic charge on the cluster and the polarity of the environment (see 76). Other more subtle factors include hydrogen bonds from the sulfides to polypeptide amides (1, 21) and the bond lengths and bond angles of the iron-sulfur cluster (81). The ligands to the Fe atoms are expected to play a major role (107). In the plant-type ferredoxins, the ligands to the [2Fe-2S] cluster are all cysteine sulfurs. The replacement of thiolate by carboxylate ligands for [4Fe-4S] clusters resulted in substantial positive shifts of the redox potential [100 mV per substituted ligand (60)]. Probably, substitutions of thiolate by nitrogen-containing residues will have a similar effect on the redox potential. The formal charge on a nitrogen ligand is 0, compared with -1 for a Cys^- ligand. The above structure would have a formal charge of 0 in the oxidized form compared to -2 for the classical $[2Fe\text{-}2S]^{2+}(CysS^-)_4$ structure. A single electron would therefore be more easily stabilized on the Rieske cluster (65). The electrostatic effect of charged amino acids around the clusters could also influence the midpoint potential. These might include histidines that are close to the cluster but not ligands to it. Notably, the lower-potential photosynthetic ferredoxins have no histidine residues in the vicinity of the cysteine residues. In this context, the surrounding amino acid residues of the conserved regions could be targets for substitution studies. Using site-directed mutagenesis, one can replace these residues systematically and examine the effects on the redox potential and its function in transferring electrons.

CONCLUDING REMARKS

The aromatic ring-hydroxylating dioxygenases and related oxygenases are built up of protein domains and redox centers. Several of these resemble other

electron-transfer systems such as those of respiration and photosynthesis. However, the aromatic dioxygenases show considerable diversity (Table 1) and appear to have multiple origins. The iron-sulfur flavoprotein might have evolved by gene fusion between the separate ferredoxin and flavoprotein (18), as found in the benzene dioxygenase. However, the iron-sulfur component of the flavoproteins is related to the plant-type ferredoxins (52), while the ferredoxin components are more closely related to the Rieske proteins (Figure 3). The diversity of the electron-transfer chains in the dioxygenases so far discovered indicates that further permutations of electron carriers will almost certainly be found in others.

ACKNOWLEDGMENTS

We thank Dr. D. P. Ballou for providing manuscripts prior to publication and Dr. A. Cooke for helpful discussions. The work described from this laboratory was supported by Shell Research Ltd. (JRM) and the Science and Engineering Research Council (RC).

Literature Cited

1. Adman, E. T. 1979. A comparison of the structures of electron transfer proteins. *Biochim. Biophys. Acta* 549:107–44
2. Axcell, B. C., Geary, P. J. 1975. Purification and some properties of a soluble benzene-oxidizing system from a strain of *Pseudomonas*. *Biochem. J.* 146:173–83
3. Batie, C. J., Ballou, D. P. 1990. Phthalate dioxygenase. *Methods Enzymol.* 188:61–70
4. Batie, C. J., Ballou, D. P., Correll, C. J. 1991. Phthalate dioxygenase reductase and related flavin-iron-sulfur containing electron transferases. In *Chemistry and Biochemistry of Flavoenzymes*, ed. F. Müller, pp. 544–54. Boca Raton: CRC Press
5. Batie, C. J., LaHaie, E., Ballou, D. P. 1987. Purification and characterization of phthalate oxygenase and phthalate oxygenase reductase from *Pseudomonas cepacia*. *J. Biol. Chem.* 262:1510–18
6. Beckmann, J. D., Ljungdahl, P. O., Lopez, J. L., Trumpower, B. L. 1987. Isolation and characterization of the nuclear gene encoding the Rieske iron-sulfur protein (RIP1) from *Saccharomyces cerevisiae*. *J. Biol. Chem.* 262:8901–9
7. Benen, J. A. E., Van Berkel, W. J. H., Van Dongen, W. M. A. M., Müller, F., De Kok, A. 1989. Molecular cloning and sequence determination of the *lpd* gene encoding lipoamide dehydrogenase from *Pseudomonas fluorescens*. *J. Gen. Microbiol.* 135:1787–97
8. Bernhardt, F.-H., Heyniann, E., Traylor, P. S. 1978. Chemical and spectral properties of putidamonooxin, the iron-containing and acid-labile-sulfur-containing monooxygenase from *Pseudomonas putida*. *Eur. J. Biochem.* 92:209–23
9. Bernhardt, F.-H., Pachowsky, H., Staudinger, H. 1975. A 4-Methoxybenzoate O-demethylase from *Pseudomonas putida*. A new type of monooxygenase. *Eur. J. Biochem.* 57:241–56
10. Bertrand, P., Gayda, J.-P., Fee, J. A., Kuila, D., Cammack, R. 1987. Comparison of the spin-lattice relaxation properties of the two classes of [2Fe-2S] clusters in proteins. *Biochim. Biophys. Acta* 916:24–28
11. Bertrand, P., Guigliarelli, B., Gayda, J. P., Beardwood, P., Gibson, J. 1985. A ligand-field model to describe a new class of 2Fe-2S clusters in proteins and their synthetic analogues. *Biochim. Biophys. Acta* 831:261–66
12. Bill, E., Bernhardt, F.-H., Trautwein, A. X. 1981. Mössbauer studies on the active Fe. . .[2Fe-2S] site of putidamonooxin, its electron transport and dioxygen activation mechanism. *Eur. J. Biochem.* 121:39–46
13. Bill, E., Bernhardt, F.-H., Trautwein, A. X., Winkler, H. 1985. Mössbauer investigation of the cofactor iron of puti-

damonooxin. *Eur. J. Biochem.* 147: 177–82
14. Bradley, F. C., Lindstedt, S., Lipscomb, J. D., Que, L., Roe, L., Rundgren, M. 1986. 4-Hydroxyphenylpyruvate dioxygenase is an iron tyrosinate protein. *J. Biol. Chem.* 261:11693–96
15. Brown, N. L., Ford, S. J., Pridmore, R. D., Fritzinger, D. C. 1983. Nucleotide sequence of a gene from the *Pseudomonas* transposon Tn*501* encoding mercuric reductase. *Biochemistry* 22:4089–95
16. Brunel, F., Davison, J. 1988. Cloning and sequencing of *Pseudomonas* genes encoding vanillate demethylase. *J. Bacteriol.* 171:4924–30
17. Bruschi, M., Guerlesquin, F. 1988. Structure, function and evolution of bacterial ferredoxins. *FEMS Microbiol. Rev.* 54:155–76
18. Cammack, R. 1983. Evolution and diversity in the iron-sulphur proteins. *Chem. Script.* 21:87–95
19. Cammack, R. 1984. Midpoint potentials of iron-sulphur proteins—a survey. In *Charge and Field Effects in Biosystems,* ed. M. J. Allen, P. N. R. Usherwood, pp. 41–51. Tunbridge Wells: Abacus
20. Cammack, R., Rao, K. K., Hall, D. O., Johnson, C. E. 1971. Mössbauer studies of adrenodoxin. The mechanism of electron transfer in a hydroxylase iron-sulphur protein. *Biochem. J.* 125:849–56
21. Carter, C. W., Jr. 1977. New stereochemical analogies between iron-sulfur electron transfer proteins. *J. Biol. Chem.* 252:7802–11
22. Clarke, P. H., Ornston, L. N. 1975. Metabolic pathways and regulation. In *Genetics and Biochemistry of* Pseudomonas, ed. P. H. Clarke, M. H. Richmond, pp. 191–261. London: Wiley
23. Cline, J. F., Hoffman, B. M., Mims, W. B., LaHaie, E., Ballou, D. P., Fee, J. A. 1985. Evidence for N coordination to Fe in the (2Fe-2S) clusters of Thermus Rieske protein and phthalate dioxygenase from *Pseudomonas. J. Biol. Chem.* 260:3251–54
24. Correll, C. C., Batie, C. J., Ballou, D. P., Ludwig, M. L. 1985. Crystallographic characterization of phthalate oxygenase reductase, an iron-sulphur flavoprotein from *Pseudomonas cepacia. J. Biol. Chem.* 260:14633–36
25. Crutcher, S. E., Geary, P. J. 1979. Properties of the iron-sulphur proteins of the benzene dioxygenase system from *Pseudomonas putida. Biochem. J.* 177:393–400
26. Dagley, S. 1986. Biochemistry of aromatic hydrocarbon degradation in pseudomonads. In *The Bacteria,* ed. J. R. Sokatch, 10:527–55. London: Academic
27. Dunham, W. R., Bearden, A. J., Salmeen, I. T., Palmer, G., Sands, R. H., et al. 1971. The two-iron ferredoxins in spinach, parsley, pig adrenal cortex, *Azotobacter vinelandii* and *Clostridium pasteurianum:* studies by magnetic field Mössbauer spectroscopy. *Biochim. Biophys. Acta* 253:134–41
28. Dus, K. M. 1984. Camphor hydroxylase of *Pseudomonas putida:* vestiges of sequence homology in cytochrome P-450_{CAM}, putidaredoxin, and related proteins. *Proc. Natl. Acad. Sci. USA* 81:1664–68
29. Ensley, B. D., Gibson, D. T. 1983. Naphthalene dioxygenase: purification and properties of a terminal oxygenase component. *J. Bacteriol.* 155:505–11
30. Ensley, B. D., Gibson, D. T., Laborde, A. L. 1982. Oxidation of naphthalene by a multicomponent enzyme system from *Pseudomonas* sp. strain NCIB 9816. *J. Bacteriol.* 149:948–54
31. Ensley, B. D., Haigler, B. E. 1990. Naphthalene dioxygenase from *Pseudomonas* NCIB 9816. *Methods Enzymol.* 188:46–52
32. Fee, J. A., Findling, K. L., Yoshida, T., Hille, R., Tarr, G. E., et al. 1984. Purification and characterization of the Rieske iron-sulfur protein from *Thermus thermophilus*. Evidence for a [2Fe-2S] cluster having non-cysteine ligands. *J. Biol. Chem.* 259:124–33
33. Fee, J. A., Kuila, D., Mather, M. W., Yoshida, T. 1986. Respiratory proteins from extremely thermophilic bacteria. *Biochim. Biophys. Acta* 853:153
34. Fox, B. C., Surerus, K. K., Munck, E., Lipscomb, J. D. 1988. Evidence for μ-oxo-bridged binuclear iron cluster in the hydroxylase component of methane monooxygenase. Mössbauer and EPR studies. *J. Biol. Chem.* 263:10553–56
35. Fukuyama, K., Hase, T., Matsumoto, S., Tsukihara, T., Katsube, Y., et al. 1980. Structure of *S. platensis* [2Fe-2S] ferredoxin and evolution of the chloroplast-type ferredoxins. *Nature* 286:522–24
36. Gabellini, N., Sebald, W. 1986. Nucleotide sequence and transcription of the *fbc* operon from *Rhodopseudomonas sphaeroides*. Evaluation of the deduced amino acid sequences of the FeS protein, cytochrome *b* and cytochrome c_1. Eur. J. Biochem. 154:569–79
37. Geary, P. J., Dickson, D. P. E. 1981. Mössbauer spectroscopic studies of the terminal dioxygenase from *Pseudomonas putida. Biochem. J.* 195:199–203

38. Geary, P. J., Mason, J. R., Joannou, C. L. 1990. Benzene dioxygenase from *Pseudomonas putida* (NCIB 12190). *Methods Enzymol.* 188:52–60
39. Geary, P. J., Saboowalla, F., Patil, D. S., Cammack, R. 1984. An investigation of the iron-sulphur proteins of benzene dioxygenase from *Pseudomonas putida* by electron-spin-resonance spectroscopy. *Biochem. J.* 217:667–73
40. Gibson, D. T., Cardini, G. E., Maseles, F. C., Kallio, R. E. 1970. Incorporation of oxygen-18 into benzene by *Pseudomonas putida*. *Biochemistry* 9:1631–35
41. Gibson, D. T., Koch, J. R., Kallio, R. E. 1968. Oxidative degradation of aromatic hydrocarbons by microorganisms. I. Enzymatic formation of catechol from benzene. *Biochemistry* 7:2653–62
42. Gibson, D. T., Subramanian, V. 1984. Microbial degradation of aromatic hydrocarbons. In *Microbial Degradation of Organic Compounds*, ed. D. T. Gibson, pp. 181–252. New York: Marcel Dekker
43. Gibson, D. T., Yeh, W.-K., Liu, T.-N., Subramanian, V. 1982. Toluene dioxygenase: a multicomponent enzyme system from *Pseudomonas putida*. In *Oxygenases and Oxygen Metabolism*, ed. M. Nozaki, S. Yamamoto, Y. Ishimura, M. J. Coon, L. Ernster, R. W. Estabrook, pp. 51–62. London: Academic
44. Gibson, J. F., Hall, D. O., Thornley, J. H. M., Whatley, F. R. 1966. The iron complex in spinach ferredoxin. *Proc. Natl. Acad. Sci. USA* 56:987–90
45. Greenfield, N. J., Wu, X. H., Jordan, F. 1989. Proton magnetic resonance spectra of adrenodoxin—features of the aromatic region. *Biochim. Biophys. Acta* 995:246–54
46. Gunsalus, I. C., Lipscomb, J. D. 1973. Structure and reactions of a microbial monooxygenase: the role of putidaredoxin. See Ref. 69a, pp. 151–71
47. Gurbiel, R. J., Ohnishi, T., Robertson, D. E., Daldal, F., Hoffman, B. M. 1991. Q-band ENDOR spectra of the Rieske protein from *Rhodobactor capsulatus* ubiquinol cytochrome-*c* oxidoreductase show 2 histidines coordinated to the [2Fe-2S] cluster. *Biochemistry* 30:11579–84
48. Gurbiel, R. J., Batie, C. J., Sivaraja, M., True, A. E., Fee, J. A., et al. 1989. Electron nuclear double resonance spectroscopy of N-15-enriched phthalate dioxygenase from *Pseudomonas cepacia* proves that 2 histidines are coordinated to the [2Fe-2S] Rieske-type clusters. *Biochemistry* 28:4861–71
49. Haigler, B. E., Gibson, D. T. 1990. Purification and properties of ferredoxin$_{NAP}$, a component of naphthalene dioxygenase from *Pseudomonas* sp. strain NCIB 9816. *J. Bacteriol.* 172:465–68
50. Haigler, B. E., Gibson, D. T. 1990. Purification and properties of NADH-ferredoxin$_{NAP}$ reductase, a component of naphthalene dioxygenase from *Pseudomonas* sp. strain NCIB-9816. *J. Bacteriol.* 172:457–64
51. Hanukoglu, I., Gutfinger, T. 1989. cDNA Sequence of adrenodoxin reductase—identification of NADP-binding sites in oxidoreductases. *Eur. J. Biochem.* 180:479–84
52. Harayama, S., Polissi, A., Rekik, M. 1991. Divergent evolution of chloroplast-type ferredoxins. *FEBS Lett.* 285:85–88
53. Harayama, S., Rekik, M., Timmis, K. N. 1986. Genetic analysis of a relaxed substrate specificity aromatic ring dioxygenase, toluate 1,2-dioxygenase, encoded by TOL plasmid pWWO of *Pseudomonas putida*. *Mol. Gen. Genet.* 202:226–34
54. Harayama, S., Timmis, K. N. 1989. Catabolism of aromatic hydrocarbons by *Pseudomonas*. In *Genetics of Bacterial Diversity*, ed. D. A. Hopwood, K. F. Chater, pp. 151–74. London: Academic
55. Harnisch, U., Weiss, H., Sebald, W. 1985. The primary structure of the iron-sulphur subunit of ubiquinol-cytochrome *c* reductase from *Neurospora*, determined by cDNA and gene sequencing. *Eur. J. Biochem.* 149:95–99
56. Howell, L. G., Spector, T., Massey, V. 1972. Purification and properties of p-hydroxybenzoate hydroxylase from *Pseudomonas fluorescens*. *J. Biol. Chem.* 247:4340–50
57. Huang, J. J., Kimura, T. 1973. Studies on adrenal steroid hydroxylases. Oxidation-reduction properties of adrenal iron-sulfur protein (adrenodoxin). *Biochemistry* 12:406–9
58. Hurt, E., Hauska, G. 1981. A cytochrome *f/b6* complex of five polypeptides with plastoquinol-plastocyanin-oxidoreductase activity from spinach chloroplasts. *Eur. J. Biochem.* 117:591–99
59. Irie, S., Doi, S., Yorifuji, T., Takagi, M., Yano, K. 1987. Nucleotide sequencing and characterization of the genes encoding benzene oxidation enzymes of *Pseudomonas putida*. *J. Bacteriol.* 169:5174–79
60. Johnson, R. W., Holm, R. H. 1978. Reaction chemistry of the iron-sulphur protein site analogues $[Fe4S4(SR)_4]^{2-}$. Sequential thiolate ligand substitution reactions with electrophiles. *J. Am. Chem. Soc.* 100:5338–44

61. Kamin, H., White-Stevens, R. H., Presswood, R. P. 1978. Salicylate hydroxylase. *Methods Enzymol.* 53:527–43
62. Karplus, P. A., Daniels, M. J., Herriott, J. R. 1991. Atomic structure of ferredoxin-NADP+ reductase—prototype for a structurally novel flavoenzyme family. *Science* 251:60–66
63. Koga, H., Yamaguchi, E., Matsunaga, K., Aramaki, H., Horiuchi, T. 1989. Cloning and nucleotide sequences of NADH-putidaredoxin reductase gene (Cama) and putidaredoxin gene (Camb) involved in cytochrome-P-450$_{CAM}$ hydroxylase of *Pseudomonas putida*. *J. Biochem.* 106:831–36
64. Kok, M., Oldenhuis, R., Van der Linden, M. P. G., Raatjes, P., Kingma, J., et al. 1989. The *Pseudomonas oleovorans* alkane hydroxylase gene. Sequence and expression. *J. Biol. Chem.* 264: 5435–41
65. Kuila, D., Fee, J. A. 1986. Evidence for a redox linked ionizable group associated with the [2Fe-2S] cluster of *Thermus* Rieske protein. *J. Biol. Chem.* 261:2768–71
66. Kuila, D., Fee, J. A., Schoonover, J. R., Woodruff, W. H., Batie, C. J., Ballou, D. P. 1987. Resonance Raman spectra of the [2Fe-2S] clusters of the Rieske protein from *Thermus* and phthalate dioxygenase. *J. Am. Chem. Soc.* 109:1559–61
67. Kurkela, S., Lehvaslaiho, H., Palva, E. T., Teeri, T. H. 1988. Cloning, nucleotide sequence and characterization of genes encoding naphthalene dioxygenase of *Pseudomonas putida* strain NCIB 9816. *Gene* 73:355–62
68. Kurowski, B., Ludwig, B. 1987. The genes of the *Paracoccus denitrificans* bc_1 complex. Nucleotide sequence and homologies between bacterial and mitochondrial subunits. *J. Biol. Chem.* 262:13805–11
69. Locher, H. H., Leisinger, T., Cook, A. M. 1991. 4-Sulphobenzoate 3,4-dioxygenase. Purification and properties of a desulphonative two-component enzyme system from *Comamonas testosteroni* T-2. *Biochem. J.* 274:833–42
69a. Lovenberg, A., ed. 1973. *Iron-Sulphur Proteins*. New York: Academic
70. Lund, J., Woodland, M. P., Dalton, H. 1985. Electron transfer reactions in the soluble methane monooxygenase of *Methylcoccus capsulatus*. *Eur. J. Biochem.* 147:297–305
71. Markus, A., Klages, U., Krauss, S., Lingens, F. 1984. Oxidation and dehalogenation of 4-chlorophenylacetate by a two-component enzyme system from *Pseudomonas* sp. strain CBS3. *J. Bacteriol.* 160:618–21
72. Markus, A., Krekel, D., Lingens, F. 1986. Purification and some properties of component A of the 4-chlorophenylacetate 3,4-dioxygenase from *Pseudomonas* species strain CBS. *J. Biol. Chem.* 261:12883–88
73. Mason, J. R. 1988. Oxygenase catalyzed hydroxylation of aromatic compounds: simple chemistry by complex enzymes. *Int. Ind. Biotechnol.* 8:19–24
74. Meyer, J., Bruschi, M., Bonicel, J. J., Bovier-Lapierre, G. E. 1986. Amino acid sequence of [2Fe-2S] ferredoxin from *Clostridium pasteurianum*. *Biochemistry* 25:6054–61
75. Moodie, F. D. L., Woodland, M. P., Mason, J. R. 1990. The reductase component of the chromosomally encoded benzoate dioxygenase from *Pseudomonas putida* C-1 is immunologically homologous with a product of the plasmid encoded *xylD* gene (toluate dioxygenase) from *Pseudomonas putida* mt-2. *FEMS Microbiol. Lett.* 71:163–67
76. Moore, G. D., Pettigrew, G. W., Rogers, N. K. 1986. Factors influencing redox potentials of electron transfer proteins. *Proc. Natl. Acad. Sci. USA* 83:4998–5000
77. Morrice, M., Geary, P., Cammack, R., Harris, A., Beg, F., Aitken, A. 1988. Primary structure of protein B from *Pseudomonas putida*, a member of a new class of 2Fe-2S ferredoxins. *FEBS Lett.* 231:336–40
78. Münck, E., Debrunner, P. G., Tsibris, J. C. M., Gunsalus, I. C. 1972. Mössbauer parameters of putidaredoxin and its selenium analogue. *Biochemistry* 11:855–63
79. Neidle, E. L., Hartnett, C., Ornston, L. N., Bairoch, A., Rekik, M., Harayama, S. 1991. Nucleotide sequences of the *Acinetobacter calcoaceticus benABC* genes for benzoate 1,2-dioxygenase reveal evolutionary relationships among multicomponent oxygenases. *J. Bacteriol.* 173:5385–95
80. Ohlendorf, D. H., Lipscomb, J. D., Weber, P. C. 1988. Structure and assembly of protocatechuate 3, 4-dioxygenase. *Nature* 336:403
81. Palmer, G. 1973. Current insights into the active center of spinach ferredoxin and other iron-sulphur proteins. See Ref. 69a, pp. 285–325
82. Pochapsky, T. C., Ye, [illegible] M. 1991. ^{1}H identification of a β-she [illegible]ucture and description of folding to [illegible]y in putidaredoxin. *Biochemistry* [illegible]850–56
83. Poulos, T. L., Finzel, B. C., Gunsalus,

I. C., Wagner, G. C., Kraut, J. 1986. The 2.6 Å crystal structure of *Pseudomonas putida* cytochrome P-450. *J. Biol. Chem.* 260:16122–30
84. Powers, L., Schagger, H., VonJagow, G., Smith, J., Chance, B., Ohnishi, T. 1989. EXAFS studies of the isolated bovine heart Rieske $[2Fe\text{-}2S]^{1+(1+,\ 2+)}$ cluster. *Biochim. Biophys. Acta* 975:293–98
85. Prince, R. C., George, G. N., Savas, J. C., Cramer, S. P., Patel, R. N. 1988. Spectroscopic properties of the hydroxylase of methane monooxygenase. *Biochim. Biophys. Acta* 952:220–29
86. Prince, R. C., Patel, R. N. 1986. Redox properties of the flavoprotein of methane monooxygenase. *FEBS Lett.* 203:127–31
87. Raju, S. G., Kamath, A. V., Vaidyanathan, C. S. 1988. Purification and properties of 4-hydroxyphenylacetic acid 3-hydroxylase from *Pseudomonas putida*. *Biochem. Biophys. Res. Commun.* 154:537–43
88. Riedel, A., Rutherford, A. W., Hauska, G., Muller, A., Nitschke, W. 1991. Chloroplast Rieske protein—EPR study on its spectral characteristics, relaxation and orientation properties. *J. Biol. Chem.* 266:17838–44
89. Rieske, J. S., Hansen, R. E., Zaugg, W. S. 1964. Studies on the electron transfer system. LVIII. Properties of a new oxidation-reduction component of the respiratory chain as studied by electron paramagnetic resonance spectroscopy. *J. Biol. Chem.* 239:3017–21
90. Romeo, C., Moriwaki, N., Yasunobu, K. T., Gunsalus, I. C., Koga, H. 1987. Identification of the coding region for the putidaredoxin reductase gene from the plasmid of *Pseudomonas putida*. *J. Protein Chem.* 6:253–61
91. Roome, P. W. J., Philley, J. C., Peterson, J. A. 1983. Purification and properties of putidaredoxin reductase. *J. Biol. Chem.* 258:2593–98
92. Rypniewski, W. R., Breiter, D. R., Benning, M. M., Wesenberg, C., Oh, B. H., et al. 1991. Crystallization and structure determination to 2.5-Å resolution of the oxidized [Fe2-S2] ferredoxin isolated from *Anabaena*-7120. *Biochemistry* 30:4126–31
93. Sauber, K., Frohner, C., Rosenberg, G., Eberspacher, J., Lingens, F. 1977. Purification and properties of pyrazon dioxygenase from pyrazon-degrading bacteria. *Eur. J. Biochem.* 74:89–97
94. Schagger, H., Borchart, U., Machleidt, W., Link, T. A., Von Jagow, G. 1987. Isolation and amino acid sequence of the "Rieske" iron sulfur protein of beef heart ubiquinol: cytochrome *c* reductase. *FEBS Lett.* 219:161–68
95. Schweizer, D., Markus, A., Seez, M., Ruf, H. H., Lingens, F. 1987. Purification and some properties of component B of the 4-chlorophenylacetate 3,4-dioxygenase from *Pseudomonas* species strain CBS3. *J. Biol. Chem.* 262:9340–46
96. Scrutton, N. S., Berry, A., Perham, R. N. 1990. Redesign of the coenzyme specificity of a dehydrogenase by protein engineering. *Nature* 343:38–43
97. Stainthorpe, A. C., Lees, V., Salmond, G. P. C., Dalton, H., Murrell, J. C. 1990. The methane monooxygenase gene cluster of *Methylococcus capsulatus* (Bath). *Gene* 91:27–34
98. Stayton, P. S., Poulos, T. L., Sligar, S. G. 1989. Putidaredoxin competitively inhibits cytochrome b_5–cytochrome-P-450_{CAM} association—a proposed molecular model for a cytochrome-P-450_{CAM} electron-transfer complex. *Biochemistry* 28:8201–5
99. Stephens, P. E., Lewis, H. M., Darlison, M. G., Guest, J. R. 1983. Nucleotide sequence of the lipoamide dehydrogenase gene of *Escherichia coli* K12. *Eur. J. Biochem.* 135:519–27
100. Subramanian, V., Liu, T.-N., Yeh, W. K., Gibson, D. T. 1979. Toluene dioxygenase: purification of an iron-sulphur protein by affinity chromatography. *Biochem. Biophys. Res. Commun.* 91:1131–39
101. Subramanian, V., Liu, T.-N., Yeh, W. K., Narro, M., Gibson, D. T. 1981. Purification and properties of NADH-ferredoxin$_{TOL}$ reductase. A component of toluene dioxygenase from *Pseudomonas putida*. *J. Biol. Chem.* 256:2723–30
102. Subramanian, V., Liu, T.-N., Yeh, W. K., Serdar, C. M., Wackett, L. P., Gibson, D. T. 1985. Purification and properties of ferredoxin$_{TOL}$. A component of toluene dioxygenase from *Pseudomonas putida* F1. *J. Biol. Chem.* 260:2355–63
103. Suzuki, M., Hayakawa, T., Shaw, J. P., Rekik, M., Harayama, S. 1991. Primary structure of xylene monooxygenase: similarities to and differences from the alkane hydroxylation system. *J. Bacteriol.* 173:1690–95
104. Tagawa, K., Arnon, D. I. 1968. Oxidation-reduction potentials and stoichiometry of electron transfer in ferredoxins. *Biochim. Biophys. Acta* 153: 602–13
105. Tan, H.-M., Mason, J. R. 1990. Cloning and expression of the plasmid-encoded benzene dioxygenase genes

from *Pseudomonas putida* ML2. *FEMS Microbiol. Lett.* 72:259–64
106. Trumpower, B. L. 1990. Cytochrome bc_1 complexes of microorganisms. *Microb. Rev* 54:101–29
107. Tsang, H. T., Batic, C. J., Ballou, D. P., Penner-Hahn, J. E. 1989. X-ray absorption spectroscopy of the [2Fe-2S] Rieske cluster in *Pseudomonas cepacia* phthalate dioxygenase—determination of core dimensions and iron ligation. *Biochemistry* 28:7233–40
107a. Tsibris, J. C. M., Tsai, R. L., Gunsalus, I. C., Orme-Johnson, W. H., Hansen, R. E., Beinert, H. 1968. The number of iron atoms in the paramagnetic centre ($g = 1.94$) of reduced putidaredoxin, a nonheme iron protein. *Proc. Natl. Acad. Sci. USA* 59:959–65
108. Tsukihara, T., Fukuyama, K., Mizushima, M., Harioka, T., Kusunoki, M., et al. 1990. Structure of the [2Fe-2S] Ferredoxin-I from the blue-green alga *Aphanothece sacrum* at 2.2 Å resolution. *J. Mol. Biol.* 216:399–410
109. Twilfer, H., Bernhardt, F.-H., Gersonde, K. 1981. An electron-spin-resonance study on the redox-active centers of the 4-methoxybenzoate monooxygenase from *Pseudomonas putida*. *Eur. J. Biochem.* 119:595–602
110. Twilfer, H., Bernhardt, F. H., Gersonde, K. 1985. Dioxygen-activating iron center in putidamonooxin. Electron spin resonance investigation of the nitrosylated putidamonooxin. *Eur. J. Biochem.* 147:171–76
111. Wackett, L. P. 1990. Toluene dioxygenase from *Pseudamonas putida* F1. *Methods Enzymol.* 188:39–46
112. Wackett, L. P., Kwart, L. D., Gibson, D. T. 1988. Benzylic monooxygenation catalyzed by toluene dioxygenase from *Pseudomonas putida*. *Biochemistry* 27: 1360–67
113. Weijer, W. J., Hofsteenge, J., Vereijken, J. M., Jekel, P. A., Beintema, J. J. 1982. Primary structure of p-hydroxybenzoate hydroxylase from *Pseudomonas fluorescens*. *Biochim. Biophys. Acta* 704:385–88
114. Wende, P., Bernhardt, F.-H., Pfleger, K. 1989 Substrate-modulated reactions of putidamonooxin—the nature of the active oxygen species formed and its reaction mechanism. *Eur. J. Biochem.* 181:189–97
115. Wende, P., Pfleger, K., Bernhardt, F.-H. 1982. Dioxygen activation by putidamonooxin: substrate-modulated reaction of activated dioxygen. *Biochem. Biophys. Res. Commun.* 104:527–32
116. Westphal, A. H., DeKok, A. 1988. Lipoamide dehydrogenase from *Azotobacter vinelandii;* molecular cloning, organization and sequence analysis of the gene. *Eur. J. Biochem.* 172:299–305
117. Wierenga, R. K., Maeyer, M. C. H., Hol, W. G. J. 1985. Interaction of pyrophosphate moieties with α-helixes in dinucleotide binding proteins. *Biochemistry* 24:1346–57
118. Woodland, M. P., Patil, D. S., Cammack, R., Dalton, H. 1986. ESR studies of protein A of the soluble methane moooxygenase from *Methylococcus capsulatus* (Bath). *Biochim. Biophys. Acta* 873:237–42
119. Yamaguchi, M., Fujisawa, H. 1978. Characterization of NADH-cytochrome *c* reductase, a component of benzoate 1,2-dioxygenase system from *Pseudomonas arvilla* C-1. *J. Biol. Chem.* 253:8848–53
120. Yamaguchi, M., Fujisawa, H. 1980. Purification and characterization of an oxygenase component in benzoate 1,2-dioxygenase system from *Pseudomonas arvilla* C-1. *J. Biol. Chem* 255:5058–63
121. Yamaguchi, M., Fujisawa, H. 1981. Reconstitution of iron-sulfur cluster of NADH-cytochrome *c* reductase, a component of benzoate 1,2-dioxygenase system from *Pseudomonas arvilla* C-1. *J. Biol. Chem.* 256:6783–87
122. Yamaguchi, M., Fujisawa, H. 1982. Subunit structure of oxygenase component in benzoate 1,2-dioxygenase system from *Pseudomonas arvilla* C-1. *J. Biol. Chem.* 257:12497–12502
123. Yamaguchi, M., Yamauchi, T., Fujisawa, H. 1975. Studies on mechanism of double hydroxylation. I. Evidence for participation of NADH-cytochrome *c* reductase in the reaction of benzoate 1,2-dioxygenase (benzoate hydroxylase). *Biochem. Biophys. Res. Commun.* 67: 264–71
124. Deleted in proof
125. Yasunobu, K. T., Tanaka, M. 1973. The types, distribution in nature, structure-function, and evolutionary data of the iron-sulphur proteins. See Ref. 69a, pp. 27–130
126. Zamanian, M., Mason, J. R. 1987. Benzene dioxygenase in *Pseudomonas putida*. Subunit composition and immunocross-reactivity with other aromatic dioxygenases. *Biochem. J.* 244:611–16
127. Zylstra, G. J., Gibson, D. T. 1989. Toluene degradation by *Pseudomonas putida*-F1—nucleotide sequence of the *todCIC2BADE* genes and their expression in *Escherichia coli*. *J. Biol. Chem.* 264:14940–46

Structure–function Analysis of the Bacterial Aromatic Ring-hydroxylating Dioxygenases

Clive S. Butler* and Jeremy R. Mason

Division of Life Sciences, King's College London, Campden Hill Road, London W8 7AH, UK

**Present address: School of Biological Sciences, Molecular and Microbiology Sector, University of East Anglia, Norwich NR4 7TJ, UK*

1. INTRODUCTION

Soil microorganisms, particularly bacteria of the genus *Pseudomonas*, are able to metabolize an enormous range of natural and synthetic organic compounds, and are important agents in the degradation and recycling of organic material (Gibson, 1988). The initial step in the aerobic microbial biodegradation of aromatic

ADVANCES IN MICROBIAL PHYSIOLOGY VOL 38
ISBN 0-12-027738-7

compounds is usually the introduction of two hydroxyl groups into the benzene ring, forming *cis*-dihydrodiols or *cis*-diol carboxylic acids. This reaction prepares the aromatic compound for further fission and catabolism. The enzymes that catalyse the insertion of molecular oxygen into aromatic substrates are called oxygenases (Hayaishi, 1962).

Oxygenases have generated a great deal of interest as they possess the ability to carry out stereo- and regio-specific reactions under mild conditions (Ziffer *et al.*, 1977; Lee et al., 1995). This has led to their use as biocatalysts for the synthesis of chemicals, which are notoriously difficult to produce by conventional chemical methods. Examples of such compounds include *cis*-glycols (Dalton, 1986) and inositol-related compounds (Ley *et al.*, 1987). Other potentially useful biotransformations are reviewed by Sheldrake (1992) and Hudlicky *et al.* (1994). In addition, developments in environmental biotechnology have resulted in biodegradation becoming a useful strategy for the removal of hazardous aromatic compounds from soil and ground water (Fetzner and Lingens, 1994).

In order to utilize the full potential of oxygenase enzymes, it is important to understand the molecular structure of the proteins. In particular, their manipulation, to effect increased substrate specificity and enhance specific activity, is dependent on an understanding of the environments of the redox centres and substrate binding-site.

2. BACTERIAL OXYGENASES

The importance of oxygenases in physiological processes can be appreciated when one considers the chemistry of dioxygen. It is generally understood that, while the reaction of the resonance-stabilized benzene ring with oxygen is thermodynamically favoured, there are significant kinetic barriers inherent in these processes. Because molecular oxygen has a triplet electronic ground state, any adiabatic process involving electron transfer from a stable, closed shell (singlet) organic species to dioxygen results initially in the formation of a triplet diradical product. In enzyme-catalysed reactions, this is accomplished by dioxygen reacting with either the unpaired *d* electrons of a transition metal ion complex or with a stable organic free radical, such as a flavin semiquinone. The resulting activated oxygen species (peroxides, hydroxyl radicals, superoxide anion, singlet oxygen) are highly reactive and, if allowed to gain access to a cell, would result in considerable oxidative damage. Thus, in addition to activation of dioxygen, oxygenase enzymes are also able to constrain the active oxygen species and direct it towards the hydroxylation of the aromatic substrate. The active sites of such enzymes have evolved to channel the free-radical reaction and yield a specific product, rather than the mixture of products, which would result if reactions of this kind were attempted

in solution (Halliwell and Gutteridge, 1984). Transition metals, such as iron, serve as catalytic centres in numerous oxygenases; some utilize non-haem Fe(II) or Fe(III) (Feig and Lippard, 1994), whereas others are haem enzymes (cytochrome P-450; Raag and Poulos, 1989). In some cases other transition metals are used to bind dioxygen. The tetrahydrobiopterin-dependent phenylalanine hydroxylase from *Chromobacterium violaceum* has been shown to utilize copper (CuII) instead of iron for enzymatic activity (Pember *et al.*, 1989) and 3,4-dihydroxyphenylacetate 2,3-dioxygenase has been reported to be a manganese-containing enzyme (Que *et al.*, 1981).

Oxygenases may be classified into two groups, the monooxygenases, which incorporate one atom of oxygen into one molecule of substrate and the dioxygenases, which incorporate both atoms of dioxygen into the substrate (Hayaishi, 1962). This general definition fails to account, however, for isopenicillin N synthase, a dioxygenase that catalyses the oxidative ring closure reactions of δ-(L-α-aminoadipoyl)-L-cysteinyl-D-valine (ACV) to form isopenicillin N, the precursor to all other penicillins (Pang *et al.*, 1984). This reaction results in the complete four-electron reduction of a single equivalent of dioxygen to form two equivalents of H_2O (Chen *et al.*, 1989). Monooxygenase-catalysed reactions result in the unincorporated oxygen atom being reduced to water. Thus, these enzymes function as part oxygenase and part oxidase and, as a consequence, are termed mixed-function oxidases (Mason, 1988). It is, however, not always possible to distinguish between a dioxygenase and monooxygenase by activity alone. For example, both toluene and naphthalene dioxygenases can catalyse monooxygenase reactions as in the oxidation of indene and indan to 1-indenol and 1-indanol, respectively (Wackett *et al.*, 1988; Brand *et al.*, 1992) or desaturation reactions (Gibson et al., 1995). Toluene dioxygenase has also been reported to catalyse the monohydroxylation of phenols to the corresponding catechols (Spain *et al.*, 1989) and the stereospecific oxidation of aryl alkyl sulphides to sulphoxides (Lee *et al.*, 1995). Conversely, 4-methoxy benzoate monooxygenase has been shown to dihydroxylate the vinylic side chain of 4-methoxystyrene (Wende *et al.*, 1982). In addition, enzymes such as the 2-oxo-1,2-dihydroquinoline 8-monooxygenase have not been demonstrated to have any dihydroxylation activity, although their structure places them clearly with the aromatic ring-hydroxylating non-haem iron dioxygenases (Rosche *et al.*, 1995).

The dioxygenases are a large group of enzymes that have been divided into distinct groups, owing to the different reactions that they catalyse. The enzymes are involved in the oxidation of aromatic compounds to produce dihydroxy non-aromatic intermediates, catalysing the cleavage of the aromatic nucleus or oxidative ring-closure reactions. The first two of these separate groups are termed the ring-hydroxylating dioxygenases and the ring-fission dioxygenases. The remainder of this chapter will focus on the ring-hydroxylating dioxygenases, referring to ring-cleavage dioxygenases and other related systems only where appropriate (see Harayama *et al.*, 1992, for a detailed review of oxygenases).

3. STRUCTURE OF RING-HYDROXYLATING DIOXYGENASES

The most extensively studied ring-hydroxylating dioxygenase enzyme systems have been isolated from *Pseudomonas* species. Gibson and co-workers (1968, 1970) were the first to show that a dioxygenase system of *Pseudomonas putida* oxidized benzene to generate *cis*-1,2-dihydroxy-cyclohexa-3,5-diene (*cis*-benzene dihydrodiol). Several other ring-hydroxylating dioxygenases have since been isolated and characterized from other strains of *Pseudomonas*: pyrazon dioxygenase (Sauber *et al.*, 1977); naphthalene dioxygenase (Ensley *et al.*, 1982; Takizawa *et al.*, 1994; Yang *et al.*, 1994); toluene dioxygenase (Subramanian *et al.*, 1979, 1981, 1985); benzoate 1,2-dioxygenase (Yamaguchi and Fujisawa, 1978, 1980, 1982); phthalate dioxygenase (Batie *et al.*, 1987); 4-chlorophenylacetate 3,4-dioxygenase (Markus *et al.*, 1986); 2-halobenzoate 1,2-dioxygenase (Fetzner *et al.*, 1992); *ortho*-halobenzoate 1,2-dioxygenase (Romanov and Hausinger, 1994; Haak et al., 1995); benzene dioxygenase (Axcell and Geary, 1975; Irie *et al.*, 1987); biphenyl dioxygenase (Haddock *et al.*, 1993; Erickson and Mondello, 1993); and 2-nitrotoluene 2,3-dioxygenase (An *et al.*, 1994). Ring-hydroxylating dioxygenases have also been isolated from *Acinetobacter* (benzoate 1,2-dioxygenase, Neidle *et al.*, 1991), *Comamonas* (4-sulphobenzoate 3,4-dioxygenase, Locher *et al.*, 1991; terephthalate 1,2-dioxygenase, Schläfli *et al.*, 1994; biphenyl dioxygenase, Hurtubise *et al.*, 1995; naphthalene dioxygenase, Goyal and Zylstra, 1996), *Alcaligenes* (chlorobenzoate 3,4-dioxygenase, Nakatsu and Wyndham, 1993; Nakatsu *et al.*, 1995), *Sphingomonas* (dibenzofuran 4,4a-dioxygenase, Bünz and Cook, 1993) and *Rhodococcus* (phthalate dioxygenase, Suemori et al., 1993; biphenyl dioxygenase, Wang et al., 1995). All the enzymes are non-haem iron dioxygenases, which oxidize the aromatic substrates to give *cis*-dihydrodiols or *cis*-diol carboxylic acids, although in some cases these products probably dehydrogenate spontaneously to give the corresponding catechol (Locher *et al.*, 1991; Romanov and Hausinger, 1994; Haak *et al.*, 1995). In addition to molecular oxygen, these enzymes have been shown to have requirements for cofactors, NADH or NADPH, and in the majority of cases, iron (reviewed by Mason and Cammack, 1992).

All of the ring-hydroxylating dioxygenases are soluble, multi-component enzymatic systems, comprising two or three separate proteins. A typical arrangement consists of a short electron-transport chain composed of an iron–sulphur flavoprotein, or a flavoprotein and an iron–sulphur ferredoxin, which transfer electrons to a catalytic terminal oxygenase (Fig. 1). The subunit composition of the ring-hydroxylating dioxygenases differs considerably (Fig. 2). If the reductase component contains a [2Fe–2S] cluster, the system tends to lack the ferredoxin component. However, an exception to this is the naphthalene dioxygenase (Ensley *et al.*, 1982), where both the reductase and the ferredoxin are present, and both contain a [2Fe–2S] cluster. Variation is also encountered in the number and size of

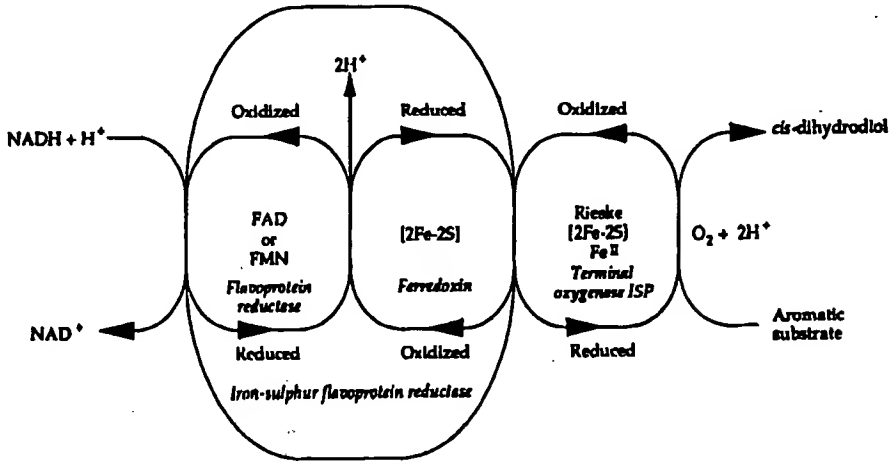

Figure 1 Biochemical organization of the multi-component ring-hydroxylating dioxygenases. A flavoprotein reductase accepts electrons from NADH and transfers them via an iron–sulphur cluster or a ferredoxin to a terminal oxygenase, which is a large iron–sulphur protein. The reduced terminal oxygenase catalyses the oxidation of aromatic substrates to *cis*-dihydroxy products.

the subunits of both the terminal oxygenase and the reductase components. These subunit variations have led to the classification of the three groups of dioxygenases by Batie and co-workers (1992) as Class I, Class II and Class III (Table 1). However, with the purification and characterization of numerous dioxygenases, it has become clear that this classification based on the enzyme as a whole may be inappropriate, since the individual components exist separately in the cell and in some cases the electron transfer components of one enzyme may complement those of another. This would suggest that each component may be classified better as an enzyme in its own right with a separate EC number.

4. ELECTRON TRANSPORT SYSTEM

4.1. The Reductase Component

The reductase component is the first component in the electron-transfer chain of dioxygenases. It acts as an oxidoreductase, catalysing the transfer of electrons from NADH to a second redox component. The majority of reductases studied use

Table 1 Multi-component hydroxylating dioxygenases.

Class	Enzyme system (reference)	Reductase M_r	Reductase Prosthetic group(s)	Ferredoxin M_r	Ferredoxin Prosthetic group(s)	Oxygenase Structure (M_r)	Oxygenase Prosthetic group(s)
IA	Phthalate dioxygenase (1,2)	34 000	FMN [2Fe–2S]	None		$\alpha(48\,000)_4$	4[2Fe–2S]$_R$, 4Fe
IA	4-Chlorophenylacetate 3,4-dioxygenase (3,4)	35 000	FMN [2Fe–2S]	None		$\alpha(46\,000)_3$	3[2Fe–2S]
IA	4-Sulphobenzoate 3,4-dioxygenase (5)	36 000	FMN [2Fe–2S]	None		$\alpha(50\,000)_2$	2[2Fe-2S]$_R$, 2Fe
IA	Chlorobenzoate 3,4-dioxygenase (6)	42 000	nd	None		$\alpha(51\,000)_n$	nd
IB	2-Halobenzoate 1,2-dioxygenase (7)	37 500	FAD [2Fe–2S]	None		$\alpha(52\,000)_3$ $\beta(20\,000)_3$	3[2Fe–2S], 3Fe
IB	Benzoate dioxygenase (8–11)	37 500	FAD [2Fe–2S]	None		$\alpha(50\,000)_3$ $\beta(20\,000)_3$	3[2Fe–2S], 3Fe
IB	2-oxo-1,2-dihydroquinoline 8-monooxygenase (12)	38 000	FAD [2Fe–2S]	None		$\alpha(55\,000)_6$	6[2Fe–2S]$_R$, ?Fe

Table 1 *continued*

Class	Enzyme system (reference)	Reductase M_r	Reductase Prosthetic group(s)	Ferredoxin M_r	Ferredoxin Prosthetic group(s)	Oxygenase Structure (M_r)	Oxygenase Prosthetic group(s)
IIA	Pyrazon dioxygenase (13)	67 000	FAD	12 000	[2Fe–2S]	180 000	[2Fe–2S]
IIA	Dibenzofuran 4,4a-dioxygenase (14)	44 000	FAD	12 000	[2Fe–2S]	$\alpha(45\,000)_2$ $\beta(23\,000)_2$	2[2Fe–2S], 2Fe
IIB	Benzene 1,2-dioxygenase (15–21)	87 168[a] (α2)	FAD	11 939[a]	[2Fe–2S]$_R$	$\alpha(51\,105^a)_2$ $\beta(22\,252^a)_2$	2[2Fe–2S]$_R$, 2Fe
IIB	Toluene 2,3-dioxygenase (22–26)	42 942[a]	FAD	11 900[a]	[2Fe–2S]$_R$	$\alpha(50\,930^a)_2$ $\beta(22\,013^a)_2$	2[2Fe–2S]$_R$, 2Fe
IIB	Biphenyl dioxygenase (27–31)	42 970[a]	FAD	11 981[a]	[2Fe–2S]$_R$	$\alpha(51\,513^a)_2$ $\beta(22\,085^a)_2$	2[2Fe–2S]$_R$, 2Fe
III	Naphthalene dioxygenase (32–36)	35 552[a]	FAD [2Fe–2S]	11 767[a]	[2Fe–2S]$_R$	$\alpha(49\,597^a)_2$ $\beta(23\,038^a)_2$	2[2Fe–2S]$_R$, 2Fe

R indicates a Rieske-type [2Fe–2S] cluster; nd, not determined; M_r observed from SDS-PAGE or [a]deduced from amino-acid sequence.

References: 1, Batie *et al.*, 1987; 2, Batie and Ballou, 1990; 3, Schweizer *et al.*, 1987; 4, Markus *et al.*, 1986; 5, Locher *et al.*, 1991; 6, Nakatsu and Wyndham, 1993; 7, Fetzner *et al.*, 1992; 8, Yamaguchi and Fujisawa, 1978; 9, Yamaguchi and Fujisawa, 1980; 10, Yamaguchi and Fujisawa, 1982; 11, Moodie *et al.*, 1990; 12, Rosche *et al.*, 1995; 13, Sauber *et al.*, 1977; 14, Bunz and Cook, 1993; 15, Axcell and Geary, 1975; 16, Geary *et al.*, 1990; 17, Zamanian and Mason, 1987; 18, Geary *et al.*, 1984; 19, Tan and Mason, 1990; 20, Tan *et al.*, 1993; 21, Crutcher and Geary, 1979; 22, Zylstra and Gibson, 1989; 23, Wackett, 1990; 24, Zylstra *et al.*, 1988; 25, Subramanian *et al.*, 1981; 26, Subramanian *et al.*, 1985; 27, Furukawa *et al.*, 1993; 28, Mondello, 1989; 29, Erickson and Mondello, 1992; 30, Gibson *et al.*, 1993; 31, Taira *et al.*, 1992; 32, Haigler and Gibson, 1990a; 33, Haigler and Gibson, 1990b; 34, Ensley *et al.*, 1982; 35, Ensley and Haigler, 1990; 36, Suen and Gibson, 1993.

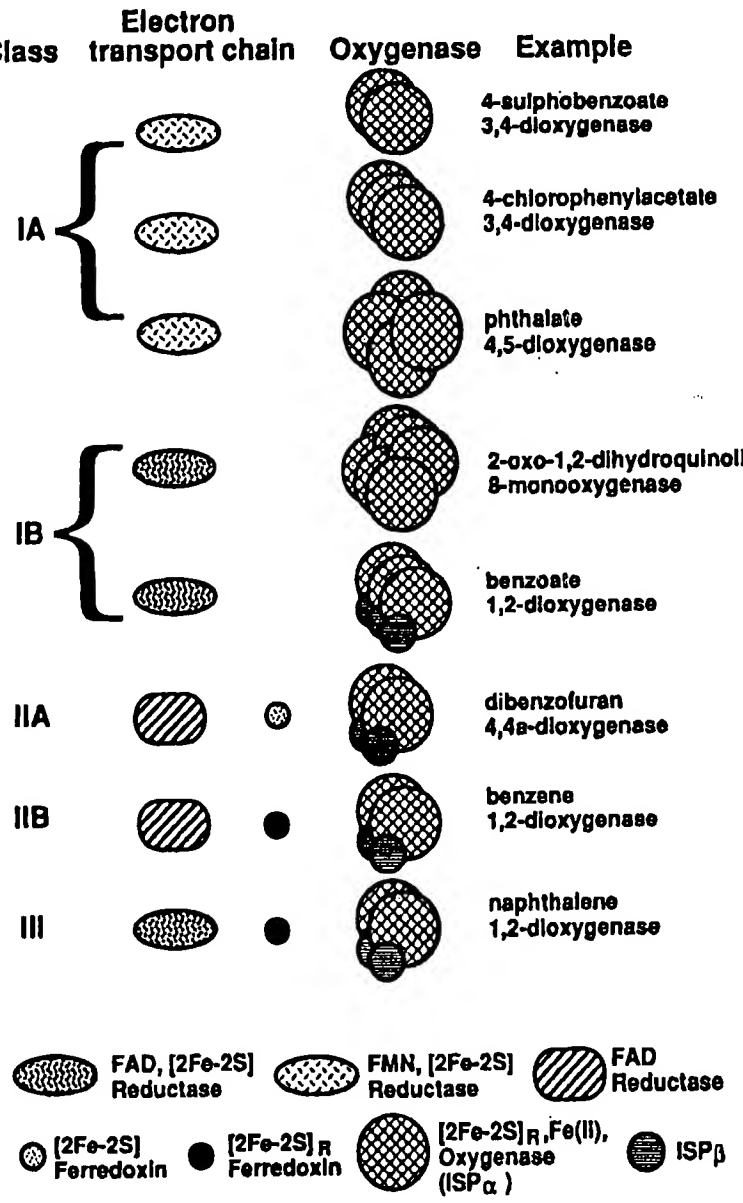

Figure 2 Schematic diagram to show the subunit composition of hydroxylating bacterial dioxygenases.

NADH as the preferred reductant. Benzene and toluene dioxygenase are specific for NADH (Axcell and Geary, 1975; Subramanian *et al.*, 1981), whereas NADPH served as an electron donor for naphthalene dioxygenase, but its activity was 43% of that observed with NADH (Ensley *et al.*, 1982). In contrast, the 2-nitrotoluene 2,3-dioxygenase has been demonstrated to be fully active in the presence of either NADH or NADPH (An *et al.*, 1994). The stereospecificity of hydride removal from NADH during catalysis by the reductases has been examined by Cook and co-workers (Schläfli *et al.*, 1995). Dioxygenases classified as members of Classes IA, IB and III were shown to be pro-R specific, whereas the reductases of the Class II enzymes dibenzofuran dioxygenase (Class IIA) and benzene dioxygenase (Class IIB) were demonstrated to be pro-S specific (Table 2).

The active site of the oxygenase component contains a single electron acceptor in the form of a [2Fe–2S] cluster. Since NADH can transfer both of its electrons simultaneously only as a hydride, the reductase is required to mediate this transition. Thus the reductases contain flavin, either as FMN or FAD. Flavins are distinctive among biological coenzymes in that they can accept two electrons, as hydrides from NADH, and transfer these electrons one at a time via the semiquinone redox state to other electron-transfer components.

All the Class I dioxygenases are two-component systems that have a reductase component with a [2Fe–2S] cluster. This class is subdivided into IA and IB, depending on whether they contain FMN or FAD, respectively. These reductase components have a relative molecular mass (M_r) ranging from 34 kDa for phthalate dioxygenase (Batie *et al.*, 1987) to 42 kDa for chlorobenzoate 3,4-dioxygenase (Nakatsu and Wyndham, 1993) and are all monomers. The properties of these iron–sulphur flavoproteins are listed in Table 2. As these flavoproteins contain a [2Fe–2S] cluster, the absorption spectra of the oxidized proteins show absorption maxima at ~340 nm and ~460 nm. The most detailed analysis has been carried out on the phthalate dioxygenase reductase (Batie *et al.*, 1992; Gassner *et al.*, 1995). The recently determined structure (Batie *et al.*, 1992; Correll *et al.*, 1992) shows the protein to be comprised of three domains. The FMN domain is at the N-terminus of the chain, and the [2Fe–2S] domain is at the C-terminus. The domains are arranged to bring the FMN and [2Fe–2S] prosthetic groups together near the centre of the molecule, with the flavin adjoining the binding site for the pyridine nucleotide. The [2Fe–2S] domain includes a four-stranded mixed β-sheet and two helices in a fold that resembles the [2Fe–2S] ferredoxin from *Anabaena* (Batie *et al.*, 1992). The amino-acid sequence of the iron–sulphur flavoprotein of benzoate dioxygenase (Neidle *et al.*, 1991) shows some homology with the plant-type ferredoxins. EPR spectra of the reduced reductases from phthalate, 4-chlorophenylacetate and benzoate dioxygenases show typical features of plant-type [2Fe–2S] clusters, together with a signal around g = 2.004 from the flavosemiquinone radical (Batie *et al.*, 1987; Schweizer *et al.*, 1987; Altier *et al.*, 1993); thus it appears that the iron–sulphur clusters of the Class I dioxygenases are of the plant type (see Section 6). These iron–sulphur flavoproteins are also capable of transferring

Table 2 Properties of the reductase component of aromatic dioxygenases.

Dioxygenase (reference)	Component	Prosthetic group(s)	Absorption (λ_{max}) (nm)	EPR (g_x, g_y, g_z)	Stereo-specificity[b]
Phthalate (1,2)	Reductase	FMN [2Fe–2S]	330, 420, 462, 495[a], 530[a]	1.900, 1.949, 2.008, 2.041	pro-R
4-Chlorophenyl-acetate (3)	B	FMN [2Fe–2S]	336, 394, 458	1.90, 1.94, 2.004, 2.03	pro-R
4-Sulphobenzoate (4)	B	FMN [2Fe–2S]	~330, ~400, 465	nd	nd
2-Halobenzoate (5)	B	FAD [2Fe–2S]	272, 343, 457	nd	pro-R
Benzoate (6)	Reductase	FAD [2Fe–2S]	273, 340, 402, 467	1.88, 1.95, 2.04	nd
Pyrazon (7)	A2	FAD	450, 475	ND	nd
Dibenzofuran (8)	A_n	FAD	nd	ND	pro-S
Benzene (9)	Reductase$_{BED}$	FAD	385, 425, 455	ND	pro-S
Toluene (10)	Reductase$_{TOL}$	FAD	372, 488, 475	ND	nd
Naphthalene (11)	Reductase$_{NAP}$	FAD [2Fe–2S]	278, 340, 420, 460, 540[a]	ND	pro-R

[a] Shoulder.
[b] Data taken from Schläfli *et al.* (1995).
nd, not determined; ND, not detected.
References: 1, Batie *et al.*, 1987; 2, Correll *et al.*, 1992; 3, Schweizer *et al.*, 1987; 4 Locher *et al.*, 1991; 5, Fetzner *et al.*, 1992; 6, Yamaguchi and Fujisawa, 1978; 7, Sauber *et al.*, 1977; 8, Bünz and Cook, 1993; 9, Geary *et al.*, 1990; 10, Subramanian *et al.*, 1981; 11, Haigler and Gibson, 1990a.

electrons directly from NADH to an artificial electron acceptor. Thus, the reductase components of benzoate, phthalate, 4-chlorophenylacetate and 2-halobenzoate dioxygenases can reduce cytochrome *c* directly in the presence NADH (Yamaguchi and Fujisawa, 1978; Batie *et al.*, 1987; Schweizer *et al.*, 1987; Fetzner *et al.*, 1992). Interestingly, studies on the 4-sulphobenzoate 3,4-dioxygenase have identified two possible reductase components (B and C), both capable of transferring electrons to the terminal oxygenase. However, owing to lower activity with component C, component B is regarded as the authentic electron donor (Locher *et al.*, 1991).

Classes II and III contain the three-component dioxygenases. Their reductases contain FAD, which has been reported to be readily lost during purification (Mason and Cammack, 1992). The Class II flavoproteins consist of a single polypeptide with an M_r ranging from 42.9 kDa for toluene dioxygenase (Zylstra and Gibson, 1989) to 67 kDa for pyrazon dioxygenase (Sauber *et al.*, 1977). All are monomeric except for the reductase of benzene dioxygenase, which is a dimer (Geary *et al.*, 1990). This class is subdivided into groups A and B. However, they vary only in the structure of the ferredoxin and terminal oxygenase components. The properties of these reductases are listed in Table 2. As no detailed structures are known for this group of reductases, the probable cofactor binding sites in the reductase proteins can only be inferred from their amino-acid sequences and comparison with other flavoproteins. When the amino-acid sequence of the reductase of benzene dioxygenase (Tan *et al.*, 1993), toluene dioxygenase (Zylstra and Gibson, 1989) and biphenyl dioxygenase (Kikuchi *et al.*, 1994) are compared with flavin-containing putidaredoxin reductase, which performs an analogous function in the cytochrome P-450-dependent camphor hydroxylase (Koga *et al.*, 1989) or other NADH-dependent flavoproteins like dihydrolipoamide dehydrogenase, it is clear that two highly conserved regions are located at the N terminus and the middle region. Both are centred around a βαβ-fold, with the consensus sequence:

Gly-Xaa-Gly-Xaa$_2$-Gly-Xaa$_3$-Ala-Xaa$_6$-Gly

(where Xaa is any amino acid and the subscript represents the number of amino-acid residues).

The N-terminus and middle conserved regions are predicted to bind the ADP moiety of FAD and NAD$^+$, respectively. Tan and co-workers (Tan *et al.*, 1993) have identified a third conserved region that is located at the C-terminus of the benzene dioxygenase reductase and forms a β-sheet (aa 265–275) with the consensus sequence of Thr-Xaa$_6$-Ala-Xaa-Gly-Asp. This conserved region is predicted to bind the O-3 group of the ribityl chain of the flavin moiety of FAD (Wierenga *et al.*, 1986; Eggink *et al.*, 1990).

Like the Class I enzyme 4-sulphobenzoate 3,4-dioxygenase, dibenzofuran 4,4a-dioxygenase has been shown to possess two reductases (A1 and A2). The two reductases, though physically similar to each other, were shown to have very different N-termini [reductase A1: Xaa-Gln-Tyr-(Asp or Gly)-Val-Leu-(Ile or Ala)-Val-Gly-Ala-Leu; reductase A2: Met-Arg-Ser-Ala-Asp-Val-Ile-Val-(Arg

or Ala or Gly)], both reductases could complement dioxygenase activity (Bünz and Cook, 1993).

The Class III enzyme naphthalene dioxygenase also consists of three components. Similar to those found in Class I, the reductase component is an iron–sulphur flavoprotein that can catalyse the reduction of cytochrome *c*. The absorption spectrum is also similar to the spectra of the iron–sulphur flavoproteins, with absorption maxima at 278, 340, 420 and 460 nm, and a broad shoulder at 540 nm (Haigler and Gibson, 1990a) (Table 2). Despite the presence of the reductase [2Fe–2S] cluster, this enzyme still requires a ferredoxin in order to transfer electrons to the terminal oxygenase. The reductase has a M_r of 36.3 kDa (Haigler and Gibson, 1990a).

4.2. The ferredoxin component

The ferredoxins are one-electron acceptors, transferring electrons from the reductase to the terminal oxygenase and are found only in ring-hydroxylating dioxygenases in Classes II and III. They are small acidic proteins with an M_r of approximately 12 kDa as determined by sequence analysis, but appear larger when observed by SDS-PAGE (Geary *et al.*, 1990). Each contains 2 gram-atoms of iron and acid-labile sulphide per mole in the form of a [2Fe–2S] cluster. In addition to transferring electrons from the flavoprotein to the terminal oxygenase, the ferredoxin can catalyse a flavoprotein-dependent reduction of other electron acceptors, such as cytochrome *c* (Axcell and Geary, 1975; Subramanian *et al.*, 1985). Studies on the toluene dioxygenase by Gibson and co-workers have shown that analogous electron-transfer proteins, such as spinach ferredoxin, ferredoxin from *Clostridium pasteurianum*, putidaredoxin and adrenodoxin cannot replace ferredoxin_{TOL} in either cytochrome *c* reduction or toluene oxidation (Subramanian *et al.*, 1985). Similarly, ferredoxin_{TOL} could not substitute for ferredoxin_{NAP} in the naphthalene dioxygenase (Haigler and Gibson, 1990b). However, ferredoxin_{BED} could substitute for ferredoxin_{TOL}, maintaining a functional toluene dioxygenase (Tan, 1991) and ferredoxin_{NAP} could replace ferredoxin_{2NT}*, maintaining a functional 2-nitrotoluene 2,3-dioxygenase (An *et al.*, 1994). Thus, ferredoxins are apparently rather specific for the dioxygenase system (class) in which they act. This specificity is reflected in the primary structure of the proteins.

The ferredoxins of different ring-hydroxylating dioxygenases possess similarities in both size and amino-acid sequence. Ferredoxin_{NAP} comprises 104 amino acids, whilst both ferredoxin_{BED} and ferredoxin_{TOL} have 107 amino acids (Mason and Cammack, 1992). Sequence analysis has revealed that ferredoxin_{BED} and ferredoxin_{TOL} are almost identical, showing 99% homology in amino-acid sequence and 75% homology in the nucleic-acid sequence. In contrast, ferredoxin_{NAP} has only 34% homology with the amino-acid sequence of ferredoxin_{BED} (Kurkela *et al.*, 1988).

*2NT is suggested to be a Class III dioxygenase similar to NAP (An *et al.*, 1994).

The EPR spectrum of the ferredoxin of the pyrazon dioxygenase resembles that of the P-450 monooxygenases, such as putidaredoxin with *g*-factors of 2.02 and 1.94 (Sauber *et al.*, 1977) (Table 3), indicating the presence of a typical plant-type ferredoxin [2Fe–2S] cluster (see Section 6). In addition, the absorption spectrum displays maxima at 411 nm and 453 nm, typical of the doublet peak in the 410–463 nm region of the absorption spectrum exhibited by other well-studied [2Fe–2S] ferredoxins (Bruschi and Guerlesquin, 1988). Similarly, the ferredoxin of dibenzofuran 4,4a-dioxygenase displays absorption maxima at 410 nm and 463 nm (Bünz and Cook, 1993), typical of the plant-type ferredoxins. In contrast, the ferredoxins of the benzene dioxygenase and toluene dioxygenase have [2Fe–2S] clusters with unusual spectroscopic and redox properties (Table 3). Ferredoxin_{TOL} displays an extinction coefficient at 460 nm that is approximately 70% of the value for the plant-type ferredoxins at 415 nm (Subramanian *et al.*, 1985), and is nearly equivalent to that of the Rieske iron–sulphur proteins (Fee *et al.*, 1986). The midpoint redox potentials of the ferredoxins of benzene dioxygenase (Geary *et al.*, 1984) and toluene dioxygenase (Subramanian *et al.*, 1985) are −155 mV and −109 mV, respectively. These are significantly higher than those of spinach ferredoxin (−420 mV), adrenodoxin (−274 mV) or putidaredoxin (−235 mV), but are closer to those of the more negative members of the Rieske iron–sulphur proteins (−140 to +350 mV) (Cammack, 1984). The resemblance to the Rieske iron–sulphur proteins is also evident from the EPR spectra of ferredoxin_{TOL} and ferredoxin_{BED}. The average *g*-factors of 1.92 and 1.84 for ferredoxin_{BED} and ferredoxin_{TOL},

Table 3 Properties of the ferredoxin component of aromatic dioxygenases.

Dioxygenase (reference)	Component	Prosthetic group	Absorption (λ_{max}) (nm)	EPR (g_x, g_y, g_z)	Redox potential (mV)
Pyrazon (1)	B	[2Fe–2S]	411, 453	1.94, 2.02	nd
Dibenzofuran (2)	B	[2Fe–2S]	410, 463	nd	nd
Benzene (3,4)	Ferredoxin_{BED}	[2Fe–2S]	280, 320, 456	1.834, 1.890, 2.026	−155
Toluene (5)	Ferredoxin_{TOL}	[2Fe–2S]	277, 327, 460	1.81, 1.86, 2.01	−109
ortho-Halobenzoate (6)	C	[2Fe–2S]	278, 321, 455	1.82, 1.905, 2.02	nd
Naphthalene (7)	Ferredoxin_{NAP}	[2Fe–2S]	280, 325, 460	nd	nd

nd, not determined.

References: 1, Sauber *et al.*, 1977; 2, Bünz and Cook, 1993; 3, Geary *et al.*, 1990; 4, Tan *et al.*, 1994; 5, Subramanian *et al.*, 1985; 6, Romanov and Hausinger, 1994; 7, Haigler and Gibson, 1990b.

respectively, are more similar to those of the Rieske clusters ($g_{av} = 1.91$) than those of the plant-type ferredoxins ($g_{av} = 1.96$). Examination of the amino-acid sequence of the ferredoxins of benzene dioxygenase (Morrice *et al.*, 1988; Tan *et al.*, 1993), toluene dioxygenase (Zylstra and Gibson, 1989), naphthalene dioxygenase (Haigler and Gibson, 1990b) and biphenyl dioxygenase (Erickson and Mondello, 1992) show that two cysteine and two histidine residues are highly conserved. This suggests that the dioxygenase ferredoxin [2Fe–2S] clusters are of the Rieske-type (see Section 6 for the coordination of iron–sulphur clusters).

Recently, site-directed mutagenesis studies were performed in our laboratory on the ferredoxin of benzene dioxygenase, in which the two conserved histidine residues were mutated to cysteines, both separately and in combination. All of these mutations prevented the insertion of the cluster *in vivo*. These data suggest that ferredoxin$_{BED}$ and ferredoxin$_{TOL}$, and by analogy ferredoxin$_{BPH}$ and ferredoxin$_{NAP}$, are of the Rieske type.

5. THE CATALYTIC TERMINAL OXYGENASE COMPONENT

The catalytic terminal oxygenase component is also an iron–sulphur protein. In addition to the [2Fe–2S] cluster, it contains the substrate binding site and a mononuclear non-haem iron; all are essential for the hydroxylation of an aromatic substrate. This component shows considerable variation in subunit configuration. Class IA oxygenases consist of a large (M_r = 46–51 kDa) subunit arranged as a dimer, trimer or tetramer for 4-sulphobenzoate 3,4-dioxygenase (Locher *et al.*, 1991), 4-chlorophenylacetate 3,4-dioxygenase (Schweizer *et al.*, 1987) and phthalate dioxygenase (Batie *et al.*, 1987), respectively. Most of the Class IB oxygenases examined to date consist of a larger (α) and a smaller (M_r ~20 kDa) (β) subunit in the configuration of $\alpha_3\beta_3$. The exception to this is the 2-oxo-1,2-dihydroquinoline 8-monoxygenase that consists of six identical α subunits (Rosche *et al.*, 1995). The Class II and III oxygenases characterized also consist of both α and β subunits but in the configuration $\alpha_2\beta_2$, e.g. benzene dioxygenase (Zamanian and Mason, 1987), or $\alpha_3\beta_3$, e.g. biphenyl dioxygenase (Haddock and Gibson, 1995). All the terminal oxygenases have one [2Fe–2S] cluster per αβ-dimer or α monomer (Mason and Cammack, 1992). Studies on benzoate 1,2-dioxygenase (Yamaguchi and Fujisawa, 1982) and naphthalene dioxygenase (Suen and Gibson, 1993, 1994), have demonstrated that the [2Fe–2S] cluster is situated in the α subunit. Whilst an early study on the toluate 1,2-dioxygenase reported the β subunit to be involved in substrate recognition (Harayama *et al.*, 1986), more recent studies on the biphenyl dioxygenase have shown that the α subunit is the major component involved in controlling substrate specificity (Furukawa *et al.*, 1993; Erickson and Mondello, 1993; Tan and Cheong, 1994).

Furukawa and co-workers have also demonstrated that substitution of the biphenyl dioxygenase α subunit with the toluene dioxygenase α subunit resulted in the formation of a functional multicomponent dioxygenase, capable of the oxidation of toluene preferentially (Furukawa *et al.*, 1993). Similarly, the replacement of the iron–sulphur protein (ISP) α subunit of biphenyl dioxygenase with the ISP α subunit of benzene dioxygenase resulted in a hybrid enzyme with greater activity towards benzene than biphenyl (Tan and Cheong, 1994). Site-directed mutagenesis has been employed to determine the region of the biphenyl dioxygenase α subunit involved in controlling substrate specificity. Comparison of the substrate specificity of two biphenyl dioxygenases from *Pseudomonas* sp. LB400 and *Pseudomonas pseudoalcaligenes* KF707 revealed that the former had a much broader substrate range than the latter; however, the enzyme from KF707 had a greater capacity to hydroxylate congeners chlorinated in the double *para* position. The replacement of four residues of the LB400 dioxygenase subunit with the corresponding residues from the KF707 enzyme produced an engineered dioxygenase with the broad substrate range of LB400 combined with better activity towards the 4,4′ congeners (Erickson and Mondello, 1993). The region responsible for this altered activity is shown underlined in Fig. 3.

The location of the mononuclear non-haem iron binding site in the Class II and III dioxygenases is still unknown. However, the location of the iron binding site in the α subunits of these dioxygenases would be consistent with the finding that the oxygenase components of phthalate dioxygenase (Batie *et al.*, 1987) and 4-chlorophenylacetate dioxygenase (Markus *et al.*, 1986), with structures α_4 and α_3, respectively, require Fe(II) for oxygenase activity. The function of the β subunit of these Class II and III dioxygenases is unknown. The deduced amino-acid sequences of the β subunits of benzene, toluene, naphthalene and benzoate/toluate oxygenases show a low but significant degree of homology to each other with nine conserved amino acids present in each subunit. Five of the nine conserved residues are charged amino acids. It is possible that the charged amino acids play a role in the association between the subunits of the oxygenase component (Neidle *et al.*, 1991). Recently, we have carried out covalent cross-linking experiments on the components of benzene dioxygenase using 1-ethyl-3-(3-dimethyl aminopropyl carbodiimide). Results indicated that the β subunit may play a role in ferredoxin "docking" with the ISP$_{BED}$ (unpublished results).

6. COORDINATION OF THE IRON–SULPHUR CLUSTERS

All ferredoxin and oxygenase components of ring-hydroxylating dioxygenases contain an iron–sulphur cluster. These specific groups are responsible for the transfer of electrons through the redox chain by the reduction and oxidation of iron. Several different types of [2Fe–2S] clusters are known in proteins (Cammack,

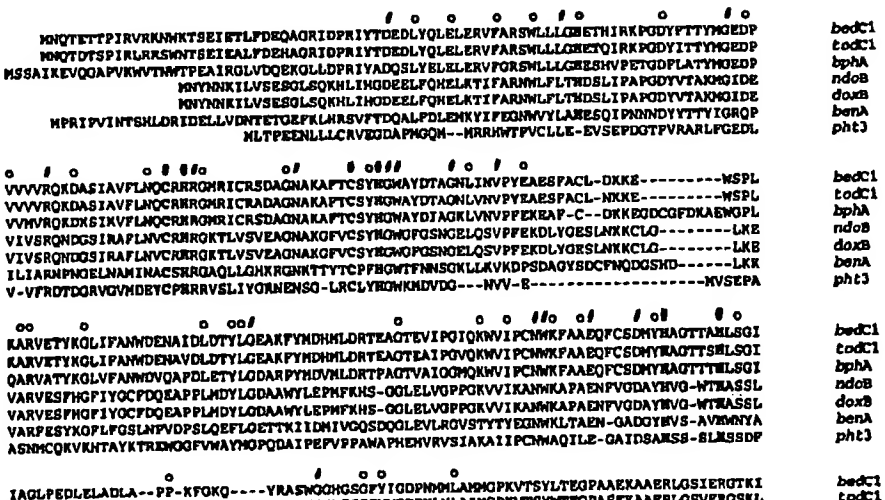

Figure 3 Alignment of the predicted amino-acid sequence from the ISP α subunits of all known classes of dioxygenases. Sequence identities are as follows: *bed*C1, benzene dioxygenase; *tod*C1, toluene dioxygenase; *bph*A, biphenyl dioxygenase; *ndo*B, naphthalene dioxygenase; *dox*B, dibenzothiophene dioxygenase; *ben*A, benzoate dioxygenase; and *pht*3, phthalate dioxygenase. Symbols indicate amino acids conserved in six (o) or seven (#) sequences, respectively. The five conserved histidines and the two conserved cysteines are highlighted. The sequence underlined indicates amino acids shown to influence the substrate specificity of biphenyl dioxygenase.

1992). The largest class consists of the plant-type ferredoxin [2Fe–2S] clusters, of which the first known example was the spinach ferredoxin, found in chloroplast membranes (Gibson *et al.*, 1966). Similar proteins have since been found in cyanobacteria (Fukuyama *et al.*, 1980). These ferredoxins are small hydrophilic proteins containing one [2Fe–2S] cluster per molecule, serving as one-electron carriers (Bruschi and Guerlesquin, 1988). The [2Fe–2S] clusters contain two atoms

of iron, bridged by two labile sulphide atoms, and are coordinated to the protein by four sulphide ligands contributed by four cysteine residues. Upon reduction, one of the iron ions becomes high-spin Fe(II), and the net spin of the coupled Fe(III) and Fe(II) ions is $S = 1/2$. Thus, these [2Fe–2S] clusters give an EPR signal in the reduced state, when measured at low temperatures, which has an average g-factor of less than two (Gibson *et al.*, 1966). The plant-type ferredoxins give an EPR signal with a g_{av} of approximately 1.96. This type of iron–sulphur cluster is also associated with the reductase components of the Class I and III dioxygenases.

The second class of proteins that contain [2Fe–2S] clusters is the Rieske proteins. These proteins are named after J. S. Rieske, who described a protein isolated from the cytochrome bc_1 complex of mitochondria (Rieske *et al.*, 1964). Similar proteins have been shown to be associated with the b_6f complex of the thylakoid membrane of chloroplasts (Riedel *et al.*, 1991) and the plasma membrane of some aerobic and photosynthetic bacteria (Fee *et al.*, 1984; Gabellini and Sebald, 1986). Examination of various physical properties has been used to distinguish between the plant-type and Rieske-type iron–sulphur clusters. The Rieske proteins have red-shifted visible spectra with maximum absorption about two-thirds of those of the plant-type ferredoxins and relatively more positive midpoint redox potentials. The EPR spectra of the reduced proteins have a lower g_{av} value, around 1.91, with a characteristic sharp derivative peak at $g \approx 2.02$ and a broad trough around $g \approx 1.80$ (Trumpower, 1990). The terminal oxygenase component of many of the ring-hydroxylating dioxygenases have both visible and EPR spectra typical of the Rieske-type iron–sulphur clusters (Table 4); as a consequence, the results of the Rieske protein studies have been compared to those of the dioxygenases (Mason and Cammack, 1992).

6.1. Evidence that the dioxygenase ISP [2Fe–2S] clusters are of the Rieske type with imidazole ligands

Many spectroscopic techniques, including electron nuclear double resonance (ENDOR), electron spin-echo envelope modulation (ESEEM), Mössbauer, resonance Raman and X-ray absorption have been used to distinguish between plant-type and Rieske [2Fe–2S] clusters. The use of these spectroscopic techniques, amino-acid sequence analysis and the application of site-directed mutagenesis has provided evidence that two of the ligands to the dioxygenase and Rieske iron–sulphur clusters are the nitrogens of histidine residues.

6.2 Spectroscopic evidence

Mössbauer spectroscopy, which depends upon the chemical state and environment of the atoms containing the ^{57}Fe Mössbauer nuclei, yields characteristic spectra for

Table 4 Properties of the oxygenase component of aromatic dioxygenases.

Dioxygenase (reference)	Component	Prosthetic group(s)	Absorption (λ_{max}) (nm)	EPR (g_x, g_y, g_z)	Redox potential (mV)
Phthalate (1)	Oxygenase	4[2Fe–2S]	325, 460, 560[a]	1.73, 1.91, 2.01	nd
4-Chlorophenyl-acetate(2)	A	3[2Fe–2S]	325, 458, 564	nd	nd
4-Sulphobenzoate (3)	A	2[2Fe–2S]	327, 467, 560	nd	nd
2-Halobenzoate (4)	A	3[2Fe–2S]	279, 325, 462, 550[a]	nd	nd
Benzoate (5,6)	Oxygenase	3[2Fe–2S] 3Fe	325, 464, 565[a]	1.77, 1.91, 2.01, 1.83, 4.2, 7.5	nd
Pyrazon (7)	A1	[2Fe–2S]	445, 545[a]	1.79, 1.91, 2.02	nd
Dibenzofuran (8)	C	2[2Fe–2S]	450, 565	nd	nd
Benzene (9–11)	ISP_{BED}	2[2Fe–2S]	326, 450, 550[a]	1.75, 1.92, 2.02	−115
Toluene (12)	ISP_{TOL}	2[2Fe–2S]	326, 450, 550[a]	nd	nd
Napthalene (13,14)	ISP_{NAP}	2[2Fe–2S]	334, 462, 566[a]	1.80, 1.91, 2.01	nd
Terephthalate (15)	Z	2[2Fe–2S]	420, 460, 520[a]	1.73, 1.91, 2.01	nd

[a] Shoulder.
nd, not determined.
References: 1, Batie *et al.*, 1987; 2, Markus *et al.*, 1986; 3, Locher *et al.*, 1991; 4, Fetzner *et al.*, 1992; 5, Yamaguchi and Fujisawa, 1980; 6, Yamaguchi and Fujisawa, 1982; 7, Sauber *et al.*, 1977; 8, Bünz and Cook, 1993; 9, Zamanian and Mason, 1987; 10, Geary *et al.*, 1990; 11, Crutcher and Geary, 1979; 12, Subramanian *et al.*, 1979; 13, Ensley and Gibson, 1983; 14, Suen and Gibson, 1993; 15, Schläfli *et al.*, 1994.

the two types of iron–sulphur cluster, particularly when they are examined in both their oxidized and reduced states. ^{57}Fe was incorporated into the ISP_{BED} component of benzene dioxygenase by growing *P. putida* ML2 on a ^{57}Fe-containing medium. The Mössbauer spectra obtained from the ISP_{BED} purified subsequently, indicated the presence of [2Fe–2S] clusters similar to those observed in the plant-type ferredoxins (Geary and Dickson, 1981); however, the main difference was the isomer shift of one of the iron sites, which was greater than in the plant-type ferredoxins, but similar to that observed in the Rieske-type protein of *Thermus thermophilus* (Fee *et al.*, 1984). The Mössbauer parameters were compared with those of the monooxygenase ferredoxin putidaredoxin, which has a [2Fe–2S] cluster with all sulphur ligation (Münck *et al.*, 1972). In the reduced state, the Fe(III) site of the dioxygenase [2Fe–2S] cluster was similar to the corresponding iron in the ferredoxin; however, the Fe(II) sites were different, as shown by the electric-field gradient and hyperfine tensors. These differences may have two possible explanations: different distortions of the cluster geometry or different ligands. Münck *et al.* (1972) considered it likely that the Fe(II) site had non-sulphur ligands as this iron atom had a larger Mössbauer isomer shift than that in putidaredoxin.

Electron-spin relaxation processes are characterisic of the iron–sulphur clusters. The electron-spin relaxation rate of the [2Fe–2S] clusters in the dioxygenases and the Rieske proteins is slower than in the plant-type ferredoxins, but faster than in hydroxylase ferredoxins, such as putidaredoxin and adrenodoxin. This observation was interpreted by Bertrand and co-workers (1987) as differences in the geometry of the [2Fe–2S] clusters.

Using ENDOR and ESEEM spectroscopy, Cline *et al.* (1985) were able to observe hyperfine interactions in the [2Fe–2S] clusters in the phthalate dioxygenase of *P. cepacia* and in the respiratory Rieske iron–sulphur protein of *T. thermophilus*. All of the recorded spectra showed resonances attributed to protons that were weakly coupled to the iron–sulphur clusters and in addition, unusually strong-hyperfine resonances were observed, which were assigned to the ^{14}N of two histidines.

Further analysis of the phthalate dioxygenase of *P. cepacia* by Gurbiel *et al.* (1989) established the nature of the nitrogen-containing ligands to the [2Fe–2S] Rieske-type cluster. Four different samples of the phthalate dioxygenase terminal oxygenase component were isolated and purified from a histidine auxotroph strain of *P. cepacia*, grown previously on a specific isotopic labelling medium. The X-band ENDOR spectra obtained with the ^{15}N-histidine enriched protein at the g_y resonance position, showed two sharp doublets (four lines) attributed to a pair of inequivalent ^{15}N nitrogen sites. However, as the spectrum at g_y corresponds to a distribution of orientations, the signal from a single ^{15}N nitrogen may give rise to more than one pair of peaks. To eliminate this possibility, Gurbiel *et al.* (1989) recorded another spectrum at g_z. This second spectrum corresponded to a unique molecular orientation and again exhibited two doublets, demonstrating conclusively that the ^{15}N ENDOR signals represent two magnetically distinct histidine

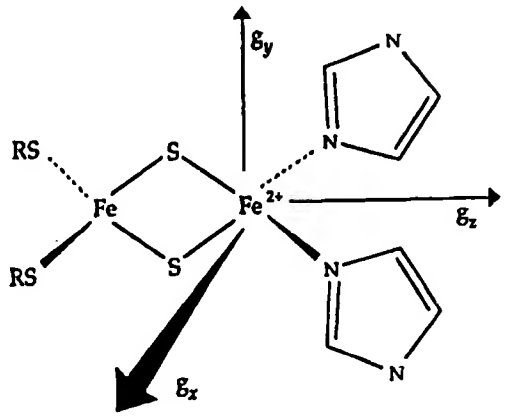

Figure 4 Structure of the Rieske-type [2Fe–2S] cluster of the phthalate dioxygenase ISP as determined by ENDOR spectroscopy. The [2Fe–2S] core and the g_y–g_z plane lie in the paper. (Adapted from Gurbiel *et al.*, 1989.)

ligands coordinated to the Rieske-type [2Fe–2S] cluster. Q-band (35 GHz) ENDOR experiments by Gurbiel *et al.* (1989) have demonstrated that the high-frequency ENDOR resonances observed with the *T. thermophilus* Rieske protein (Cline *et al.*, 1985), assigned previously to a strongly coupled nitrogen, were in fact due to protons. Analysis of the ^{15}N hyperfine coupling tensors and the ^{15}N quadrupole coupling tensors have indicated a roughly tetrahedral coordination at Fe(II), with the N–Fe–N ligand plane corresponding to the g_z–g_x plane. These data led Gurbiel and co-workers to propose a model for the structure of the Rieske-type [2Fe–2S] cluster of phthalate dioxygenase, shown in Fig. 4.

The model proposed by Gurbiel *et al.* (1989) was in keeping with data previously obtained by Kuila *et al.* (1987), who determined the resonance Raman spectra of the Rieske proteins of *T. thermophilus* and phthalate dioxygenase of *P. cepacia*. Raman spectroscopy examines the vibrational modes of the metal centre. For the plant-type [2Fe–2S] clusters, the modes display a centrosymmetric pattern; however, for the dioxygenase cluster, the spectrum showed additional vibration modes, indicating a major perturbation from centrosymmetry. From these results it was concluded that both nitrogens were ligated to one iron atom (Kuila *et al.*, 1987).

X-ray absorption spectroscopy has also been applied to the terminal oxygenase component of phthalate dioxygenase of *P. cepacia* by Tsang *et al.* (1989). In order to study the [2Fe–2S] cluster selectively, the mononuclear iron site was either depleted or reconstituted with cobalt or zinc. The results obtained showed that the iron environment in the Rieske cluster is structurally indistinguishable from that found in the plant-type [2Fe–2S] clusters, thus strongly supporting the suggestion

that the unusually high reduction potentials for the Rieske clusters are due to electrostatic rather than structural effects. Based on the model by Gurbiel *et al.* (1989), Tsang *et al.* (1989) estimated the average Fe–Fe distance to be 2.68 Å for both the oxidized and reduced clusters, and the bridging and terminal Fe–S distance to be 2.20 Å and 2.31 Å, respectively, for the oxidized cluster. It was not possible, however, to estimate the number or distances of any nitrogen ligands.

More recently, Britt *et al.* (1991) and Shergill and Cammack (1994) have conducted ESEEM spectroscopy on the Rieske centres in spinach cytochrome b_6f complex, bc_1 complex and bovine heart mitochondrial membranes. The ESEEM spectra indicate a nitrogen coordination environment similar to that proposed by Gurbiel *et al.* (1989) for the phthalate dioxygenase, supporting the suggested coordination of two histidine ligands to the Rieske [2Fe–2S] cluster. Recently, we have employed the two-dimensional ESEEM technique of hyperfine sublevel correlation spectroscopy (HYSCORE) to correlate unambiguously pairs of ESEEM frequencies belonging to different nitrogen nuclei of ISP_{BED}. The results confirm the assignment of parameters to the two histidine ligands but also provide evidence for the involvement of a weakly coupled peptide nitrogen (Shergill *et al.*, 1995).

6.3. Comparison of the amino-acid sequences of [2Fe–2S] Rieske proteins and the dioxygenase ISP α subunits

The amino-acid sequence for many iron–sulphur proteins from various organisms has been determined either by direct amino acid sequencing or deduced from the DNA sequence of the respective genes. A comparison of the amino-acid sequences of the ISP α subunit from benzene dioxygenase (Tan *et al.*, 1993), toluene dioxygenase (Zylstra and Gibson, 1989), benzoate dioxygenase (Neidle *et al.*, 1991), naphthalene dioxygenase (Simon *et al.*, 1993), dibenzothiophene dioxygenase* (Denome *et al.*, 1993), biphenyl dioxygenase (Erickson and Mondello, 1992) and phthalate dioxygenase (Nomura *et al.*, 1992) is shown in Fig. 3. The alignment reveals that four cysteines and two histidines are highly conserved across all three classes of dioxygenase and, in addition, a fifth histidine positioned near to the N terminus is conserved amongst six of the dioxygenases sequenced.

The amino-acid sequence of other Rieske-type iron–sulphur proteins has been determined. The amino-acid sequence of the Rieske subunit of *Rhodopseudomonas sphaeroides* (Gabellini and Sebald, 1986) and *Rhodobacter capsulatus* (Davidson and Daldal, 1987) have been deduced from their nucleotide sequences. The sequence shows that four cysteines and three histidines are highly conserved;

*Dibenzothiophene dioxygenase genes (*dox*) found in *Pseudomonas* sp. encode proteins that are ⩾ 99% similar in amino-acid sequence to naphthalene dioxygenase. As the deduced pathway metabolizes naphthalene as well as dibenzothiophene, this enzyme has not yet been classified as a separate dioxygenase.

similarly, the amino-acid sequences of the cytochrome b_6f complex Rieske protein (Pfefferkorn and Meyer, 1986) and the mitochondrial C-III of *Saccharomyces cerevisiae* (Beckmann *et al.*, 1987) also contain four conserved cysteine and three conserved histidine residues. The amino-acid composition of the *T. thermophilus* Rieske protein (Fee *et al.*, 1984), which coordinates two identical [2Fe–2S] clusters per protein molecule, contains four cysteine residues, indicating that only two cysteine residues could coordinate each [2Fe–2S] cluster. When these Rieske protein sequences were compared with the dioxygenase sequences it appeared that two cysteine and two histidine residues were fully conserved giving rise to the following consensus sequence (Mason and Cammack, 1992):

Cys-Xaa-His-Xaa$_{16-17}$-Cys-Xaa$_2$-His

(where Xaa is any amino acid and the subscript represents the number of amino-acid residues).

In the conserved regions of the sequence of six of the dioxygenases, each histidine residue is flanked by a single glycine residue either next to it or one residue away. Glycine residues occur in turns of protein secondary structure (Hanukoglu and Gutfinger, 1989); thus it has been suggested that the iron–sulphur cluster is situated in a cleft within the protein (Mason and Cammack, 1992).

6.4. Site-directed mutagenesis experiments on Rieske iron–sulphur proteins

The use of site-directed mutagenesis has helped considerably in determining the structure and function of proteins. To date no directed mutagenesis studies have been reported on the ISP components of the ring-hydroxylating dioxygenases. Such studies have been carried out on the mitochondrial Rieske protein of *S. cerevisiae* (Graham and Trumpower, 1991; Graham *et al.*, 1992) and on the Rieske protein of the cytochrome bc_1 complex of *R. capsulatus* (Davidson *et al.*, 1992).

Graham and Trumpower (1991) have prepared site-directed mutants of the *S. cerevisiae* Rieske protein, in which conserved cysteines at positions 159, 164, 178 and 180 were changed to serines, and conserved histidines at positions 161 and 181 were converted to arginines. The mutation of any one of these six fully conserved residues resulted in an inactive iron–sulphur protein, lacking the iron–sulphur cluster. EPR spectra of the Rieske protein mutated at either of these six positions, showed no detectable $g_y = 1.89$ signal. Mutation of each of the six conserved residues was shown by immunological blotting not to prevent post-translational import of the Fe–S protein precursor into mitochondria, where it is processed into a mature protein. In addition, a histidine at position 184, which is conserved only in respiring organisms, was replaced by an arginine residue. This mutation resulted in the correct assembly of the iron–sulphur cluster and the yeast was able to grow on non-fermentable carbon sources. Therefore, it seems that mutation of each of

the conserved amino-acid residues C159, H161, C164, C178, C180 and H181 affects the insertion or the stability of the Rieske [2Fe–2S] cluster in the protein. Examination of the cytochrome bc_1 complex purified from one of the site-directed mutants showed that the other eight subunits of the complex are present. The mutant Rieske protein lacking the iron–sulphur cluster was more easily lost from the bc_1 complex during purification compared to the wild-type complex. From these observations it has been suggested that the insertion of the iron–sulphur protein is the final step in the assembly of the bc_1 complex and that insertion of the iron–sulphur cluster plays a role in stabilizing the Rieske protein in the complex (Graham and Trumpower, 1991).

Yeast cells expressing mutated Rieske proteins were only able to grow fermentatively, owing to the specific loss of function of the cytochrome bc_1 complex, which suggested that the four conserved cysteines and two histidines were specifically required for the function of the iron–sulphur protein. Consideration of the spectroscopic data (Gurbiel *et al.*, 1989; Kuila *et al.*, 1987; Britt *et al.*, 1991) has led Graham and Trumpower (1991) to suggest that two of the four cysteines, and the two histidines 161 and 181 are the most likely ligands to the [2Fe–2S] cluster. On the basis of geometric and spatial requirements for liganding the iron–sulphur cluster, they proposed that the two coordinating cysteines are C164 and C178, and that C159 and C180 are essential, and may form a disulphide bond that maintains the correct environment for the [2Fe–2S] cluster to be stably inserted into the apoprotein (Fig. 5a).

Davidson and co-workers (Davidson *et al.*, 1992) have also prepared site-directed mutants of the bc_1 complex in an overproducing strain of *R. capsulatus*, in order to assign the amino-acid ligands of the Rieske [2Fe–2S] cluster. Comparison of the amino-acid sequences from numerous bc_1 complex Rieske subunits identified two highly conserved regions that Davidson and co-workers have assigned as box I and box II (Fig. 6). Each box contains two conserved cysteines (box I C133 and C138; box II C153 and C155) and a conserved histidine (box I H135; box II H156). In addition, another histidine, H159, which is conserved in some of the sequences and replaced by a glutamine in others, could not be excluded as a potential iron–sulphur ligand. This amino-acid residue and those in the box regions were all targets for site-directed mutagenesis. All of the mutants, except C155S, H159A and H159S, lacked an EPR spectrum typical of the Rieske type [2Fe–2S] cluster, and analysis of the SDS-PAGE and Western blots showed that the chromatophore membranes of the mutants either lacked or had drastically decreased levels of the Rieske apoprotein, leading to the conclusion that substitution of any of the six highly conserved residues had led to the loss of the cluster and the degradation of the mutant subunits. These data favoured H135 and H156 as the two imidazole ligands to the iron–sulphur cluster. Of the four cysteines, C155S was the only mutant that contained a [2Fe–2S] cluster, as detected by EPR spectroscopy. This suggested that C155 was not a ligand to the cluster. This was supported by C155 being located next to a likely nitrogen ligand, H156. Davidson

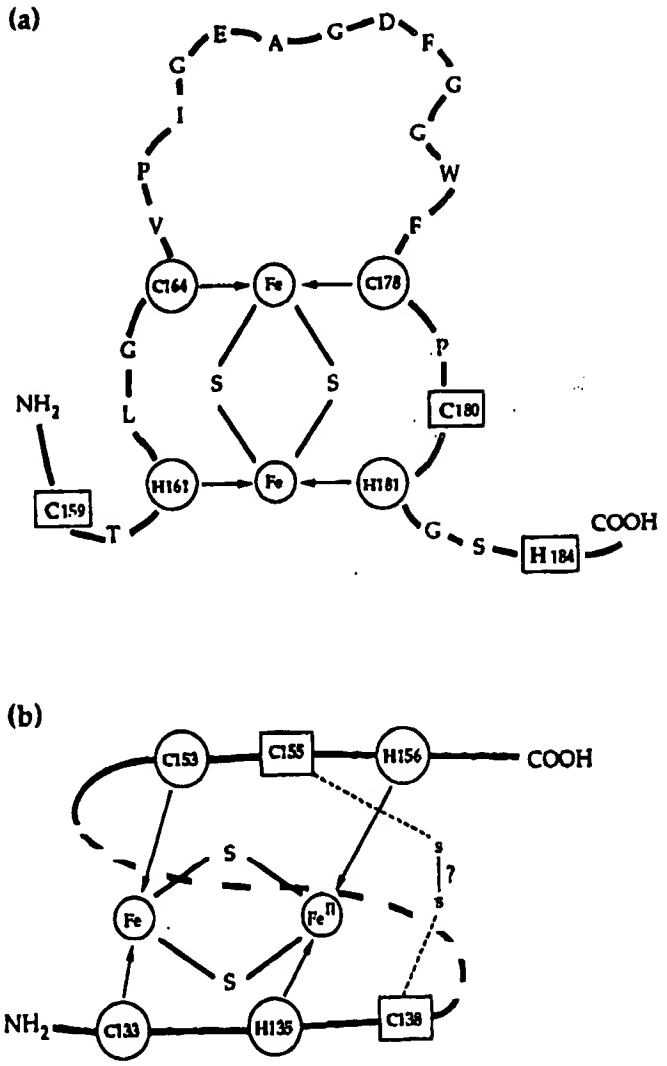

Figure 5 (a) Model for the [2Fe–2S] cluster binding region of the *S. cerevisiae* Rieske iron–sulphur protein. The conserved cysteines 164 and 178 and histidines 161 and 181 are the proposed ligands to the iron–sulphur cluster. Cysteines 159 and 180 may form a disulphide bond to maintain the correct environment for the [2Fe–2S] cluster to be inserted stably into the apoprotein. NH_2 and COOH represent the amino and carboxyl ends of the protein. (Adapted from Graham and Trumpower, 1991.) (b) Model for the [2Fe–2S] cluster binding region of the *R. capsulatus* Rieske protein. The proposed ligands are circled, and S–S represents the putative disulphide bridge between the conserved, non-liganding residues. NH_2 and COOH represents the amino and carboxyl ends of the protein. (Adapted from Davidson *et al.*, 1992.)

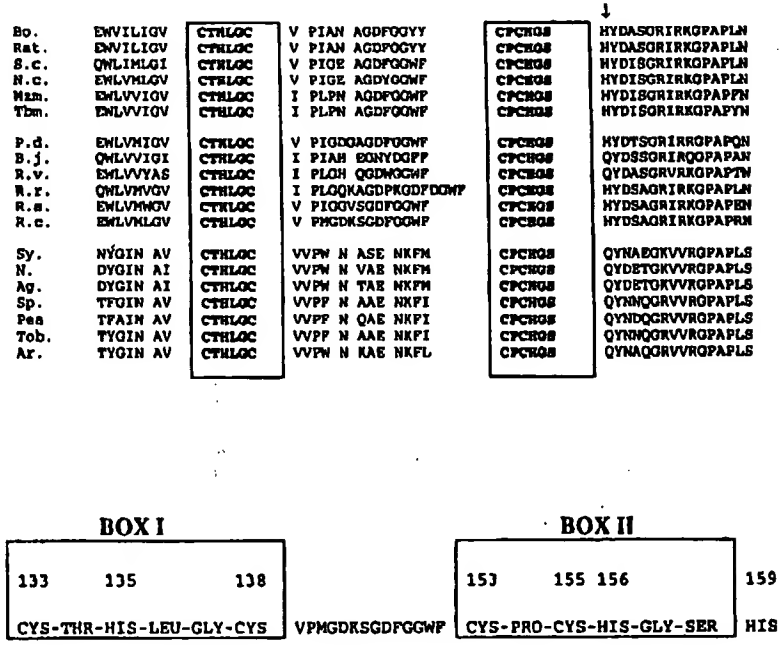

Figure 6 Alignment of the carboxyl termini of all available Rieske sequences showing conserved boxes I and II. The sequence identities are as follows: Bo., bovine; Rat., rat; S.c., *Saccharomyces cerevisiae*; N.c., *Neurospora crassa*; Mzm., maize mitochondrion; Tbm., tobacco mitochondrion; P.d., *Paracoccus denitrificans*; B.j., *Bradyrhizobium japonicum*; R.v., *Rhodopseudomonas viridis*; R.r., *Rhodospirillum rubrum*; R.s., *Rhodobacter sphaeroides*; R.c., *Rhodobacter capsulatus*. The lower group shows the available *b6f* Rieske sequences. Sy., *Synechococcus* sp. PCC 7009; N., *Nostoc*; Ag., *Agmenellum quadriplicatum*; Sp., spinach; Pea, pea; Tob., tobacco; Ar., *Arabadopsis*. The putative [2Fe–2S] cluster binding region of the *R. capsulatus* Rieske protein is shown in boxes I and II. The position of the non-conserved His adjacent to box II is indicated by an arrow. (Adapted from Davidson *et al.*, 1992.)

and co-workers (1992) have assigned C153 as a ligand by assuming that both boxes I and II provide a cysteine and histidine residue as ligands. On this basis there was insufficient data to assign which of C133 and C138 was the potential cysteinyl ligand from box I. Comparing the amino-acid sequences of the Rieske proteins with those of the bacterial dioxygenases, Davidson's group have proposed that the four ligands are box I; C133, H135 and box II; C153; H156. This assignment is in total agreement with the amino-acid sequence consensus put forward by Mason and Cammack (1992). This model differs slightly from that proposed by Graham and Trumpower (1991) who suggest that C138 (*R. capsulatus* numbering) is the box I cysteinyl ligand.

In addition to suggesting the ligands to the iron–sulphur cluster, Davidson *et al.*

(1992) have proposed an internal disulphide bond formed between the two remaining cysteine residues, C138 and C155, as previously suggested for the Rieske protein of *S. cerevisiae* (Graham and Trumpower, 1991). As the two histidine ligands both coordinate to the Fe(II) ion of the [2Fe–2S] cluster (Fee *et al.*, 1984; Gurbiel *et al.*, 1989; Britt *et al.*, 1991), and that the Fe–Fe axis is in the plane of the membrane (Salerno *et al.*, 1979), these data, together with the liganding roles attributed to the specific amino-acid residues suggest that a simple loop between boxes I and II cannot suffice. For C133, H135, C153 and H156 to act as ligands and lie in the membrane, the intervening region (amino-acid residues 136–155) between the two boxes, must twist back upon itself to bring the appropriate residues parallel to each other (Fig. 5b) (Davidson *et al.*, 1992).

The assignment of C159 (*S. cerevisiae* numbering) as a ligand to the [2Fe–2S] cluster by Davidson *et al.* (1992), led Graham and co-workers to assess their proposed structure. After more extensive mutagenesis, Graham *et al.* (1992) isolated a mutant in which threonine at position 160 was changed to alanine, eliminating an electronegative residue proximal to C159. This change had almost no effect on cytochrome *c* reductase activity. In contrast, a mutant proximal to C164, in which proline 166 was converted to serine, reduced the cytochrome *c* reductase activity to less than 20% of the wild-type activity, while exchanging an adjacent hydrophobic residue to another (valine 165 to alanine) had very little effect on cytochrome *c* reductase activity. Thus Graham *et al.* (1992) still favour their initial speculation that C164 is a ligand rather than C159, as proposed by Davidson *et al.* (1992).

7. THE CATALYTIC NON-HAEM IRON CENTRE

Protein systems that use the reaction of dioxygen with non-haem Fe(II) are functionally quite diverse. These highly evolved biological Fe(II) complexes are active sites for dioxygen chemistry, typically functioning by binding and activating dioxygen in preparation for its insertion into unactivated C–H or C–C bonds. There are three broad classes of O_2-reactive non-haem iron-containing enzymes containing mononuclear, dinuclear and polynuclear non-haem iron centres. Probably the most extensively studied class is that of the dinuclear non-haem iron- containing enzymes. Examples from this group of enzymes are methane monooxygenase, haemerythrin and ribonucleotide reductase, of which perhaps methane monooxygenase has been the most comprehensively characterized (reviewed by Feig and Lippard, 1994). The ring-hydroxylating dioxygenases have been reported to contain a mononuclear iron centre (Mason and Cammack, 1992), although very little structural information about this centre has been reported. Consequently, any discussion of its possible binding site and mode of action can be only speculative.

Oxygenases containing mononuclear iron centres have been characterized.

Examples of such oxygenases are the extradiol catechol dioxygenases, 4-methoxybenzoate monooxygenase and isopenicillin N synthase (reviewed by Feig and Lippard, 1994). The ring cleavage dioxygenase, protocatechuate 3,4-dioxygenase from *P. aeruginosa* has been studied in detail, resulting in the structure of this molecule being determined by X-ray crystallography (Ohlendorf *et al.*, 1988; Ohlendorf *et al.*, 1994). The coordination geometry of the non-haem iron centre has been described as trigonal bipyramidal with Tyr447 and His462 serving as axial ligands, and Tyr408 His460 and solvent serving as equatorial ligands (Ohlendorf *et al.*, 1994). Resonance Raman investigations into the structures of 4-hydroxyphenylpyruvate dioxygenase (Bradley *et al.*, 1986) and chlorocatechol dioxygenase (Broderick and O'Halloran, 1991) have revealed the presence of enhanced vibrations characteristic of tyrosinate coordination to the iron centre. The structure for isopenicillin N synthase proposed by Orville and co-workers (1992) also shows that the mononuclear iron centre is ligated by histidines but suggests that an aspartate may act as an additional ligand.

The activation of dioxygen requires a centre capable of single-electron transfer. Although all of the ring-hydroxylating dioxygenases have a terminal oxygenase with Rieske-type [2Fe–2S] clusters, there is no evidence for the cluster serving as an oxygen binding site; sulphide is prone to oxidative damage (Mason and Cammack, 1992). For the non-haem iron to activate dioxygen for the dihydroxylation of the substrate, its binding site is presumed to be close to that of the substrate. As substrate specificity of the ring-hydroxylating dioxygenases has been shown to be controlled by the α subunit of the ISP component (Furukawa *et al.*, 1993; Erickson and Mondello, 1993), it is thought that the binding site for the non-haem iron is also situated on this subunit. Analysis of the amino-acid sequences of the ISPα subunits of benzene, toluene, benzoate/toluate and naphthalene dioxygenases by Neidle and co-workers (1991) identified two histidines and two tyrosines near the middle of the sequence. This led Neidle *et al.* to speculate that these conserved residues are ligands to the iron centre. However, a more thorough comparison of the amino-acid sequences of all classes of the ring-hydroxylating dioxygenases (Fig. 3) shows that the tyrosine residues are not conserved in all ring-hydroxylating dioxygenases. It is thus possible that the coordination of the mononuclear non-haem iron in these dioxygenases involves the highly conserved asparagine (N208; BDO numbering), aspartate (D219) and glutamate (E214) in addition to the histidines (H222 and H228). Such residues have been shown to be involved in the ligation of iron centres in the soybean lipoxygenase L-1 (Minor *et al.*, 1993), isopenicillin N synthase (Orville *et al.*, 1992) and methane monooxygenase (Rosenzweig *et al.*, 1993). The possible involvement of histidines H222 and H228 in the active site of ISP_{BED} has been supported recently by site-directed mutagenesis experiments in our laboratory in which all four conserved histidines (Fig. 4) were mutated. All four mutants resulted in a complete loss of activity, although only mutants H98C and H119C gave rise to a loss of EPR signal, indicative of their role in coordination of the iron–suphur cluster (Fig. 7).

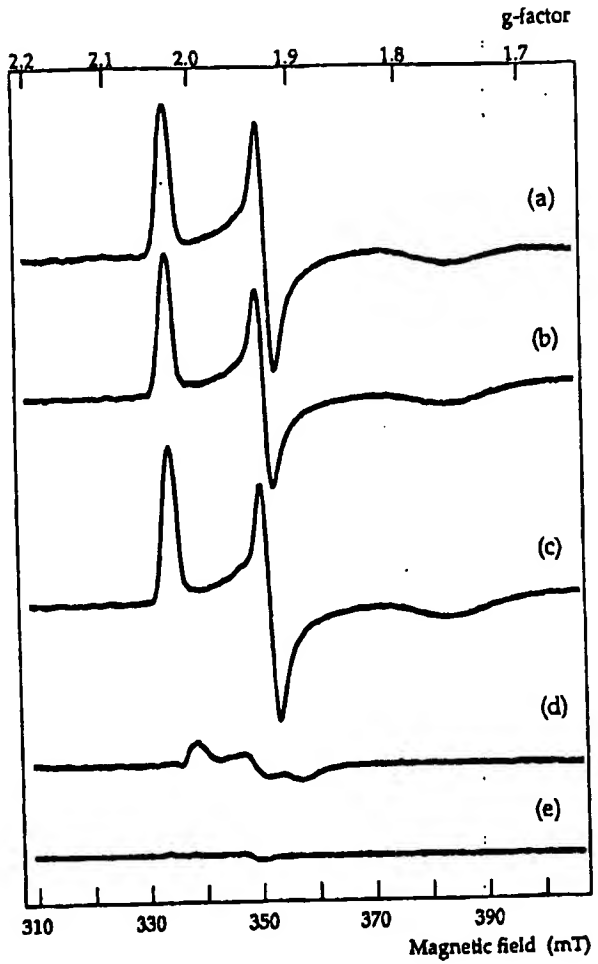

Figure 7 EPR spectra of dithionite-reduced cell extracts of *E. coli* cells expressing wild-type and mutant ISP_{BED} α subunits. Spectra are from wild-type (a) and mutants (b) H222M, (c) H228C, (d) H98C and (e) H119C. Each spectrum has been resolved by the subtraction of the spectrum from the cell extract of *E. coli* cells not expressing an ISP_{BED} α subunit. Conditions of measurement: microwave power 2 mW, microwave frequency 9.37 GHz, modulation amplitude 0.5 mT, temperature 30 K, 5 scans.

The mononuclear non-haem iron centres should be observable using EPR spectroscopy though for some types of ligand field, the reaction may become too broad to be detected. The only EPR signals due to the high-spin Fe(III) centre in the ring-hydroxylating dioxygenases that have been reported are by Altier *et al.* (1993) for the benzoate 1,2-dioxygenase. Their results show that the high spin

Fe(III) has *g*-factors of 7.5, 4.2 and 1.83. This result is similar to that reported for the iron site of chlorocatechol dioxygenase (g = 9.83 and 4.25) (Broderick and O'Halloran, 1991) and 4-methoxybenzoate monooxygenase with *g*-factors around 6.0 and 4.3 (Bill *et al.*, 1981; Twilfer *et al.*, 1981). In the case of oxidized, fully active 4-methoxybenzoate monooxygenase, the $g = 6$ signals shifted upon addition of substrates, whereas the $g = 4.3$ signals did not. This led the authors to suggest that a change occurred in the microenvironment in the presence of substrate. A recent magnetic circular dichroism study on the mononuclear ferrous active site of phthalate dioxygenase from *P. cepacia* showed that a change of ligation, a decrease in coordination from six to five, occurred on substrate binding. This displacement of an iron ligand may prepare the ferrous centre for dioxygen activation (Gassner *et al.*, 1993). In the EPR study on the benzene dioxygenase by Geary and co-workers (1984) the detection of the mononuclear non-haem iron was limited to a minor signal observed at $g = 4.3$, but no significant changes in this signal were observed on addition of benzene either alone or in combination with dioxygen.

The mechanism of dioxygen activation by the ring-hydroxylating dioxygenase reaction remains to be elucidated. An important property of the dioxygen molecule is its propensity to accept electrons in pairs and single electron-transfer reactions are less frequently encountered. Therefore, in mononuclear systems, it is less certain how two-electron redox reactions are accommodated. Since an external reductant, such as NADH or a [2Fe–2S] cluster, is usually present, it is possible that the mononuclear iron centre, cycles through two one-electron transfer steps during each round of catalysis. A mechanism has been proposed by Twilfer *et al.* (1985), who envisaged the activation of the dioxygen at the iron centre by successive electron transfers from the reductase, followed by the reaction of the peroxo complex with the substrate:

$$\mathrm{Fe(III) \xrightarrow{1e^-} Fe(II) \xrightarrow{O_2} Fe(II){\cdot}O_2 \rightarrow Fe(III){\cdot}O_2^- \xrightarrow{1e^-} Fe(II){\cdot}O_2^- \rightarrow Fe(III){\cdot}O_2^{2-}}$$

Twilfer *et al.* (1985) obtained a series of nitrosyl analogues of the oxo-derivatives using nitric oxide. Since NO is an odd-electron species, it can convert Fe(II), which is normally undetectable by EPR spectroscopy, to an EPR-detectable species. EPR signals were observed for high-spin (S = 3/2) Fe(II)·NO (or Fe(III)·NO^-) species, with *g*-factors $g_\perp = 4$, $g_\parallel = 2$. The *g*-factors of signals changed upon binding of substrates (Twilfer *et al.*, 1985).

8. CONCLUDING REMARKS

The bacterial aromatic ring-hydroxylating dioxygenases represent a broad range of multi-component enzymes, which, despite their diverse microbial origins, possess many properties and mechanisms in common. This has enabled their

classification based on structural properties. This classification has been supported by sequence comparisons based on nucleotide and primary amino-acid sequences. Comparison of the low homology sequences has also enabled the identification of highly conserved functional motifs, e.g. iron–sulphur ligation domains, whereas analysis of high homology sequences has allowed the characterization of amino acids involved in more specific functions, such as the control of substrate specificity. This combination of sequence analysis with structure–function studies will prove invaluable for future protein engineering of improved enzymes for both biocatalysis and environmental remediation.

ACKNOWLEDGEMENTS

We thank our colleagues Dr J. K. Shergill and Professor R. Cammack for their critical help and advice. Portions of this work were supported in the authors' laboratory by awards from the Engineering and Physical Sciences Research Council (GR/J00151), and a studentship from the Biotechnology and Biological Sciences Research Council (CSB).

REFERENCES

Altier, D.J., Fox, B.G., Münck, E. and Lipscomb, J.D. (1993) EPR and Mössbauer characterization of benzoate 1,2-dioxygenase from *P. putida*. *J. Bioinorg. Chem.* **52**, 300.

An, D., Gibson, D.T. and Spain, J.C. (1994) Oxidative release of nitrite from 2-nitro-toluene by a three-component enzyme system from *Pseudomonas* sp. strain JS42. *J. Bacteriol.* **176**, 7462–7467.

Axcell, B.C. and Geary, P.J. (1975) Purification and some properties of a soluble benzene-oxidizing system from a strain of *Pseudomonas*. *Biochem. J.* **146**, 173–183.

Batie, C.J. and Ballou, D.P. (1990) Phthalate dioxygenase. In: *Methods in Enzymology*, Vol. 188, *Hydrocarbons and Methylotrophy* (M.E. Lidstrom, ed.), pp. 61–70. Academic Press, New York.

Batie, C.J., LaHaie, E. and Ballou, D.P. (1987) Purification and characterization of phthalate oxygenase and phthalate oxygenase reductase from *Pseudomonas cepacia*. *J. Biol. Chem.* **262**, 1510–1518.

Batie, C.J., Ballou, D.P. and Correll, C.J. (1992) Phthalate dioxygenase reductase and related flavin–iron–sulphur containing electron transferases. In *Chemistry and Biochemistry of Flavoenzymes*. (F. Müller, ed.), pp. 544–554. CRC Press, Boca Raton.

Beckmann, J.D., Ljungdahl, P.O., Lopez, J.L. and Trumpower, B.L. (1987) Isolation and characterization of the nuclear gene encoding the Rieske iron–sulfur protein (RIP1) from *Saccharomyces cerevisiae*. *J. Biol. Chem.* **262**, 8901–8909.

Bertrand, P., Guigliarelli, B., Gayda, J.-P., Beardwood, P. and Gibson, J. (1985) A ligand-field model to describe a new class of 2Fe–2S clusters in proteins and their synthetic analogues. *Biochim. Biophys. Acta* **831**, 261–266.

Bertrand, P., Gayda, J.-P., Fee, J.A., Kuila, D. and Cammack, R. (1987) Comparison of the spin-lattice relaxation properties of the two classes of [2Fe–2S] clusters in proteins. *Biochim. Biophys. Acta* **916**, 24–28.

Bill, E., Bernhardt, F.-H. and Trautwein, A.-X. (1981) Mössbauer studies on the active Fe...[2Fe–2S] site of putidamonooxin, its electron transport and dioxygen activation mechanism. *Eur. J. Biochem.* **121**, 39–46.

Bradley, F.C., Lindstedt, S., Lipscomb, J.D., Que, L., Roe, A.L. and Rundgren, M. (1986) 4-Hydroxyphenylpyruvate dioxygenase is an iron–tyrosinate protein. *J. Biol. Chem.* **261**, 11693–11696.

Brand, J.M., Cruden, D.L., Zylstra, G.J. and Gibson, D.T. (1992) Stereospecific hydroxylation of indan by *Escherichia coli* containing the cloned toluene dioxygenase genes from *Pseudomonas putida* F1. *Appl. Environ. Microbiol.* **58**, 3407–3409.

Britt, R.D., Sauer, K., Klein, M.P., Knaff, D.B., Krianciunas, A., Yu, C.A., Yu, L. and Malkin, R. (1991) Electron Spin Echo Envelope Modulation Spectroscopy supports the suggested coordination of two histidine ligands to the Rieske FeS-centres of the cytochrome b_6f complex of spinach and cytochrome bc_1 complexes of *Rhodospirillum rubrum*, *Rhodobacter sphaeroides* R-26 and bovine heart mitochondria. *Biochemistry* **30**, 1892–1901.

Broderick, J.B. and O'Halloran, T.V. (1991) Overproduction, purification and characterization of chlorocatechol dioxygenase, a non-heme iron dioxygenase with broad substrate tolerance. *Biochemistry* **30**, 7349–7358.

Bruschi, M. and Guerlesquin, F. (1988) Structure, function and evolution of bacterial ferredoxins. *FEMS Microbiol. Rev.* **54**, 155–176.

Bünz, P.V. and Cook, A.M. (1993) Dibenzofuran 4,4a-dioxygenase from *Sphingomonas* sp. strain RW1: Angular dioxygenation by a three-component enzyme system. *J. Bacteriol.* **175**, 6467–6475.

Cammack, R. (1984) Midpoint potentials of iron–sulphur proteins—a survey. In: *Charge and Field Effects in Biosystems* (M.J. Allen and P.N.R. Usherwood, eds), pp. 41–51. Abacus, Tunbridge Wells.

Cammack, R. (1992) Iron–sulfur clusters in enzymes: themes and variations. *Adv. Inorg. Chem.* **38**, 281–322.

Chen, V.J., Orville, A.M., Harpel, M.R., Frolik, C.A., Surerus, K.K., Münck, E. and Lipscomb, J.D. (1989) Spectroscopic studies of isopenicillin N synthase. A mononuclear non-heme Fe^{2+} oxidase with metal coordination sites for small molecules and substrate. *J. Biol. Chem.* **264**, 21677–21681.

Cline, J.F., Hoffman, B.M., Mims, W.B., LaHaie, E., Ballou, D.P. and Fee, J.A. (1985) Evidence for N coordination to Fe in the [2Fe–2S] clusters of *Thermus* Rieske protein and phthalate dioxygenase from *Pseudomonas*. *J. Biol. Chem.* **260**, 3251–3254.

Correll, C.C., Batie, C.J., Ballou, D.P. and Ludwig, M.L. (1992) Phthalate dioxygenase reductase: a modular structure for electron transfer from pyridine nucleotides to [2Fe–2S]. *Science* **258**, 1604–1610.

Crutcher, S.E. and Geary, P.J. (1979) Properties of the iron–sulphur proteins of the benzene dioxygenase system from *Pseudomonas putida*. *Biochem. J.* **177**, 393–400.

Dalton, H. (1986) Biotransformations for industry. *SERC Bull.* **3**, 8–9.

Davidson, E. and Daldal, F. (1987) Primary structure of the bc_1 complex of *Rhodopseudomonas capsulata*: nucleotide sequence of the *pet* operon encoding the Rieske cytochrome b and cytochrome c_1 apoproteins. *J. Mol. Biol.* **195**, 13–24.

Davidson, E., Ohnishi, T., Atta-Asafo-Adjei, E. and Daldal, F. (1992) Potential ligands to the [2Fe–2S] Rieske cluster of the cytochrome bc_1 complex of *Rhodobacter capsulatus* probed by site-directed mutagenesis. *Biochemistry* **31**, 3342–3351.

Denome, S.A., Stanley, D.C., Olson, E.S. and Young, K.D. (1993) Metabolism of

dibenzothiophene and naphthalene in *Pseudomonas* strains: complete DNA sequence of an upper naphthalene catabolic pathway. *J. Bacteriol.* **175**, 6890–6901.

Eggink, G., Engel, H., Vriend, G., Terpstra, P. and Witholt, B. (1990) Rubredoxin reductase of *Pseudomonas oleovorans*. Structural relationships to other flavoprotein oxidoreductases based on one NAD and two FAD fingerprints. *J. Mol. Biol.* **212**, 135–142.

Ensley, B.D. and Gibson, D.T. (1983) Naphthalene dioxygenase: purification and properties of a terminal oxygenase component. *J. Bacteriol.* **155**, 505–511.

Ensley, B.D. and Haigler, B.E. (1990) Naphthalene dioxygenase from *Pseudomonas* NCIB 9816. In: *Methods in Enzymology*, Vol. 188, *Hydrocarbons and Methylotrophy* (M.E. Lidstrom, ed.), pp. 46–52. Academic Press, New York.

Ensley, B.D., Gibson, D.T. and LaBorde, A.L. (1982) Oxidation of naphthalene by a multicomponent enzyme system from *Pseudomonas* sp. strain NCIB 9816. *J. Bacteriol.* **149**, 948–954.

Erickson, B.D. and Mondello, F.J. (1992) Nucleotide sequencing and transcriptional mapping of the genes encoding biphenyl dioxygenase, a multicomponent polychlorinated-biphenyl-degrading enzyme in *Pseudomonas* strain LB400. *J. Bacteriol.* **174**, 2903–2912.

Erickson, B.D. and Mondello, F.J. (1993) Enhanced biodegradation of polychlorinated biphenyls after site-directed mutagenesis of a biphenyl dioxygenase gene. *Appl. Environ. Microbiol.* **59**, 3858–3862.

Fee, J.A., Findling, K.L., Yoshida, T., Hille, R., Tarr, G.E., Hearshen, D.O., Dunham, W.R., Day, E.P., Kent, T.A. and Münck, E. (1984). Purification and characterization of the Rieske iron–sulfur protein from *Thermus thermophilus*: Evidence for a [2Fe–2S] cluster having non-cysteine ligands. *J. Biol. Chem.* **259**, 124–133.

Fee, J.A., Kuila, D., Mather, M.W. and Yoshida, T. (1986) Respiratory proteins from extremely thermophilic bacteria. *Biochim. Biophys. Acta* **853**, 153–185.

Feig, A.L. and Lippard, S.J. (1994) Reactions of non-heme iron (II) centers with dioxygen in biology and chemistry. *Chem. Rev.* **94**, 759–805.

Fetzner, S. and Lingens, F. (1994) Bacterial dehalogenases: biochemistry, genetics and biotechnological applications. *Microbiol. Rev.* **58**, 641–685.

Fetzner, S., Müller, R. and Lingens, F. (1992) Purification and some properties of 2-halobenzoate 1,2-dioxygenase, a two-component enzyme system from *Pseudomonas cepacia* 2CBS. *J. Bacteriol.* **174**, 279–290.

Fukuyama, K., Hase, T., Matsumoto, S., Tsukihara, T and Katsube, Y. (1980) Structure of *S. platensis* [2Fe–2S] ferredoxin and evolution of the chloroplast-type ferredoxins. *Nature* **286**, 522–524.

Furukawa, K., Hirose, J., Suyama, A., Zaiki, T. and Hayashida, S. (1993) Gene components responsible for discrete substrate specificity in the metabolism of biphenyl (*bph* operon) and toluene (*tod* operon) *J. Bacteriol.* **175**, 5224–5232.

Gabellini, N. and Sebald, W. (1986) Nucleotide sequence and transcription of the *fbc* operon from *Rhodopseudomonas sphaeroides*. Evaluation of the deduced amino-acid sequences of the FeS protein, cytochrome *b* and cytochrome c_1. *Eur. J. Biochem.* **154**, 569–579.

Gassner, G.T., Ballou, D.P., Landrum, G.A. and Whittaker, J.W. (1993) Magnetic circular dichroism studies on the mononuclear ferrous active site of phthalate dioxygenase from *Pseudomonas cepacia* show a change of ligation state on substrate binding. *Biochemistry* **32**, 4820–4825.

Gassner, G.T., Ludwig, M.L, Gatti, D.L., Correll, C.C and Ballou, D.P. (1995) Flavoprotein structure and mechanism. 7. Structure and mechanism of the iron–sulfur flavoprotein phthalate dioxygenase reductase. FASEB J. **9**, 1411–1418.

Geary, P.J. and Dickson, D.P.E. (1981) Mössbauer spectroscopic studies of the terminal

dioxygenase protein of benzene dioxygenase from *Pseudomonas putida*. *Biochem. J.* **195**, 199–203.

Geary, P.J., Mason, J.R. and Joannou, C.L. (1990) Benzene dioxygenase from *Pseudomonas putida* ML2 (NCIB 12190) In: *Methods in Enzymology*, Vol 188, *Hydrocarbons and Methylotrophy* (M.E. Lidstrom, ed.), pp. 52–60. Academic Press, New York.

Geary, P.J., Saboowalla, F., Patil, D. and Cammack, R. (1984) An investigation of the iron–sulphur proteins of benzene dioxygenase from *Pseudomonas putida* by electron-spin-resonance spectroscopy. *Biochem. J.* **217**, 667–673.

Gibson, D.T. (1988) Microbial metabolism of aromatic hydrocarbons and the carbon cycle In: *Microbial Metabolism and the Carbon Cycle* (S.R. Hagedm, R.S. Hanson and D.A. Kunz, eds), pp. 33–58. Harwood Academic Publishers, New York.

Gibson, J.F., Hall, D.O., Thornley, J.H.M. and Whatley, F.R. (1966) The iron complex in spinach ferredoxin. *Proc. Natl Acad. Sci.* **56**, 987–990.

Gibson, D.T., Koch, J.R. and Kallio, R.E. (1968) Oxidative degradation of aromatic hydrocarbons by microorganisms. I. Enzymatic formation of catechol from benzene. *Biochemistry* **7**, 2653–2662.

Gibson, D.T., Maseles, F.C. and Kallio, R.E. (1970) Incorporation of oxygen-18 into benzene by *Pseudomonas putida*. *Biochemistry* **9**, 1631–1635.

Gibson, D.T., Cruden, D.L., Haddock, J.D., Zylstra, G.J. and Brand, J.M. (1993) Oxidation of polychlorinated biphenyls by *Pseudomonas* sp. strain LB400 and *Pseudomonas pseudoalcaligenes* KF707. *J. Bacteriol.* **175**, 4561–4564.

Gibson, D.T., Resnick, S.M., Lee, K., Brand, J.M., Torok, D.S., Wackett, L.P., Schocken, M.J. and Haigler, B.E. (1995) Desaturation, dioxygenation and monooxygenation reactions catalyzed by naphthalene dioxygenase from *Pseudomonas* sp strain 9816-4. *J. Bacteriol.* **177**, 2615–2621.

Goyal, A.K. and Zylstra, G.J. (1996) Molecular cloning of novel genes for polycyclic aromatic hydrocarbon degradation from *Comamonas testosteroni* GZ39. *Appl. Environ. Microbiol.* **62**, 230.

Graham, L.A. and Trumpower, B.L. (1991) Mutational analysis of the mitochondrial Rieske iron–sulphur protein of *Saccharomyces cerevisiae*. *J. Biol. Chem.* **266**, 22485–22492.

Graham, L.A., Brandt, U., Sargent, J.S. and Trumpower, B.L. (1992) Mutational analysis of assembly and function of the iron–sulphur protein of the cytochrome bc_1 complex in *Saccharomyces cerevisiae*. *J. Bioenerg. Biomemb.* **25**, 245–257.

Gurbiel, R.J., Batie, C.J., Sivaraja, M., True, A.E., Fee, J.A., Hoffman, B.M. and Ballou, D.P. (1989) Electron-nuclear resonance spectroscopy of ^{15}N-enriched phthalate dioxygenase from *Pseudomonas cepacia* proves that two histidines are coordinated to the [2Fe–2S] Rieske-type clusters. *Biochemistry* **28**, 4861–4871.

Haak, B., Fetzner, S. and Lingens, F. (1995) Cloning, nucleotide sequence and expression of the plasmid-encoded genes for the two-component 2-halobenzoate 1,2-dioxygenase from *Pseudomonas cepacia* 2CBS. *J. Bacteriol.* **177**, 667–675.

Haddock, J.D. and Gibson, D.T. (1995). Purification and characterization of the oxygenase component of biphenyl 2,3-dioxygenase from *Pseudomonas* sp. Strain LB400. *J. Bacteriol.* **177**, 5834–5839.

Haddock, J.D., Nadim, L.M. and Gibson, D.T. (1993) Oxidation of biphenyl by a multicomponent enzyme system from *Pseudomonas* sp. strain LB400. *J. Bacteriol.* **175**, 395–400.

Haigler, B.E. and Gibson, D.T. (1990a) Purification and properties of NADH–ferredoxin$_{NAP}$ reductase, a component of naphthalene dioxygenase from *Pseudomonas* sp. strain NCIB 9816. *J. Bacteriol.* **172**, 457–464.

Haigler, B.E. and Gibson, D.T. (1990b) Purification and properties of ferredoxin$_{NAP}$, a

component of naphthalene dioxygenase from *Pseudomonas* sp. strain NCIB 9816. *J. Bacteriol.* **172**, 465–468.

Halliwell, B. and Gutteridge, J.M.C. (1984) Oxygen toxicity, oxygen radicals, transition metals and disease. *Biochem. J.* **219**, 1–14.

Hanukoglu, I. and Gutfinger, T. (1989) cDNA Sequence of adrenodoxin reductase-identification of NADP-binding sites in oxidoreductases. *Eur. J. Biochem.* **180**, 479–484.

Harayama, S., Rekik, M. and Timmis, K.N. (1986) Genetic analysis of a relaxed substrate specificity aromatic ring dioxygenase, toluate 1,2-dioxygenase, encoded by TOL plasmid pWWO of *Pseudomonas putida*. *Mol. Gen. Genet.* **202**, 226–234.

Harayama, S. Kok, M. and Neidle, E.L. (1992) Functional and evolutionary relationships among diverse oxygenases. *Annu. Rev. Microbiol.* **46**, 565–601.

Hayaishi, O. (1962) *Oxygenases*. Academic Press, New York, London.

Hudlicky, T., Mandel, M., Rouden, J., Lee, R.S., Bachman, B., Dudding, T., Yost, K.J. and Merola, J.S. (1994) Microbial oxidation of aromatics in enantiocontrolled synthesis. Part 1. Expedient and general asymmetric synthesis of inositols and carbohydrates *via* an unusual oxidation of a polarized diene with potassium permanganate. *J. Chem. Soc. Perkin. Trans. 1* 1553–1567.

Hurtubise, Y., Barriault, D., Powlowski, J. and Sylvestre, M. (1995) Purification and characterization of the *Comamonas testosteroni* B-356 biphenyl dioxygenase components. *J. Bacteriol.* **177**, 6610–6618.

Irie, S., Doi, S., Yorifuji, T., Takagi, M. and Yano, K. (1987) Nucleotide sequencing and characterization of the genes encoding benzene oxidation enzymes of *Pseudomonas putida*. *J. Bacteriol.* **169**, 5174–5179.

Kikuchi, Y., Nagata, Y., Hinata, M., Kimbara, K., Fukuda, M., Yano, K. and Takagi, M. (1994) Identification of the *bphA4* gene encoding ferredoxin reductase involved in biphenyl and polychlorinated biphenyl degradation in *Pseudomonas* sp. strain KKS102. *J. Bacteriol.* **176**, 1689–1694.

Koga, H., Yamaguchi, E., Matsunaga, K., Aramaki, H. and Horiuchi, T. (1989) Cloning and nucleotide sequences of NADH-putidaredoxin reductase gene (*camA*) and putidaredoxin gene (*camB*) involved in cytochrome P-450cam hydroxylase of *Pseudomonas putida*. *J. Biochem.* **106**, 831–836.

Kuila, D., Fee, J.A., Schoonover, J.R., Woodruff, W.H., Batie, C.J. and Ballou, D.P. (1987) Resonance Raman spectra of the [2Fe–2S] clusters of the Rieske protein from *Thermus* and phthalate dioxygenase. *J. Am. Chem. Soc.* 109:1559–1561.

Kurkela, S., Lehväslaiho, H., Palva, E.T. and Teeri, T.H. (1988) Cloning, nucleotide sequence and characterization of genes encoding naphthalene dioxygenase of *Pseudomonas putida* strain NCIB9816. *Gene* **73**, 355–362.

Lee, L., Brand, J.M. and Gibson, D.T. (1995) Stereospecific sulfoxidation by toluene and naphthalene dioxygenases. *Biochem. Biophys. Res. Commun.* **212**, 9–15.

Ley, S.V., Sternfeld, F. and Taylor, S. (1987) Microbial oxidation in synthesis: a six step preparation of (±)-pinitol from benzene. *Tetrahedron Lett.* **28**, 225–226.

Locher, H.H., Leisinger, T. and Cook, A.M. (1991) 4-Sulphobenzoate 3,4-dioxygenase. Purification and properties of a desulphonative two-component enzyme system from *Comamonas testosteroni* T-2. *Biochem. J.* **274**, 833–842.

Markus, A., Krekel, D. and Lingens, F. (1986) Purification and some properties of component A of the 4-chlorophenylacetate 3,4-dioxygenase from *Pseudomonas* species strain CBS. *J. Biol. Chem.* **261**, 12883–12888.

Mason, J.R. (1988) Oxygenase catalysed hydroxylation of aromatic compounds: simple chemistry by complex enzymes. *Int. Ind. Biotechnol.* **8**, 19–24.

Mason, J.R. and Cammack, R. (1992) The electron-transport proteins of hydroxylating bacterial dioxygenases. *Annu. Rev. Microbiol.* **46**, 277–305.

Minor, W., Steczko, J., Bolin, J.T., Otwinowski, Z. and Axelrod, B. (1993) Crystallographic determination of the active site iron and its ligands in soybean lipoxygenase L-1. *Biochemistry* **32**, 6320–6323.

Mondello, F.J. (1989) Cloning and expression in *Escherichia coli* of the *Pseudomonas* strain LB400 genes encoding polychlorinated biphenyl degradation. *J. Bacteriol.* **171**, 1725–1732.

Moodie, F.D.L., Woodland, M.P. and Mason, J.R. (1990) The reductase component of the chromosomally encoded benzoate dioxygenase from *Pseudomonas putida* C-1 is immunologically homologous with a product of the plasmid encoded *xylD* gene (toluate dioxygenase) from *Pseudomonas putida* mt-2. *FEMS Microbiol. Lett.* **71**, 163–168.

Morrice, N., Geary, P., Cammack, R., Harris, A., Beg, F. and Aitken, A. (1988) Primary structure of protein B from *Pseudomonas putida*, member of a new class of 2Fe–2S ferredoxins. *FEBS Lett.* **231**, 336–340.

Münck, E., Debrunner, P.G., Tsibris, J.C.M. and Gunsalus, I.C. (1972) Mössbauer parameters of putidaredoxin and its selenium analogue. *Biochemistry* **11**, 855–863.

Nakatsu, C.H. and Wyndham, R.C. (1993) Cloning and expression of the transposable chlorobenzoate-3,4-dioxygenase genes of *Alcaligenes* sp. strain BR60. *Appl. Environ. Microbiol.* **59**, 3625–3633.

Nakatsu, C.H., Straus, N.A. and Wyndham, R.C. (1995) The nucleotide sequence of the Tn*5271* chlorobenzoate (*cbaAB*) dioxygenase unites the Class IA oxygenases in a single lineage. *Microbiology* **141**, 485–495.

Neidle, E.L., Hartnett, C., Ornston, L.N., Bairoch, A., Rekik, M. and Harayama, S. (1991) Nucleotide sequences of *Acinetobacter calcoaceticus benABC* genes for benzoate 1,2-dioxygenase reveal evolutionary relationships among multicomponent oxygenases. *J. Bacteriol.* **173**, 5385–5395.

Nomura, Y., Nakagawa, M., Ogawa, N., Harashima, S. and Oshima, Y. (1992) Genes in PHT plasmid encoding the initial degradation pathway of phthalate in *Pseudomonas putida*. *J. Ferment. Bioeng.* **74**, 333–344.

Ohlendorf, D.H., Lipscomb, J.D. and Weber, P.C. (1988) Structure and assembly of protocatechuate 3,4-dioxygenase. *Nature* **336**, 403–405.

Ohlendorf, D.H., Orville, A.M. and Lipscomb, J.D. (1994) Structure of protocatechuate 3,4-dioxygenase from *Pseudomonas aeruginosa* at 2.14 Å resolution. *J. Mol. Biol.* **244**, 586–608.

Orville, A.M., Chen, V.J., Kriauciunas, A., Harpel, M.R., Fox, B.G., Münck, E. and Lipscomb, J.D. (1992) Thiolate ligation of the active site Fe^{2+} of isopenicillin N synthase derives from substrate rather than endogenous cysteine: spectroscopic studies of site-specific cys > ser mutated enzymes. *Biochemistry* **31**, 4602–4612.

Pang, C.-P., Chakravarti, B., Adlington, R.M., Ting, H.-H., White, R.L., Jayatilake, G.S., Baldwin, J.E. and Abraham, E.P. (1984) Purification of isopenicillin N synthase. *Biochem. J.* **222**, 789–795.

Pember, S.O., Johnson, K.A., Villafranca, J.J. and Benkovic, S.J. (1989) Mechanistic studies on phenylalanine hydroxylase from *Chromobacterium violaceum*. Evidence for the formation of an enzyme–oxygen complex. *Biochemistry* **28**, 2124–2130.

Pfefferkorn, B. and Meyer, H.E. (1986) N-terminal amino-acid sequence of the Rieske iron–sulfur protein from the cytochrome b_6/f-complex of spinach thylakoids. *FEBS Lett.* **206**, 233–237.

Que, L. Jr, Widom, J. and Crawford, R.L. (1981) 3,4-dihydroxyphenylacetate 2,3-dioxygenase: a manganese(II) dioxygenase from *Bacillus brevis*. *J. Biol. Chem.* **256**, 10941–10944.

Raag, R. and Poulos, T.L. (1989) Crystal structure of the carbon monoxide–substrate–cytochrome $P\text{-}450_{CAM}$ ternary complex. *Biochemistry* **28**, 7586–7592.

Riedel, A., Rutherford, A.W., Hauska, G., Muller, A. and Nitschke, W. (1991) Chloroplast Rieske protein—EPR study on its spectral characteristics, relaxation and orientation properties. *J. Biol. Chem.* **266**, 17838–17844.

Rieske, J.S., Zaugg, W.S. and Hansen, R.E. (1964) Properties of a new oxidation–reduction component of the respiratory chain as studied by electron paramagnetic resonance spectroscopy. *J. Biol. Chem.* **239**, 3017–3022.

Romanov, V. and Hausinger, R.P. (1994) *Pseudomonas aeruginosa* 142 uses a three-component *ortho*-halobenzoate 1,2-dioxygenase for the metabolism of 2,4-dichloro- and 2-chlorobenzoate. *J. Bacteriol.* **176**, 3368–3374.

Rosche, B., Tshisuaka, B., Fetzner, S. and Lingens, F. (1995) 2-Oxo-1,2-dihydroquinoline 8-monooxygenase, a two-component enzyme system from *Pseudomonas putida* 86. *J. Biol. Chem.* **270**, 17836–17842.

Rosenzweig, A.C., Frederick, C.A., Lippard, S.J. and Nordlund, P. (1993) Crystal structure of a bacterial non-haem iron hydroxylase that catalyses the biological oxidation of methane. *Nature* **366**, 537–543.

Salerno, J.C., Blum, H. and Ohnishi, T. (1979) The orientation of iron–sulphur clusters and a spin-coupled ubiquinone pair in the mitochondrial membrane. *Biochim. Biophys. Acta* **547**, 270–281.

Sauber, K., Fröhner, C., Rosenberg, G, Eberspöcher, J. and Lingens, F. (1977) Purification and properties of pyrazon dioxygenase from pyrazon-degrading bacteria. *Eur. J. Biochem.* **74**, 89–97.

Schläfli, H.R., Baker, D.P., Leisinger, T. and Cook, A.M. (1995) Stereospecificity of hydride removal from NADH by reductases of multi-component non-heme iron oxygenase systems. *J. Bacteriol.* **177**, 831–834.

Schläfli, H.R., Weiss, M.A., Leisinger, T. and Cook, A.M. (1994) Terephthalate 1,2-dioxygenase system from *Comamonas testosteroni* T-2: purification and some properties of the oxygenase component. *J. Bacteriol.* **176**, 6644–6652.

Schweizer, D., Markus, A., Seez, M., Ruf, H.H. and Lingens, F. (1987) Purification and some properties of component B of the 4-chlorophenylacetate 3,4-dioxygenase from *Pseudomonas species* strain CBS3. *J. Biol. Chem.* **262**, 9340–9346.

Sheldrake, G.N. (1992) Biologically derived arene *cis*-dihydrodiols as synthetic building blocks. In: *Chirality in Industry* (A.N. Collins, G.N. Sheldrake and J. Crosby, eds), pp. 127–166. Wiley, Chichester.

Shergill, J.K. and Cammack, R. (1994) ESEEM and ENDOR studies of the Rieske iron–sulphur protein in bovine heart mitochondrial membranes. *Biochim. Biophys. Acta* **1185**, 35–42.

Shergill, J.K., Joannou, C.L., Bratt, P.J., Mason, J.R. and Cammack, R. (1995) Coordination of the Rieske-type [2Fe–2S] cluster of the terminal iron–sulphur protein of *Pseudomonas putida* benzene 1,2-dioxygenase, studied by one- and two-dimensional electron spin-echo envelope modulation spectroscopy. *Biochemistry* **34**, 16533–16542.

Simon, M.J., Osslund, T.D., Saunders, R., Ensley, B.D., Suggs, S., Harcourt, A., Suen, W.-C., Cruden, D.L., Gibson, D.T. and Zylstra, G.J. (1993) Sequences of the genes encoding naphthalene dioxygenase in *Pseudomonas putida* strains G7 and NCIB 9816–4. *Gene* **127**, 31–37.

Spain, J.C., Zylstra, G.J., Blake, C.K. and Gibson, D.T. (1989) Monohydroxylation of phenol and 2,5-dichlorophenol by toluene dioxygenase in *Pseudomonas putida* F1. *Appl. Environ. Microbiol.* **55**, 2648–2652.

Subramanian, V., Te-Ning, L., Yeh, W.K. and Gibson, D.T. (1979) Toluene dioxygenase: purification of an iron–sulfur protein by affinity chromatography. *Biochem. Biophys. Res. Commun.* **91**, 1131–1139.

Subramanian, V., Liu, T.-N., Yeh, W.-K., Narro, M. and Gibson, D.T. (1981) Purification and

properties of NADH-ferredoxin$_{TOL}$ reductase. A component of toluene dioxygenase from *Pseudomonas putida*. *J. Biol. Chem.* **256**, 2723–2730.

Subramanian, V., Liu, T.-N., Yeh, W.-K., Serdar, C.M., Wackett, L.P. and Gibson, D.T. (1985) Purification and properties of ferredoxin$_{TOL}$, A component of toluene dioxygenase from *Pseudomonas putida* F1. *J. Biol. Chem.* **260**, 2355–2363.

Suemori, A., Kurane, R. and Tomizuka, N. (1993) Purification and properties of phthalate oxygenase from *Rhodococcus erythropolis* S-1. *Biosci. Biotechnol. Biochem.* **57**, 1482–1486.

Suen, W.-C. and Gibson, D.T. (1993) Isolation and preliminary characterization of the subunits of the terminal component of naphthalene dioxygenase from *Pseudomonas putida* NCIB 9816–4. *J. Bacteriol.* **175**, 5877–5881.

Suen, W.-C. and Gibson, D.T. (1994) Recombinant *Escherichia coli* strains synthesize active forms of naphthalene dioxygenase and its individual α and β subunits. *Gene* **143**, 67–71.

Taira, K., Hirose, J., Hayashida, S. and Furukawa, K. (1992) Analysis of *bph* operon from the polychlorinated biphenyl-degrading strain of *Pseudomonas pseudoalcaligenes* KF707. *J. Biol. Chem.* **267**, 4844–4853.

Takizawa, N., Kaida, N., Torigoe, S., Moritani, T., Sawada, T., Satoh, S. and Kiyohara, H. (1994) Identification and characterization of genes encoding polycyclic aromatic hydrocarbon dioxygenase and polycyclic aromatic hydrocarbon dihydrodiol dehydrogenase in *Pseudomonas putida* OUS82. *J. Bacteriol.* **176**, 2444–2449.

Tan, H.-M. and Mason, J.R. (1990) Cloning and expression of the plasmid-encoded benzene dioxygenase genes from *Pseudomonas putida* ML2. *FEMS Microbiol. Lett.* **72**, 259–264.

Tan, H.-M. (1991) The benzene dioxygenase genes from *Pseudomonas putida* ML2: cloning, expression and identification of functional domains. Ph.D. thesis, University of London.

Tan, H.-M., Tang, H.-Y., Joannou, C.L., Abdel-Wahab, N.H. and Mason, J.R. (1993) The *Pseudomonas putida* ML2 plasmid-encoded genes for benzene dioxygenase are unusual in codon usage and low in G + C content. *Gene* **130**, 33–39.

Tan, H.-M. and Cheong, C.-M. (1994) Substitution of the ISP α subunit of biphenyl dioxygenase from *Pseudomonas* results in a modification of the enzyme activity. *Biochem. Biophys. Res. Commun.* **204**, 912–917.

Tan H.-M., Joannou, C.L., Cooper, C.E., Butler, C.S., Cammack, R. and Mason, J.R. (1994) The effect of ferredoxin$_{BED}$ over-expression on benzene dioxygenase activity in *Pseudomonas putida* ML2. *J. Bacteriol.* **176**, 2507–2512.

Trumpower, B.L. (1990) Cytochrome bc_1 complexes of microorganisms. *Microbiol. Rev.* **54**, 101–129.

Tsang, H.-Y., Batie, C.J., Ballou, D.P. and Penner-Hahn, J.E. (1989) X-ray absorption spectroscopy of the [2Fe–2S] Rieske clusters in *Pseudomonas cepacia* phthalate dioxygenase. Determination of core dimensions and iron ligation. *Biochemistry* **28**, 7233–7240.

Twilfer, H., Bernhardt, F.-H. and Gersonde, K. (1981) An electron-spin-resonance study on the redox-active centers of the 4-methoxybenzoate monooxygenase from *Pseudomonas putida*. *Eur. J. Biochem.* **119**, 595–602.

Twilfer, H., Bernhardt, F.H. and Gersonde, K. (1985) Dioxygen-activating iron centre in putidamonooxin. Electron spin resonance investigation of the nitrosylated putidamonooxin. *Eur. J. Biochem.* **147**, 171–176.

Wackett, L.P. (1990) Toluene dioxygenase from *Pseudomonas putida* F1. In: *Methods in Enzymology*, Vol 188, *Hydrocarbons and Methylotrophy* (M.E. Lidstrom, ed.), pp. 39–46. Academic Press, New York.

Wackett, L.P., Kwart, L.D. and Gibson, D.T. (1988) Benzylic monooxygenation catalysed by toluene dioxygenase from *Pseudomonas putida*. *Biochemistry* **27**, 1360–1367.

Wang, Y., Garnon, J., Labbe, D., Bergeron, H. and Lau, P.C.K. (1995) Sequence and

expression of the *bpdC1C2BADE* genes involved in the initial steps of biphenyl/chlorobiphenyl degradation by *Rhodococcus* sp M5. *Gene* **164**, 117–122.
Wende, P., Pfleger, K. and Bernhardt, F.H. (1982) Dioxygen activation by putidamonooxin: substrate-modulated reaction of activated dioxygen. *Biochem. Biophys. Res. Commun.* **104**, 527–532.
Wierenga, R.K., Terpstra, P. and Hol, W.G.J. (1986) Prediction of the occurrence of the ADP-binding βαβ-fold in proteins, using an amino-acid sequence fingerprint. *J. Mol. Biol.* **187**, 101–107.
Yamaguchi, M. and Fujisawa, H. (1978) Characterization of NADH-cytochrome *c* reductase, a component in benzoate 1,2-dioxygenase system from *Pseudomonas arvilla* C-1. *J. Biol. Chem.* **253**, 8848–8853.
Yamaguchi, M. and Fujisawa, H. (1980) Purification and characterization of an oxygenase component in benzoate 1,2-dioxygenase system from *Pseudomonas arvilla* C-1. *J. Biol. Chem.* **255**, 5058–5063.
Yamaguchi, M. and Fujisawa, H. (1982) Subunit structure of oxygenase component in benzoate-1,2-dioxygenase system from *Pseudomonas arvilla* C-1. *J. Biol. Chem.* **257**, 12497–12502.
Yang, Y., Chen, R.F. and Shiaris, M.P. (1994) Metabolism of naphthalene, fluorene and phenanthrene: preliminary characterization of a cloned gene cluster from *Pseudomonas putida* NCIB 9816. *J. Bacteriol.* **176**, 2158–2164.
Zamanian, M. and Mason, J.R. (1987) Benzene dioxygenase in *Pseudomonas putida*. Subunit composition and immuno-cross-reactivity with other aromatic dioxygenases. *Biochem. J.* **244**, 611–616.
Ziffer, H., Kabuto, K., Gibson, D.T., Kobal, V.M. and Jerina, D.M. (1977) The absolute stereochemistry of several *cis*-dihydrodiols microbially produced from substituted benzenes. *Tetrahedron* **33**, 2491–2496.
Zylstra, G.J. and Gibson, D.T. (1989) Toluene degradation by *Pseudomonas putida* F1. Nucleotide sequence of *todC1C2BADE* genes and their expression in *Escherichia coli*. *J. Biol. Chem.* **264**, 14940–14946.
Zylstra, G.J., McCombie, W.R., Gibson, D.T. and Finette, B.A. (1988) Toluene degradation by *Pseudomonas putida* F1: Genetic organization of the *tod* operon. *Appl. Environ. Microbiol.* **54**, 1498–1503.

Thiol Template Peptide Synthesis Systems in Bacteria and Fungi

Rainer Zocher and Ullrich Keller

Institut für Biochemie und Molekulare Biologie, Technische Universität Berlin, Franklinstraße 29, D-10587 Berlin-Charlottenburg, Germany

Abbreviations: Abu, α-amino butyric acid; ACMS, actinomycin synthetase; ACP, acyl carrier protein; ACV, δ-(L-α-aminoadipyl)-cysteinyl-D-valine; ACVS, δ-(L-α-aminoadipyl)-cysteinyl-D-valine synthetase; AdoHCy, S-adenosyl-L-homocysteine;

ADVANCES IN MICROBIAL PHYSIOLOGY VOL 38
ISBN 0-12-027738-7

JOURNAL OF BACTERIOLOGY, Sept. 1991, p. 5385–5395
0021-9193/91/175385-11$02.00/0

Vol. 173, No. 17

Nucleotide Sequences of the *Acinetobacter calcoaceticus benABC* Genes for Benzoate 1,2-Dioxygenase Reveal Evolutionary Relationships among Multicomponent Oxygenases

ELLEN L. NEIDLE,[1]† CHRISTOPHER HARTNETT,[1]‡ L. NICHOLAS ORNSTON,[1]* AMOS BAIROCH,[2] MONIQUE REKIK,[2] AND SHIGEAKI HARAYAMA[2]

Department of Biology, Yale University, New Haven, Connecticut 06511,[1] and Department of Medical Biochemistry, Faculty of Medicine, University of Geneva, 1211 Geneva 4, Switzerland[2]

Received 22 January 1991/Accepted 13 June 1991

The nucleotide sequences of the *Acinetobacter calcoaceticus benABC* genes encoding a multicomponent oxygenase for the conversion of benzoate to a nonaromatic *cis*-diol were determined. The enzyme, benzoate 1,2-dioxygenase, is composed of a hydroxylase component, encoded by *benAB*, and an electron transfer component, encoded by *benC*. Comparison of the deduced amino acid sequences of BenABC with related sequences, including those for the multicomponent toluate, toluene, benzene, and naphthalene 1,2-dioxygenases, indicated that the similarly sized subunits of the hydroxylase components were derived from a common ancestor. Conserved cysteine and histidine residues may bind a [2Fe-2S] Rieske-type cluster to the α-subunits of all the hydroxylases. Conserved histidines and tyrosines may coordinate a mononuclear Fe(II) ion. The less conserved β-subunits of the hydroxylases may be responsible for determining substrate specificity. Each dioxygenase had either one or two electron transfer proteins. The electron transfer component of benzoate dioxygenase, encoded by *benC*, and the corresponding protein of the toluate 1,2-dioxygenase, encoded by *xylZ*, were each found to have an N-terminal region which resembled chloroplast-type ferredoxins and a C-terminal region which resembled several oxidoreductases. These BenC and XylZ proteins had regions similar to certain monooxygenase components but did not appear to be evolutionarily related to the two-protein electron transfer systems of the benzene, toluene, and naphthalene 1,2-dioxygenases. Regions of possible NAD and flavin adenine dinucleotide binding were identified.

The complete degradation of benzoate by aerobic bacteria can occur by either of two catabolic pathways. In both reaction sequences, benzoate is converted to a nonaromatic *cis*-diol, 2-hydro-1,2-dihydroxybenzoate, and then to catechol (51) (Fig. 1). Catechol is cleaved between the two hydroxyl groups when benzoate is metabolized via the *ortho* (or β-ketoadipate) pathway, and subsequent reactions yield the tricarboxylic acid cycle intermediates succinate and acetyl coenzyme A (59). Catechol cleavage via the *meta* pathway occurs adjacent to the hydroxyl groups, and subsequent reactions lead to the formation of pyruvate and acetaldehyde. The *ortho*- and *meta*-fission routes do not usually operate concurrently, and regulatory factors determine how benzoate is degraded when genes encoding both pathways are present in the host cell (39).

The genes responsible for the conversion of benzoate to its corresponding *cis*-diol have been isolated from two different soil bacteria: *benABC* from the chromosome of *Acinetobacter calcoaceticus* (42) and *xylXYZ* from TOL plasmid pWW0 of *Pseudomonas putida* (78). The *benABC*-encoded benzoate 1,2-dioxygenase exhibits narrow substrate specificity, showing little or no oxidation of most substituted benzoates. In contrast, the plasmid-encoded *meta* pathway toluate 1,2-dioxygenase, encoded by *xylXYZ*, catalyzes the hydroxylation not only of benzoate but of many 3- and 4-substituted benzoates including toluates (78). Benzoate 1,2-dioxygenase and toluate 1,2-dioxygenase are each multicomponent enzymes consisting of three different polypeptides of about 53, 19, and 38 kDa (19, 21, 42).

The similar sizes of the polypeptides and the similarity among the biochemical reactions catalyzed by the *benABC*- and *xylXYZ*-encoded enzymes raise questions about their evolutionary origins. Benzoate and toluate 1,2-dioxygenases are structurally related to a family of multicomponent aromatic ring-hydroxylating dioxygenases (9). These dioxygenases contain an aromatic ring hydroxylase component composed of two different subunits. The sizes of these α and β subunits, about 50 and 20 kDa, respectively, are similar in different dioxygenases. Studies of benzoate 1,2-dioxygenase from the soil bacterium *Pseudomonas arvilla* C-1 indicate that the structure of this native enzyme is $\alpha_3\beta_3$ (75). Each α-subunit contains one iron-sulfur cluster [2Fe-2S], whereas the isolated β-subunit does not contain any detectable iron or labile sulfide. One mononuclear Fe(II) atom may also be associated with each hydroxylase component (75).

In addition to the hydroxylase component, the dioxygenases described above usually contain one or two electron transport proteins. The benzoate 1,2-dioxygenase of *P. arvilla* has a single iron-sulfur flavoprotein exhibiting an NADH-cytochrome *c* reductase activity that is responsible for the electron transfer from NADH to the aromatic ring hydroxylase. This enzyme is a 38-kDa polypeptide with one iron-sulfur cluster of the [2Fe-2S] type and one molecule of flavin adenine dinucleotide (FAD) (73, 74). The involvement of similar proteins in the electron transfer reactions of benzoate 1,2-dioxygenase from *A. calcoaceticus* and toluate 1,2-dioxygenase from *P. putida* have been suggested by our previous genetic studies (19, 21, 42). In the benzene, toluene, and naphthalene dioxygenase systems, however, two

* Corresponding author.
† Present address: Microbiology Department, University of Texas Medical School, Houston, TX 77225.
‡ Present address: Neurogen Corporation, Branford, CT 06405.

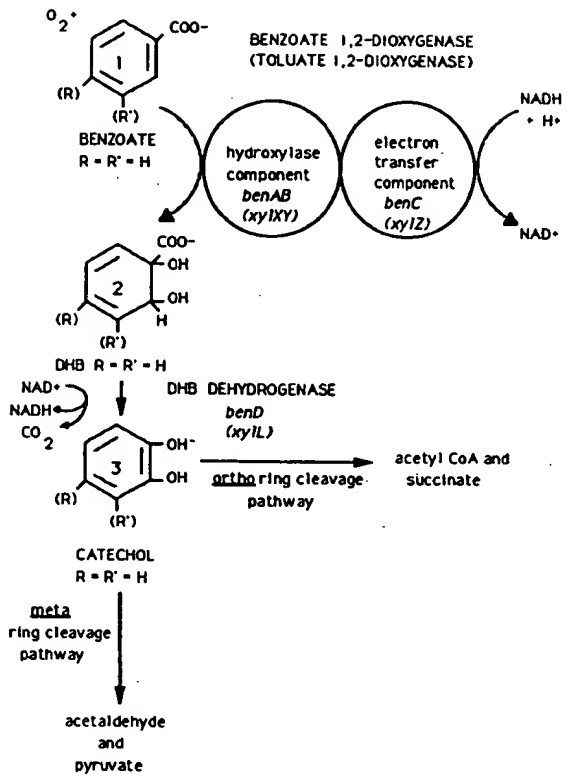

FIG. 1. Multicomponent dioxygenases initiate benzoate (1) degradation by converting it to 2-hydro-1,2-dihydroxybenzoate (DHB, 2). Benzoate and toluate 1,2-dioxygenases are each composed of a two-subunit hydroxylase, encoded by *benAB* and *xylXY*, respectively, and an electron transfer oxidoreductase encoded by *benC* and *xylZ*, respectively. DHB is converted to catechol (3) by an NAD-dependent dehydrogenase, the gene product of *benD* or *xylL*. The chromosomal *ben* genes, isolated from *A. calcoaceticus*, encode enzymes specific for the substrate R=R'=H. The plasmid-borne *xyl* genes, isolated from *P. putida* TOL plasmid pWW0, encode enzymes with broader substrate specificity and can degrade compounds with methyl substitutions at positions R and R'.

different proteins are required for the electron transfer reaction (2, 16, 17, 60, 61).

To better understand the evolutionary relationships among aromatic ring-hydroxylating dioxygenases, we sequenced *benABC* and *xylXYZ*. The sequencing of the latter genes is presented elsewhere (20). In this report, we present the nucleotide sequence of the *A. calcoaceticus benABC* genes. The deduced amino acid sequences of the gene products responsible for the hydroxylation of benzoate were compared with those of enzymes which catalyze similar reactions.

MATERIALS AND METHODS

Bacterial strains, plasmids, and bacteriophages. Recombinant plasmids derived from pUC19 (69, 76) carrying wild-type DNA of *A. calcoaceticus* BD413 (29) (designated ADP1 in our collection) from the chromosomal *ben* region have been previously described (42). The 3.4-kbp insert of pIB1354 carrying *benABC* was subcloned into the replicative form of bacteriophages M13mp18 and M13mp19 (76). Similar subclones were generated from smaller *Kpn*I-*Kpn*I, *Kpn*I-*Eco*RI, and *Kpn*I-*Sal*I restriction endonuclease fragments of the *ben* DNA. *Escherichia coli* JM101 *supE thi* Δ(*lac-proAB*) (F' *traD36 proAB laqI*^{q} ZΔM15) (69) was used as a host for recombinant plasmids and bacteriophages.

The Cyclone I Biosystem of International Biotechnologies, Inc. (New Haven, Conn.) was used to generate nested deletions of the insert DNA of recombinant bacteriophages. Using this method, the exposed single-stranded ends of cloned DNA fragments were progressively digested by T4 DNA polymerase. Overlapping clones entirely covering both strands of the *benABC* genes were isolated.

DNA sequencing. Procedures described in the "M13 Cloning/Dideoxy Sequencing Instruction Manual" (4a) were followed for the isolation and propagation of M13 phages and for the generation of single-stranded DNA sequencing templates. DNA sequence was determined by the dideoxy chain termination method (56) with commercial kits obtained from Bethesda Research Laboratories, Inc. (Gaithersburg, Md.) and United States Biochemical Corp. (Cleveland, Ohio). α-^{35}S-dATP was purchased from Amersham Corp. (Arlington Heights, Ill.). As described previously (41), sequencing reaction mixtures were electrophoretically separated on 8% polyacrylamide gels with 42% urea in Tris-borate-EDTA buffer. Gels were dried under vacuum with a gel slab drier (model 224; Bio-Rad Laboratories, Richmond, Calif.) before autoradiography with Kodak X-Omat film.

DNA sequence analysis. Computer-assisted sequence analysis was done with software packages PC/GENE (Genofit; Intelligenetics; developed by A. Bairoch) and MicroGenie (Beckman). Protein similarities were detected by scanning version 13 of the SWISS-PROT protein sequence data bank (A. Bairoch; distributed by the EMBL Data Library) with an algorithm based on that of Lipman and Pearson (37). Computer-calculated alignments were used to assess the significance of sequence similarities (40), and secondary structure predictions were computed by using the conformational parameters of Chou and Fasman (7).

Nucleotide sequence accession number. The sequence of the *A. calcoaceticus* 3,353-bp *Hin*dIII-*Eco*RI restriction endonuclease fragment described in this report has been deposited with GenBank under accession number M62649.

RESULTS

Nucleotide sequence of *benABC* genes. The *benABC* genes were previously localized to a 3.4 kbp *Hin*dIII-*Eco*RI restriction endonuclease fragment cloned from the *A. calcoaceticus* ADP1 chromosome (42). The nucleotide sequence of this 3,353-bp DNA fragment was determined and, as shown in Fig. 2, it contained three open reading frames. Computer analysis by three different methods (12, 32, 57) suggested that each open reading frame would be likely to encode a protein. The first open reading frame, corresponding to *benA*, started at nucleotide 347 (Fig. 2). An ATG translational start codon was preceded by the putative ribosome binding sequence GGAG (58). Translation would yield a protein product of 52,079 Da, the size of the predicted *benA*-encoded hydroxylase subunit (42).

The second open reading frame, corresponding to *benB*, started at nucleotide 1729. An initiation codon at this position was preceded by the ribosome binding sequence GGAG. The deduced molecular mass of the *benB* product, 20,073 Da, was in agreement with previous in vitro analysis (42). The ATG initiation codon of *benB* overlapped with the

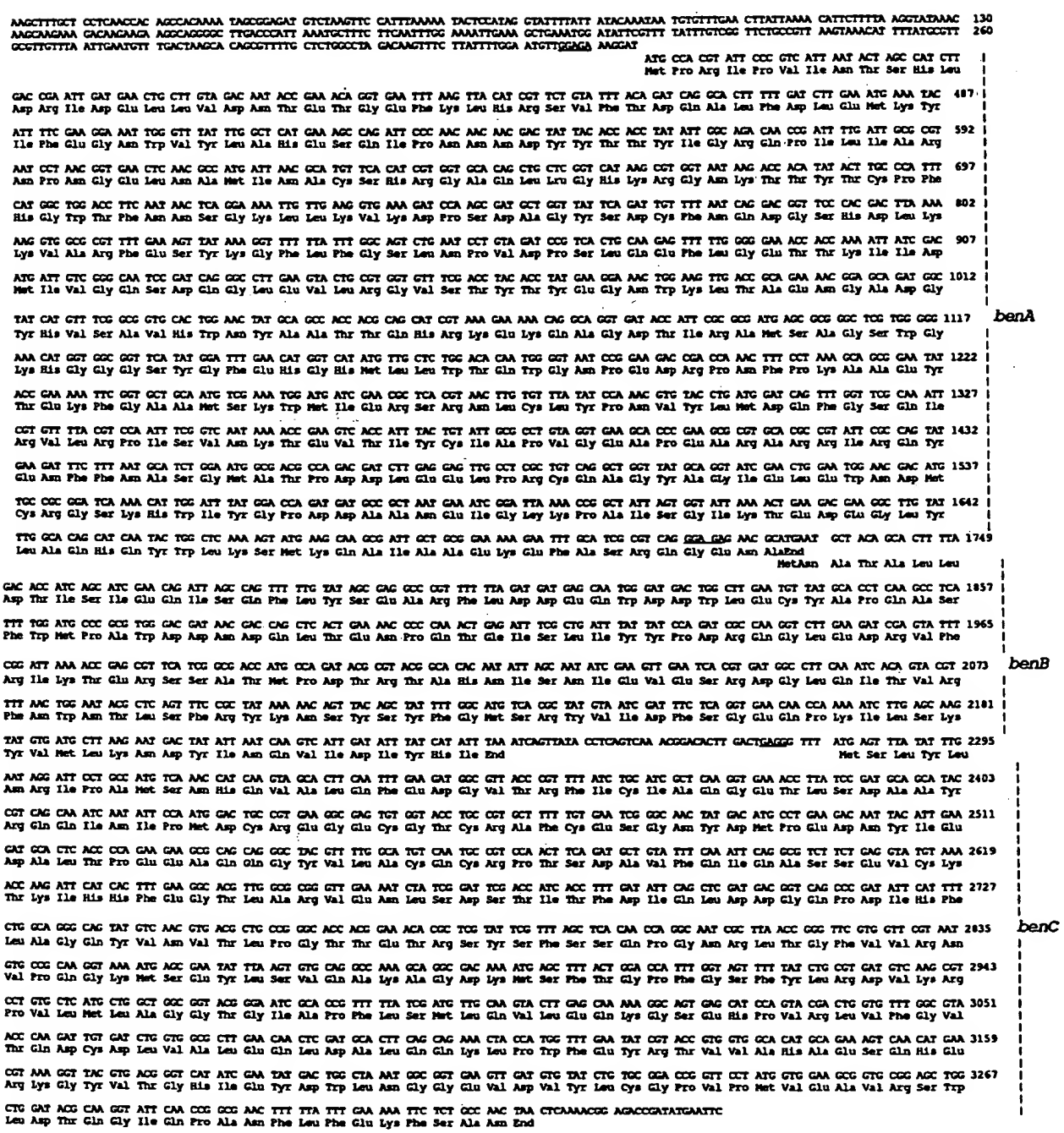

FIG. 2. DNA sequence of the 3,353-bp chromosomal *A. calcoaceticus* *Hin*dIII-*Eco*RI restriction endonuclease fragment carrying the *benABC* genes. The open reading frame corresponding to each gene is marked by broken lines, and within each open reading frame, nucleotides are arranged as codons above the deduced amino acid sequence. Numbers indicate the nucleotide positions of adjacent bases. Possible ribosome binding sites are underlined at positions 336, 1718, and 2273. A second possible initiation codon and ribosome binding site for the translation of *benC* are found at positions 2299 and 2311, respectively.

TGA stop codon of *benA*. This arrangement, which may be involved in translational coupling, has been observed previously with catabolic genes, in particular those, like *benA* and *benB*, encoding nonidentical enzymatic subunits (44).

Two possible translational initiation sites were found for the third open reading frame, *benC*. At positions 2281 and 2311, potential initiation codons were preceded by the ribosome binding sequences GAGG and AGGA, respectively. Sequence comparisons described below suggested that *benC* starts at position 2281. Translational initiation at

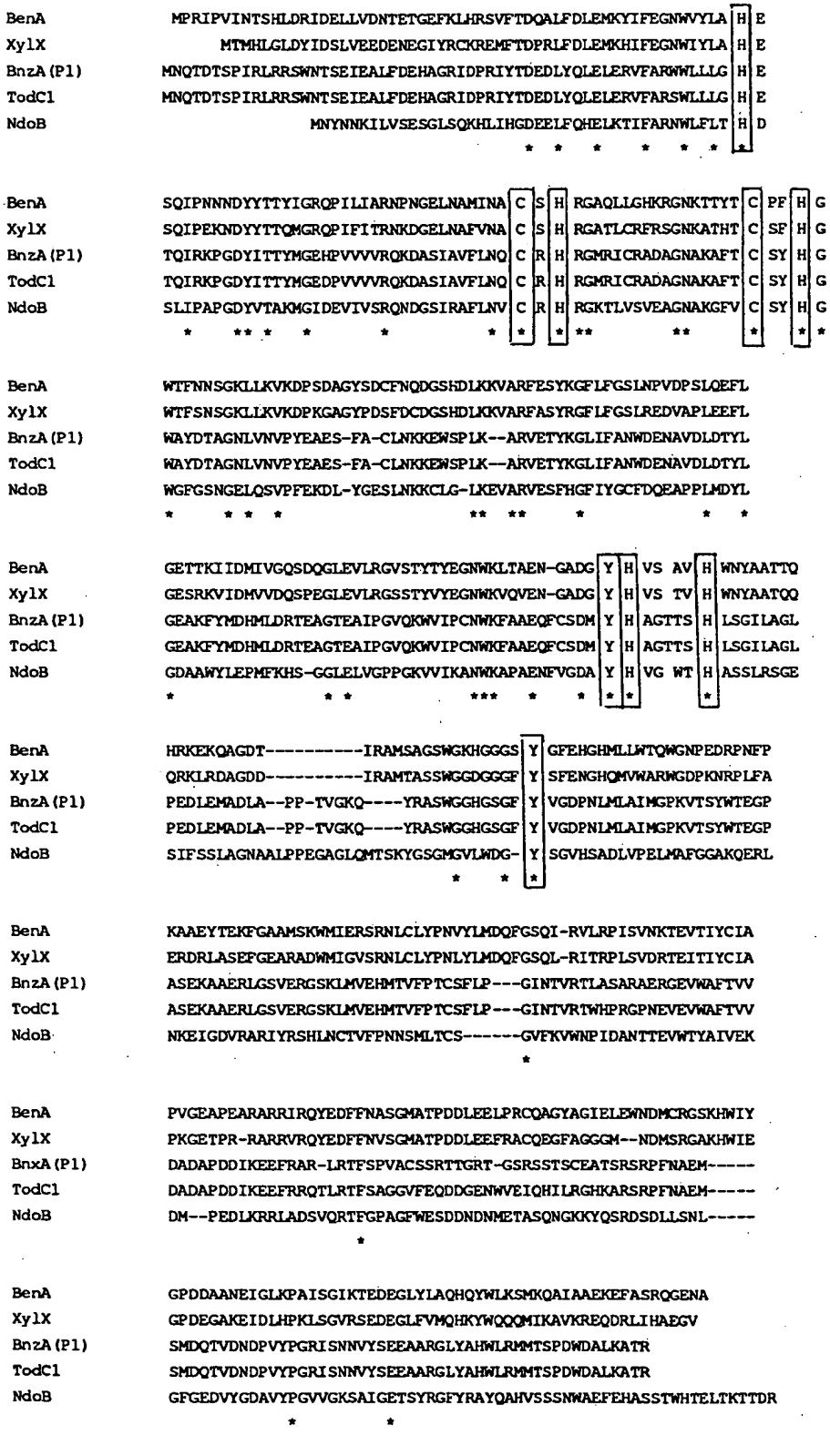
BenA MPRIPVINTSHLDRIDELLVDNTETGEFKLHRSVFTDQALFDLEMKYIFEGNWVYLA H E
XylX MTMHLGLDYIDSLVEEDENEGIYRCKREMFTDPRLFDLEMKHIFEGNWIYLA H E
BnzA(P1) MNQTDTSPIRLRRSWNTSEIEALFDEHAGRIDPRIYTDEDLYQLELERVFARWWLLLG H E
TodC1 MNQTDTSPIRLRRSWNTSEIEALFDEHAGRIDPRIYTDEDLYQLELERVFARSWLLLG H E
NdoB MNYNNKILVSESGLSQKHLIHGDEELFQHELKTIFARNWLFLT H D
BenA SQIPNNNDYYTTYIGRQPILIARNPNGELNAMINA C S H RGAQLLGHKRGNKTTYT C PF H G
XylX SQIPEKNDYYTTQMGRQPIFITRNKDGELNAFVNA C S H RGATLCRFRSGNKATHT C SF H G
BnzA(P1) TQIRKPGDYITTYMGEHPVVVVRQKDASIAVFLNQ C R H RGMRICRADAGNAKAFT C SY H G
TodC1 TQIRKPGDYITTYMGEDPVVVVRQKDASIAVFLNQ C R H RGMRICRADAGNAKAFT C SY H G
NdoB SLIPAPGDYVTAKMGIDEVIVSRQNDGSIRAFLNV C R H RGKTLVSVEAGNAKGFV C SY H G
BenA WTFNNSGKLLKVKDPSDAGYSDCFNQDGSHDLKKVARFESYKGFLFGSLNPVDPSLQEFL
XylX WTFSNSGKLLKVKDPKGAGYPDSFDCDGSHDLKKVARFASYRGFLFGSLREDVAPLEEFL
BnzA(P1) WAYDTAGNLVNVPYEAES-FA-CLNKKEWSPLK--ARVETYKGLIFANWDENAVDLDTYL
TodC1 WAYDTAGNLVNVPYEAES-FA-CLNKKEWSPLK--ARVETYKGLIFANWDENAVDLDTYL
NdoB WGFGSNGELQSVPFEKDL-YGESLNKKCLG-LKEVARVESFHGFIYGCFDQEAPPLMDYL
BenA GETTKIIDMIVGQSDQGLEVLRGVSTYTYEGNWKLTAEN-GADG Y H VS AV H WNYAATTQ
XylX GESRKVIDMVVDQSPEGLEVLRGSSTYVYEGNWKVQVEN-GADG Y H VS TV H WNYAATQQ
BnzA(P1) GEAKFYMDHMLDRTEAGTEAIPGVQKWVIPCNWKFAAEQFCSDM Y H AGTTS H LSGILAGL
TodC1 GEAKFYMDHMLDRTEAGTEAIPGVQKWVIPCNWKFAAEQFCSDM Y H AGTTS H LSGILAGL
NdoB GDAAWYLEPMFKHS-GGLELVGPPGKVVIKANWKAPAENFVGDA Y H VG WT H ASSLRSGE
BenA HRKEKQAGDT----------IRAMSAGSWGKHGGGS Y GFEHGHMLLWTQWGNPEDRPNFP
XylX QRKLRDAGDD----------IRAMTASSWGGDGGGF Y SFENGHQMVWARWGDPKNRPLFA
BnzA(P1) PEDLEMADLA--PP-TVGKQ----YRASWGGHGSGF Y VGDPNLMLAIMGPKVTSYWTEGP
TodC1 PEDLEMADLA--PP-TVGKQ----YRASWGGHGSGF Y VGDPNLMLAIMGPKVTSYWTEGP
NdoB SIFSSLAGNAALPPEGAGLQMTSKYGSGMGVLWDG- Y SGVHSADLVPELMAFGGAKQERL
BenA KAAEYTEKFGAAMSKWMIERSRNLCLYPNVYLMDQFGSQI-RVLRPISVNKTEVTIYCIA
XylX ERDRLASEFGEARADWMIGVSRNLCLYPNLYLMDQFGSQL-RITRPLSVDRTEITIYCIA
BnzA(P1) ASEKAAERLGSVERGSKLMVEHMTVFPTCSFLP---GINTVRTLASARAERGEVWAFTVV
TodC1 ASEKAAERLGSVERGSKLMVEHMTVFPTCSFLP---GINTVRTWHPRGPNEVEVWAFTVV
NdoB NKEIGDVRARIYRSHLNCTVFPNNSMLTCS------GVFKVWNPIDANTTEVWTYAIVEK
BenA PVGEAPEARARRIRQYEDFFNASGMATPDDLEELPRCQAGYAGIELEWNDMCRGSKHWIY
XylX PKGETPR-RARRVRQYEDFFNVSGMATPDDLEEFRACQEGFAGGGM--NDMSRGAKHWIE
BnxA(P1) DADAPDDIKEEFRAR-LRTFSPVACSSRTTGRT-GSRSSTSCEATSRSRPFNAEM-----
TodC1 DADAPDDIKEEFRRQTLRTFSAGGVFEQDDGENWVEIQHILRGHKARSRPFNAEM-----
NdoB DM--PEDLKRRLADSVQRTFGPAGFWESDDNDNMETASQNGKKYQSRDSDLLSNL-----
BenA GPDDAANEIGLKPAISGIKTEDEGLYLAQHQYWLKSMKQAIAAEKEFASRQGENA
XylX GPDEGAKEIDLHPKLSGVRSEDEGLFVMQHKYWQQQMIKAVKREQDRLIHAEGV
BnzA(P1) SMDQTVDNDPVYPGRISNNVYSEEAARGLYAHWLRMMTSPDWDALKATR
TodC1 SMDQTVDNDPVYPGRISNNVYSEEAARGLYAHWLRMMTSPDWDALKATR
NdoB GFGEDVYGDAVYPGVVGKSAIGETSYRGFYRAYQAHVSSSNWAEFEHASSTWHTELTKTTDR

FIG. 3. The α-subunits of the hydroxylase components of five multicomponent aromatic ring dioxygenases appear to be homologous. BenA, XylX, BnzA (P1) (27), TodC1 (79), and NdoB (34) are approximately 50-kDa components of the benzoate, toluate, benzene, toluene, and naphthalene 1,2-dioxygenases, respectively. Positions at which amino acid residues of all proteins are identical are indicated by asterisks. Conserved histidines and tyrosines which may coordinate mononuclear Fe(II) atoms are enclosed by boxes. Two conserved cysteines are also enclosed by boxes, and these residues together with the closest conserved histidines may bind a Rieske-type [2Fe-2S] center. Gaps introduced into the amino acid sequences for the purpose of alignment are indicated by dashes.

this position would yield a 38,787-Da protein, in good agreement with the predicted size of 38 kDa (42).

Codon usage and G+C content of *benABC*. The G+C content of the *benA*, *-B*, and *-C* genes, 45, 41, and 47%, respectively, reflected the characteristic 38 to 47% value found in *Acinetobacter* species (28). Similar codon usage was observed among the three genes and was much like that found in previously sequenced *A. calcoaceticus* structural genes (6, 8, 13, 14, 41, 45, 54). The most marked preference for particular codons was observed for arginine, for which two of six possible codons predominated. The CGT and CGC codons were used 50 to 63% and 13 to 30% of the time, respectively. The bias toward using preferred codons was found in *E. coli* to be a measure of gene expression levels (1).

Although relatively few genes have been sequenced from *Acinetobacter* species, a comparison of codon usage in bacteria of this genus with that found in *E. coli* (1) suggested that the general patterns of codon usage are similar. Differences included a bias toward using the GCA codon for alanine and the CAA codon for glutamine by *Acinetobacter* species. The *E. coli* preference for the CTG (leucine) codon was not observed in *benABC*. A comparison of codons used for proline showed that the *E. coli* bias toward CCG was replaced by one in *Acinetobacter* species for CCA. The TCC codon for serine was used in fewer than 10% of the serine residues by *Acinetobacter* species but not by *E. coli*.

Choice of related sequences for comparison with the deduced amino acid sequences of BenABC. The deduced amino acid sequences of the protein components of the *A. calcoaceticus* benzoate 1,2-dioxygenase system were compared with those of other aromatic ring-hydroxylating dioxygenases for which sequence data are available. These include the benzene, naphthalene, toluene, and toluate dioxygenases. Irie et al. (27) determined the nucleotide sequence of a chromosomal DNA fragment of *P. putida* carrying four genes, *bnzABCD*, encoding the benzene 1,2-dioxygenase system. The *bnzABCD* gene products have been designated P1 to P4, and we use these designations parenthetically. Sequence data for three components of naphthalene 1,2-dioxygenase, encoded by *ndoABC*, were derived from DNA of *P. putida* NCIB 9816 carrying a naphthalene-degrading plasmid (34). The nucleotide sequences of the *todC1C2BA* genes for toluene 1,2-dioxygenase have been determined from chromosomal DNA of *P. putida* F1 (79). In addition, we have determined the nucleotide sequence of the TOL plasmid pWW0 *xylXYZ* genes encoding toluate 1,2-dioxygenase (20).

In the hydroxylase components, the greatest degree of similarity was found in the N-terminal region of the α-subunits. The amino acid sequences of BenA, XylX, BnzA (P1) (27), TodC1 (79), and NdoB (34) were all found to be similar (Fig. 3). Pairwise comparisons showed that 62% of the aligned BenA and XylX residues were identical, whereas comparison of the BenA sequence with each of the others in Fig. 3 revealed 20 to 24% identity. These values reflected the averaging of approximately 30% identity in the N-terminal regions of the protein sequences and 10% identity in the C-terminal regions. Each of these proteins is an approximately 50-kDa subunit of a dioxygenase hydroxylase component. Two cysteine residues and two histidine residues, conserved among all the hydroxylase subunits, were found to align with conserved residues in Rieske iron-sulfur proteins (Fig. 4). As discussed below, these residues may bind a Rieske-type [2Fe-2S] cluster (53).

```
BenA        MINA C S H RGAQLLGHKRGNKTTYT C PF H G    MULTICOMPONENT
XylX        FVNA C S H RGATLCRFRSGNKATHT C SF H G    DIOXYGENASES:
BnzA(P1)    FLNQ C R H RGMRICRADAGNAKAFT C SY H G    HYDROXYLASE
TodC1       FLNQ C R H RGMRICRADAGNAKAFT C SY H G    α-SUBUNITS
NdoB        FLNV C R H RGKTLVSVEAGNAKGFV C SY H G

R.n.        LIGV C T H LGCVPIAN-AGCFGGYY C PC H G    RIESKE
R.c.        MLGV C T H LGCVPMGDLSGDFGGWF C PC H G    IRON-SULFUR
S.c.        MLGI C T H LGCVPIGE-AGDFGGWF C PC H G    PROTEINS
P.d.        MIGV C T H LGCVPIGDGAGDFGGWF C PC H G
B.j.        VIGI C T H LGCIPIAHE-GNYDGFF C PC H G
                 *   *  *       *       *    * *

TodB1       VQDT C T H GDWALSDGYLDGDIVE C TL H FG    MULTICOMPONENT
NdoA        TDNL C T H GSARMSDGYLEGREIE C PL H QG    DIOXYGENASES:
BnzC(P3)    VQDT C T H GDWALSDGYLDGDIVE C TL H FG    "FERREDOXIN"
                * * * *    ***** *   * * * *  *     COMPONENTS
```

FIG. 4. Two conserved cysteines and histidines may coordinate [2Fe-2S] clusters. Similar alignments of these residues, enclosed in boxes, suggested that the aromatic dioxygenase subunits, BenA, XylX, BnzA (P1) (27), TodC1 (79), and NdoB (34), are Rieske-type iron-sulfur proteins. The small iron-sulfur proteins, TodB1, NdoA, and BnzC (P3), of the toluene, naphthalene, and benzene dioxygenases, respectively, also have cysteines and histidines similarly aligned with those of the Rieske iron-sulfur proteins of *Rattus norvegicus* (R.n.) (43), *Rhodobacter capsulatus* (R.c.) (10), *S. cerevisiae* (S.c.) (3), *Paracoccus denitrificans* (P.d.) (35), and *Bradyrhizobium japonicum* (B.j.) (66). Residues identical in all aligned positions are indicated by asterisks.

```
BenB                    MNATALLDTISIEQISQFLYSEARFLDDEQWDDWLE-CYAPQASFWMPAWDDN---DQLTENPQTEISLIYYPDRQGLED
XylY                          MTISYEAVRDFLYREARYLDDKQWESWLE-MYAPDATFWMPAWDDR---DQLTEDPQSQISLIWYGNRSGLED
NdoC    MMINIQEDKLVSAHDAEEILRFFNCHDSALQQEATTLLTQEAHLLDIQAYRAWLEHCVGSEVQYQVISRELRAASERR--YKLNEAMNVYNENFQQLKV
BnzB(P2)        MIDSANRADVFLRKPAPVAPELQHEVEQFYYWEAKLLNDRRFEEWFAL-LAEDIHYFMPIRTTRIMRDSRLEYSGSREYAHFDDDATMMKG
TodC2           MIDSANRADVFLRKPAPVAPELQHEVEQFYYWEAKLLNDRRFEEWFAL-LAEDIHYFMPIRTTRIMRDSRLEYSGSREYAHFDDDATMMKG
                                                ** *       *                                          .

BenB    RVFRIKTERSSATMPDTRTAHNISNIEVESRDGLQITVRFNWNTLSFRYK---NSYSYFGMSRYVI--DFSGEQPKILSKYVMLKNDYINQVIDIYHI
XylY    RVFRIKTERSSATIPDTRTSHNISNLELLEQSDGVCKLRYNWHTMNYRYK---TVDHFFGTNFCTL--DTCGETPLITAKKVVLKNDYIRQVIDVYHV
NdoC    RVEHQLDPQNWGNSPKLRFTRFITNVQAAMDVNDKELLHIRSNVILHRARRGNQVDVFYAAREDKWKRGEGGVR-KLVQRFVDYPERILQTHNLMVFL
BnzB(P2) RLRKITSDVSWSENPASRTRHLVSNVMI-VGAEAEGEYEISSAFIVYRNRLERQLDIFAGERRDTLRRNTSEAGFEIVNRTILIDQSTILANNLSFFF
TodC2   RLRKITSDVSWSENPASRTRHLVSNVMI-VGAEAEGEYEISSAFIVYRNRLERQLDIFAGERRDTLRRNTSEAGFEIVNRTILIDQSTILANNLSFFF
        *               * *     *                 *
```

FIG. 5. Alignment of the β-subunits of the aromatic hydroxylase components. BenB, XylY, NdoC (34), BnzB (P2) (27), and TodC2 (79) are the approximately 20-kDa proteins of the benzoate, toluate, naphthalene, benzene, and toluene dioxygenases, respectively. Nine residues marked by asterisks are identical in all sequences. Dashes indicate sequence gaps.

Amino acid sequence similarities were also discovered among BenB, XylY, NdoC (34), BnzB (P2) (27), and TodC2 (79) (Fig. 5). In the aligned sequences of BenB and XylY, 56% of the amino acids were identical. In pairwise comparisons of BenB with each of the other sequences shown in Fig. 5, 16 to 18% of the amino acids were identical. Although these values are relatively low, the sequence similarities were shown to be significant by the method of Needleman and Wunsch (40), with similarity scores above 4.2. Each of these proteins is an approximately 20-kDa β-subunit of a hydroxylase, and nine residues, marked by asterisks in Fig. 5, were found to be invariant among the protein sequences.

The BenC and XylZ electron transfer components were compared with both ferredoxins and oxidoreductases. BenC was similar to XylZ (49% identical residues) but not to any components of the aromatic dioxygenases with two-protein electron transfer systems. Homology was detected, however, between BenC and XylA, a protein component of xylene monooxygenase (62) (Fig. 6). XylA may be involved in the transfer of electrons from NADH to XylM, the hydroxylase component of this two-subunit monooxygenase. The BenC and XylA sequence similarities extended throughout the entire length of the proteins; 28% of the aligned residues were identical.

As shown in Fig. 6 and 7, the N-terminal region of BenC was found to resemble chloroplast-type ferredoxins. Residues important for ferredoxin structure and function (4, 49) were conserved in BenC, including the four cysteine residues which coordinate [2Fe-2S] clusters. In addition, this ferredoxinlike region of BenC was similar to the C-terminal region of VanB, a 33-kDa protein involved in vanillate demethylation (5) (Fig. 6). In this region, 24% of the aligned VanB and BenC amino acid residues were identical, including those, like the four cysteines, which are conserved among chloroplast-type ferredoxins.

The C-terminal region of BenC was found to be homologous to the C-terminal regions of ferredoxin-$NADP^+$ reductases from spinach (30) and from *Spirulina* species (77). In the alignment shown in Fig. 6, 20% of the BenC C-terminal residues were identical to those of a ferredoxin reductase. A stretch of roughly 130 amino acids between positions 190 and 320 of BenC was also found to resemble a similarly sized region of two other oxidoreductases: NADPH-cytochrome P-450 reductase isolated from *Saccharomyces cerevisiae* (72), pigs (18), rats (50), and rabbits (31); and NADPH-sulfite reductase isolated from *E. coli* and *Salmonella typhimurium* (46, 48). In this region, the identity between BenC amino acid residues and those of each aligned oxidoreductase was 21 to 37%. The regions of strongest homology, shown in Fig. 8, may be involved in NAD(P) and FAD binding.

DISCUSSION

Nonaromatic *cis*-diols are common intermediates in the degradation of a wide variety of aromatic compounds. Such diols are usually formed by reactions catalyzed by multicomponent dioxygenases. All the hydroxylating dioxygenases studied to date have been composed of a hydroxylase component, usually composed of nonidentical α- and β-subunits, and a one- or two-protein electron transfer system (9). In this study, we compared the sequences encoding *A. calcoaceticus* benzoate 1,2-dioxygenase with those of the *P. putida* pWW0 TOL plasmid encoding toluate 1,2-dioxygenase. In addition, comparisons were made with sequences for functionally related enzymes.

The hydroxylase components of various multicomponent dioxygenases were found to be similar. The sizes of the α and β subunits in the different dioxygenases discussed are roughly 50 and 20 kDa, respectively. A comparison of the amino acid sequences of the benzoate, toluate, benzene, toluene, and naphthalene 1,2-dioxygenases suggested that the α-subunits and the β-subunits are each derived from common ancestors. The conservation of amino acid sequences was strongest in the N-terminal region of the α-polypeptides. This region may be responsible for common hydroxylase functions such as recognition and activation of two oxidizable carbons of the aromatic ring, reception of electrons from the electron transfer components, binding to the β-subunit, and binding and activation of oxygen.

The binding of oxygen, which usually involves metal cofactors, may be mediated by mononuclear Fe(II). One such iron was shown to be associated with each α-subunit of the benzoate 1,2-dioxygenase from *P. arvilla* (75). The iron atom is likely to be coordinated by tyrosine and histidine residues of the polypeptide. Five invariant histidines and two invariant tyrosines were detected in the alignment of the five α-subunits (Fig. 3). Some of these residues may be involved in iron binding.

The arrangement of two of the invariant histidines with two conserved cysteine residues (Fig. 4), however, sug-

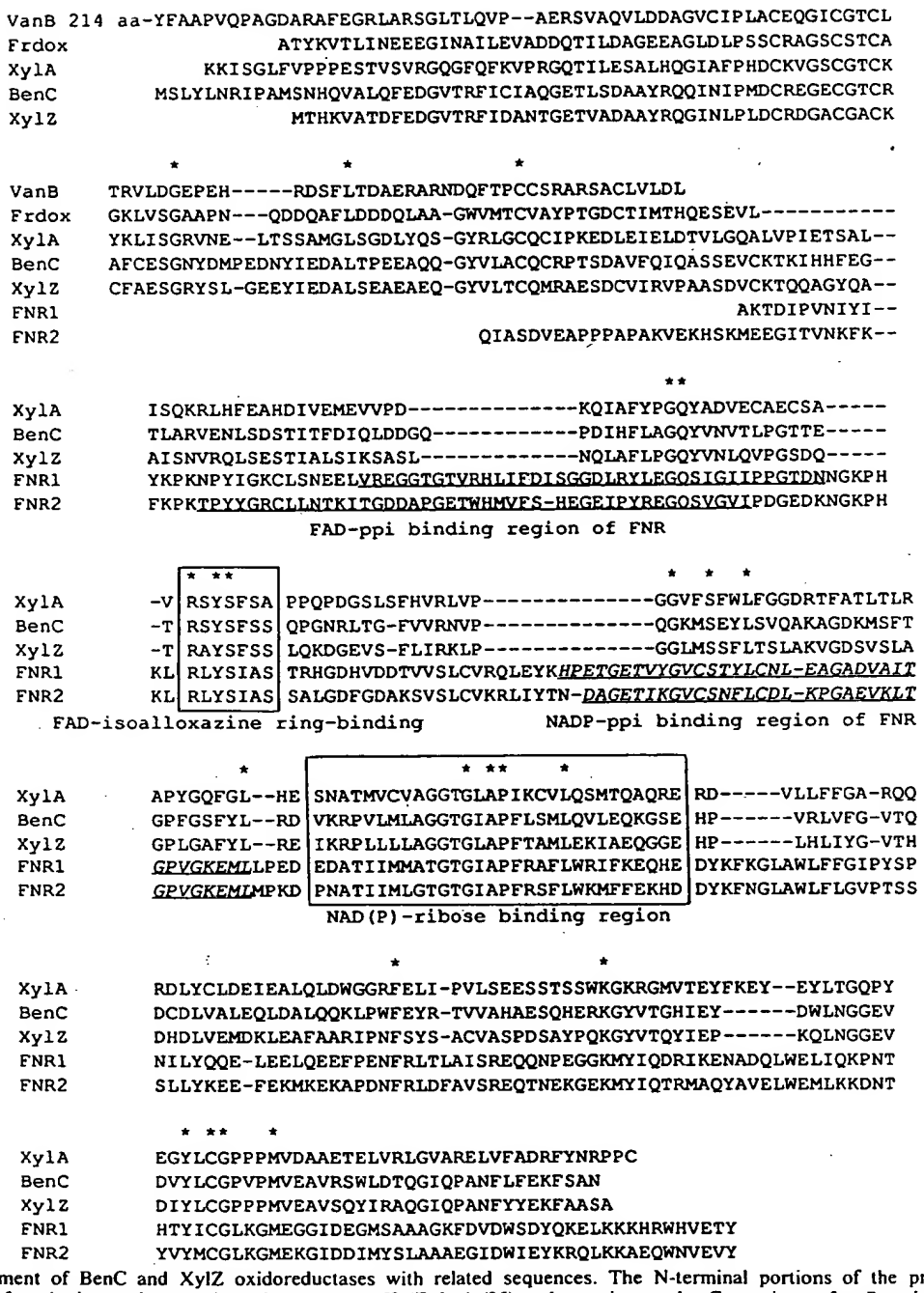

FIG. 6. Alignment of BenC and XylZ oxidoreductases with related sequences. The N-terminal portions of the proteins resemble chloroplast-type ferredoxins such as *Aphanothece sacrum* II (Frdox) (25) and a region at the C terminus of a *Pseudomonas* vanillate demethylase component (VanB) (5). The C-terminal regions of BenC and XylZ resemble ferredoxin-$NADP^+$ oxidoreductases from *Spirulina* species (FNR1) (77) and spinach (FNR2) (30). XylA, a component of xylene monooxygenase (62), is similar throughout the length of the proteins. Boxes indicate possible FAD-isoalloxazine ring- and NAD(P)-ribose-binding regions. Portions of FNR1 and -2 which may bind the FAD-PP_i moiety are underlined. Portions of FNR1 and -2 which may bind the NADP-PP_i moiety are underlined and italicized. Asterisks indicate identical residues in the aligned sequences, and dashes indicate gaps.

gested that these particular residues are involved in the coordination of a Rieske-type (53) iron-sulfur cluster. The biochemical study of benzoate 1,2-dioxygenase demonstrated that one [2Fe-2S] iron-sulfur center is associated with each α-subunit (75). Iron-sulfur center binding is mediated by four cysteines in proteins such as ferredoxins, whereas coordination is mediated by two cysteines and two histidines in Rieske iron-sulfur proteins (11, 15). These small (roughly 20-kDa) electron transport proteins are characterized by a relatively high redox potential (67).

```
                   *         *   *   * *     *       *        * *        *                *     *       *
BenC     40 AYRQQINIPMD  C  REGE  C  GT  C  RAFCESGNYDMPEDNYIEDALTPEEAQQGYVLA  C  QCRPTSDAVFQIQASSE 110
XylZ     29 AYRQGINLPLD  C  RDGA  C  GA  C  KCFAESGRYSL-GEEYIEDALSEAEAEQGYVLT  C  QMRAESDCVIRVPAASD 98
fer1     31 AEEQGIELPYS  C  RAGA  C  ST  C  AGKVLSGTIDQSEQSFLDD----DQMGAGFLLT  C  VAYPTSDCKVQTHAEDD 96
fer2     36 AEEQGYDLPFS  C  RAGA  C  ST  C  AGKLVSGTVDQSDQSFLDD----DQIEAGYVLT  C  VAYPTSDVTIQTHKEED 102
fer3    198 AEEQGIDLPYS  C  RAGA  C  ST  C  AGKVVSGTVDQSDQSFLDD----DQIAAGFVLT  C  VAYPTSDVTIETHKEED 264
fer4     30 AEEEGIELPYS  C  RAGA  C  ST  C  AGKVTEGTVDQSDQSFLDD----EQMLKGYVLT  C  IAYPESDCTILTHVEQE 96
fer5     30 AEEAGLDLPYS  C  RAGA  C  ST  C  AGTITSGTIDQSDQSFLDD----DQIEAGYVLT  C  VAYPTSDCTIKTHQEEG 96
fer6     30 AEEAGLDLPYS  C  RAGA  C  ST  C  AGKITSGSIDQSDQSFLDD----DQIEAGYVLT  C  VAYPTSDCTIQTHQEEG 96
fer7     30 AEEAGLDLPYS  C  RAGA  C  ST  C  AGKIKSGTVDQSDQSFLDD----DQIEAGYVLT  C  VAYPTSDCTIETHKEEL 96
fer8     29 AEEAGLDLPYS  C  RAGA  C  ST  C  AGKLVTGTIDQSDQSFLDD----DQVEAGYVLT  C  VAYPTSDVTIETHKEED 95
fer9     28 AEEAGLDLPYS  C  RAGA  C  ST  C  AGKITAGSVDQSDQSFLDD----DQIEAGYVLT  C  VAYPTSDCTIETHKEED 94
fer10    52 AEAQGYDWPFS  C  RAGA  C  AN  C  ASIVKEGEIDMDMQQILSDE---EVEEKDVRLT  C  IGSPAADEVIVYNAKHL 119
```

FIG. 7. The N-terminal regions of the BenC and XylZ electron transfer proteins resemble chloroplast-type ferredoxins (fer1 to -10). Conserved cysteines which bind a [2Fe-2S] center are enclosed in boxes. Additional conserved residues are indicated by asterisks, and gaps are marked by dashes. Ferredoxins 1 to 10 are from the following organisms: 1, *Bumilleriopsis filiformis* (26); 2, *Anabaena variabilis* (68); 3, *Anacystis nidulans* (52); 4, *Porphyra umbilicalis* (64); 5, *Spirulina platensis* (23); 6, *Spirulina maxima* (65); 7, *Chlorogloeopsis fritschia* (63); 8, *Aphanizomenon flos-aquae* (36); 9, *Synechocystis* sp. (22); 10, *Halobacterium halobium* (24).

The amino acid alignment shown in Fig. 4 substantiates the idea that the hydroxylase α-subunits of the benzoate, toluate, benzene, toluene, and naphthalene dioxygenases are all Rieske-type iron-sulfur proteins. This suggestion has been made previously on the basis of the physical properties of some of the dioxygenases (11). Spectroscopic studies of the functionally similar phthalate dioxygenase from *Pseudomonas cepacia* have clearly shown that in this enzyme, two histidines coordinate a [2Fe-2S] Rieske-type cluster (15). The specific residues involved in iron-sulfur binding by Rieske proteins have not previously been identified, but the sequence alignment presented in Fig. 4 suggests that they would be the conserved amino acids which are enclosed in boxes in the figure.

The low degree of homology detected among the five β-subunits of the hydroxylase components suggested that these subunits are not directly involved in the common catalytic functions of the dioxygenases. The product of the *xylY* gene, the β-subunit of toluate 1,2-dioxygenase, appears to be important for the determination of the substrate specificity of this enzyme (21). Of the nine conserved residues among the β-subunits, five are charged amino acids. It is possible that, as for the association between cytochromes *c* and b_5 (70), the charged amino acids play a role in the association between the α- and β-subunits of the hydroxylases.

The sizes and numbers of the electron transfer components of the multicomponent aromatic oxygenases vary. A comparison of the available sequences of electron transfer components suggested that variation reflects different evolutionary ancestry of the electron transfer proteins. In the naphthalene, toluene, and benzene 1,2-dioxygenases, two redox proteins are involved in the transfer of electrons from NADH to the hydroxylase component. One is a flavoprotein that has NADH oxidase activity, and the other is a ferredoxin, which has one Rieske-type [2Fe-2S] cluster. In the benzoate and toluate 1,2-dioxygenases, a single protein that contains both flavin and a [2Fe-2S] center performs the electron transfer. BenC and XylZ were each found to have a ferredoxinlike N-terminal region and an oxidoreductaselike C-terminal region (Fig. 6). Neither of these regions appeared to be homologous to their functional counterparts in the toluene and benzene dioxygenase systems.

The benzoate and toluate dioxygenases use a chloroplast-type ferredoxin for transferring electrons to the terminal hydroxylase. As shown in Fig. 7, the N-terminal regions of BenC and XylZ are homologous to chloroplast-type ferredoxins. Many residues in the 12 aligned sequences are identical, including the four cysteines which coordinate a [2Fe-2S] center in the ferredoxins (49). Similar examples of a ferredoxinlike region occurring within a larger protein were found in two monooxygenase components, VanB (5) and XylA (62) (Fig. 6). In VanB, the ferredoxinlike region occurs in the C-terminal portion of the protein. Most examples to

```
      Possible NAD-ribose binding            Possible FAD-isoalloxazine ring
       region of BenC and XylZ               binding region of BenC and XylZ

BenC        220 KRPVLMLAGGTGIAPFLSMLQVL
                ***:*:******:***   **   :
XylZ        207 KRPLLLLAGGTGLAPFTAMLEKI         BenC        167 RSYSFSS
                   **:*:: *******    :*         XylZ        153 RAYSFSS
SR(E.c.)    452 ETPVIMIGPGTGIAPFRAFMQQR         SR(S.t.)    386 RLYSIAS
                   **:*:: ******* *  :*         SR(E.c.)    386 RLYSIAS
SR(S.t.)    452 ETPVIMIGPGTGIAPFRSFMQQR         P450R(rat)  454 RYYSIAS
                   **:*:: ***:***::  :*         P450R(pig)  453 RYYSIAS
P450R(pig)  524 TTPVIMVGPGTGVAPFIGFIQER         b5R          66 RPYTPIS
                   **:*:: *******::  :*
P450R(rat)  525 TTPVIMVGPGTGIAPFMGFIQER
                  *: *** **:* * * ***
VanB        104 SSRSLLFAGGIGITPILAMAQVL
                  : * *:****** * *   : ::
b5R         146 VKSVGMIAGGTGITPMLQVIRAI
```

FIG. 8. Possible NAD- and FAD-binding regions of aromatic dioxygenase flavoproteins BenC, XylZ, BnzD (P4) (27), and TodA (79). Possible cofactor-binding regions of BenC and XylZ are aligned with those of sulfite reductase of *E. coli*, [SR(E.c.)] and *S. typhimurium* [SR(S.t.)] (46), cytochrome P-450 oxidoreductase of pig, [P450R(pig)] (18) and rat [P450R(rat)] (50), vanillate demethylase (VanB) (5), and cytochrome b_5 reductase (b5R) (33). An asterisk above a residue indicates identity with the BenC amino acid; a colon indicates similarity.

date of ferredoxinlike segments in larger proteins involve "bacterial-type" [4Fe-4S] centers in complex membrane proteins (4).

The benzene, naphthalene, and toluene dioxygenases have separate electron transport proteins that resemble Rieske iron-sulfur proteins. Each of these dioxygenases has a small 12- to 15-kDa electron transfer component containing a [2Fe-2S] center (27, 34, 38, 79). Previous observations of redox potential and spectroscopic properties suggested that these small proteins were unlike previously characterized ferredoxins (38). Some similarities to Rieske iron-sulfur proteins have been noted (17, 61). As shown in Fig. 4, similar alignments of two cysteines and two histidines in the Rieske-type hydroxylase components, the Rieske iron-sulfur proteins, and the toluene, naphthalene, and benzene "ferredoxin" components suggest that these electron transport proteins of the dioxygenases are more similar to Rieske iron-sulfur proteins than to other ferredoxins.

The protein components of benzoate and toluate dioxygenases involved in NADH oxidation are dissimilar to those of the benzene and toluene dioxygenases. The similarities observed between the BenC and XylZ C-terminal regions and a number of oxidoreductases (Fig. 6 and 8) suggested that these portions of the proteins are responsible for direct interaction with NADH. One of the oxidoreductases resembling BenC and XylZ is the NADPH-sulfite reductase involved in cysteine biosynthesis (46, 48). It is interesting that homology has previously been found between two regulatory proteins, one controlling transcription of the genes for sulfite reductase in *E. coli* and *S. typhimurium* (47) and the other controlling transcription of genes needed for benzoate metabolism in *A. calcoaceticus* (41).

Sequence comparisons failed to reveal significant similarity between BenC and the reductase components of the benzene and toluene dioxygenases that closely resemble each other (27, 79). We found two regions of roughly 30 amino acids in BnzD (P4) and TodA, identical in both proteins, which fit the consensus sequence (55, 71) for a secondary structure βαβ-fold. These regions, which are likely to be involved in binding FAD and NAD, start at amino acid positions 3 and 145 in the protein sequences of BnzD (P4) and TodA. No sequences within BenC or XylZ fit this consensus sequence, although regions involved in cofactor binding by these proteins may still have βαβ-type secondary structures.

The most highly conserved regions in the alignments of BenC and XylZ with FAD- and NAD(P)-binding oxidoreductases are likely to be those of cofactor binding (Fig. 6 and 8). The regions shown in Fig. 8 which are comparable to that of BenC near amino acid position 220 have previously been suggested to play a role in NADP-ribose binding (18, 46, 50). The additional short, highly conserved region depicted in Fig. 8 has previously been suggested to be part of a region which binds the FAD isoalloxazine ring in spinach ferredoxin-$NADP^+$ reductase and cytochrome P-450 reductase (30, 50, 72).

The regions of the ferredoxin reductases underlined in Fig. 6 may play a role in binding FAD-PP_i and NAD(P)-PP_i moieties (50). The underlined ferredoxin reductase sequences and those of BenC and XylZ are similar, with six amino acids identical in all aligned sequences and with 27% of the BenC amino acid residues identical to those of a reductase. Gaps have been introduced in the sequence alignments, however, and the role these regions play in cofactor binding by BenC or XylZ remains to be determined.

Although the sequence of the oxidoreductase of the naphthalene dioxygenase is not presently available, biochemical studies suggest that this protein is similar to the benzoate and toluate dioxygenase oxidoreductases (16). The sizes of these three proteins are similar, and spectroscopic studies of the NADH-ferredoxin$_{NAP}$ reductase suggest that it is a flavin protein with a [2Fe-2S] chloroplast-type ferredoxin. This chloroplast-type ferredoxin functions in conjunction with the separate Rieske-type ferredoxin$_{NAP}$ protein. The naphthalene dioxygenase system, therefore, appears to be unique in having two proteins and three redox centers for the transfer of electrons to the terminal hydroxylase.

The xylene monooxygenase (62) also has an electron transport component like those of the benzoate and toluate dioxygenases (Fig. 6). The hydroxylating region of this monooxygenase, however, was not found to be similar to the hydroxylase components of the dioxygenases which are related to each other. It therefore appears that there are at least two classes of oxygenase components and at least three classes of electron transfer components in multicomponent oxygenases. The partnerships of hydroxylase and electron transfer components seem to have changed during the course of evolution.

ACKNOWLEDGMENTS

This research was supported by grants to L.N.O. from the Army Research Office, the Celgene Corporation, and the National Science Foundation. Research in the laboratory of S.H. was supported by the Swiss National Science Foundation.

We thank David P. Ballou for helpful discussion.

REFERENCES

1. **Andersson, S. G. E., and C. G. Kurland.** 1990. Codon preferences in free-living microorganisms. Microbiol. Rev. **54**:198–210.
2. **Axcell, B. C., and P. J. Geary.** 1975. Purification and some properties of a soluble benzene-oxidizing system from a strain of *Pseudomonas*. Biochem. J. **146**:173–183.
3. **Beckman, J. D., P. O. Ljungdahl, J. L. Lopez, and B. L. Trumpower.** 1987. Isolation and characterization of the nuclear gene encoding the Rieske iron-sulfur protein (RIP1) from *Saccharomyces cerevisiae*. J. Biol. Chem. **262**:8901–8909.
4. **Beinert, H.** 1990. Recent developments in the field of iron-sulfur proteins. FASEB J. **4**:2483–2491.

4a. **Bethesda Research Laboratories.** 1989. M13 cloning/dideoxy sequencing instruction manual. Bethesda Research Laboratories, Inc., Gaithersburg, Md.

5. **Brunel, F., and J. Davison.** 1988. Cloning and sequencing of *Pseudomonas* genes encoding vanillate demethylase. J. Bacteriol. **171**:4924–4930.
6. **Chen, Y.-C. J., O. P. Peoples, and C. T. Walsh.** 1988. *Acinetobacter* cyclohexanone monooxygenase: gene cloning and sequence determination. J. Bacteriol. **170**:781–789.
7. **Chou, P. Y., and G. D. Fasman.** 1978. Prediction of the secondary structure of proteins from their amino acid sequence. Adv. Enzymol. **47**:45–148.
8. **Cleton-Jansen, A.-M., N. Goosen, K. Vink, and P. van de Putte.** 1989. Cloning, characterization and DNA sequencing of the gene encoding the M_r 50,000 quinoprotein glucose dehydrogenase from *Acinetobacter calcoaceticus*. Mol. Gen. Genet. **217**: 430–436.
9. **Dagley, S.** 1986. Biochemistry of aromatic hydrocarbon degradation in pseudomonads, p. 527–555. *In* J. R. Sokatch (ed.), The bacteria, vol. 10. Academic Press, Inc., New York.
10. **Davidson, E., and F. Daldal.** 1987. *fbc* operon, encoding the Rieske Fe-S protein cytochrome *b* and cytochrome *c1* apoproteins previously described from *Rhodopseudomonas sphaeroides*, is from *Rhodopseudomonas capsulata*. J. Mol. Biol. **195**: 25–29.
11. **Fee, J. A., K. L. Findling, T. Yoshida, R. Hille, G. E. Tarr, D. O. Hearshen, W. R. Dunham, E. P. Day, T. A. Kent, and E.**

Munck. 1984. Purification and characterization of the Rieske iron-sulfur protein from *Thermus thermophilus*. J. Biol. Chem. 259:124–133.
12. Fickett, J. W. 1982. Recognition of protein coding regions in DNA sequences. Nucleic Acids Res. 10:5303–5318.
13. Gatz, C., and W. Hillen. 1986. *Acinetobacter calcoaceticus* encoded mutarotase: nucleotide sequence analysis of the gene and characterization of its secretion in *Escherichia coli*. Nucleic Acids Res. 14:2891–2903.
14. Goosen, N., H. P. A. Horsman, R. G. M. Huinen, and P. van de Putte. 1989. *Acinetobacter calcoaceticus* genes involved in biosynthesis of the coenzyme pyrrolo-quinoline-quinone: nucleotide sequence and expression in *Escherichia coli* K-12. J. Bacteriol. 171:447–455.
15. Gurbiel, R. J., C. J. Batie, M. Sivaraja, A. E. True, J. A. Fee, B. M. Hoffman, and D. P. Ballou. 1989. Electron-nuclear double resonance spectroscopy of ^{15}N-enriched phthalate dioxygenase from *Pseudomonas cepacia* proves that two histidines are coordinated to the [2Fe-2S] Rieske-type clusters. Biochemistry 28:4861–4871.
16. Haigler, B. E., and D. T. Gibson. 1990. Purification and properties of NADH-ferredoxin$_{NAP}$ reductase, a component of naphthalene dioxygenase from *Pseudomonas* sp. strain NCIB 9816. J. Bacteriol. 172:457–464.
17. Haigler, B. E., and D. T. Gibson. 1990. Purification and properties of ferredoxin$_{NAP}$, a component of naphthalene dioxygenase from *Pseudomonas* sp. strain NCIB 9816. J. Bacteriol. 172:465–468.
18. Haniu, M., T. Iyanagi, P. Miller, T. D. Lee, and J. E. Shively. 1986. Complete amino acid sequence of NADPH-cytochrome P-450 reductase from porcine hepatic microsomes. Biochemistry 25:7906–7911.
19. Harayama, S., and M. Rekik. 1990. The meta cleavage operon of TOL degradative plasmid pWW0 comprises 13 genes. Mol. Gen. Genet. 221:113–120.
20. Harayama, S., M. Rekik, A. Bairoch, E. L. Neidle, C. Hartnett, and L. N. Ornston. Submitted for publication.
21. Harayama, S., M. Rekik, and K. N. Timmis. 1986. Genetic analysis of a relaxed substrate specificity aromatic ring dioxygenase, toluate 1,2-dioxygenase, encoded by TOL plasmid pWWO of *Pseudomonas putida*. Mol. Gen. Genet. 202:226–234.
22. Hase, T., K. Inoue, H. Matsubara, M. M. Williams, and L. J. Rogers. 1982. Amino acid sequence of *Synechocystis* 6714 ferredoxin: a unique structural feature of unicellular blue-green algal ferredoxin. J. Biochem. 92:1347–1355.
23. Hase, T., K. Wada, M. Ohmiya, and H. Matsubara. 1976. Amino acid sequence of the major component of *Nostoc muscorum* ferredoxin. J. Biochem. 80:993–999.
24. Hase, T., S. Wakabayashi, H. Matsubara, L. Kerscher, D. Oesterhelt, K. K. Rao, and D. O. Hall. 1978. Complete amino acid sequence of *Halobacterium halobium* ferredoxin containing an *N*-acetyllysine residue. J. Biochem. 83:1657–1670.
25. Hase, T., S. Wakabayashi, K. Wada, and H. Matsubara. 1978. Amino acid sequence of *Aphanothece sacrum* ferredoxin II (minor component). Structural characteristics and evolutionary implications. J. Biochem. 83:761–770.
26. Inoue, K., T. Hase, P. Boger, and H. Matsubara. 1983. Amino acid sequence of a ferredoxin from *Bumilleriopsis filiformis*, a yellow-green alga: relationship with red algae, Protoflorideophyceae, and filimentous blue-green algae. J. Biochem. 94: 1451–1455.
27. Irie, S., S. Doi, T. Yorifuji, M. Takagi, and K. Yano. 1987. Nucleotide sequencing and characterization of the genes encoding benzene oxidation enzymes of *Pseudomonas putida*. J. Bacteriol. 169:5174–5179.
28. Juni, E. 1978. Genetics and physiology of *Acinetobacter*. Annu. Rev. Microbiol. 32:349–371.
29. Juni, E., and A. Janik. 1969. Transformation of *Acinetobacter calcoaceticus* (*Bacterium anitratum*). J. Bacteriol. 98:281–288.
30. Karplus, P. A., A. Walsh, and J. R. Herriott. 1984. Amino acid sequence of spinach ferredoxin:NADP$^+$ oxidoreductase. Biochemistry 23:6576–6583.
31. Katagiri, M., H. Murakami, Y. Yabusaki, T. Sugiyama, M. Okamoto, T. Yamano, and H. Ohkawa. 1986. Molecular cloning and sequence analysis of full-length cDNA for rabbit liver NADPH-cytochrome P-450 reductase mRNA. J. Biochem. 100: 945–954.
32. Kolaskar, A. S., and B. V. Reddy. 1985. A method to locate protein coding sequences in DNA of prokaryotic systems. Nucleic Acids Res. 13:185–194.
33. Kuma, F., and H. Inomata. 1972. Studies on methemoglobin reductase. J. Biol. Chem. 247:556–560.
34. Kurkela, S., H. Lehvaslaiho, E. Tapio Palva, and T. H. Teeri. 1988. Cloning, nucleotide sequence and characterization of genes encoding naphthalene dioxygenase of *Pseudomonas putida* strain NCIB9816. Gene 73:355–362.
35. Kurowski, B., and B. Ludwig. 1987. The genes of the *Paracoccus denitrificans* bc_1 complex. J. Biol. Chem. 262:13805–13811.
36. Lee, I. S., T. Hase, H. Matsubara, K. H. Kwok, and D. W. Krogmann. 1983. Amino acid sequence of ferredoxin I from *Aphanizomenon flos-aquae*. Biochim. Biophys. Acta 744:53–56.
37. Lipman, D. J., and W. R. Pearson. 1985. Rapid and sensitive protein similarity searches. Science 227:1435–1441.
38. Morrice, N., P. Geary, R. Cammack, A. Harris, F. Beg, and A. Aitken. 1988. Primary structure of protein B from *Pseudomonas putida*, member of a new class of 2Fe-2S ferredoxins. FEBS Lett. 231:336–340.
39. Nakazawa, T., and T. Yokota. 1973. Benzoate metabolism in *Pseudomonas putida* (*arvilla*) mt-2: demonstration of two benzoate pathways. J. Bacteriol. 115:262–267.
40. Needleman, S. B., and C. D. Wunsch. 1970. A general method applicable to the search for similarities in the amino acid sequence of two proteins. J. Mol. Biol. 48:443–453.
41. Neidle, E. L., C. Hartnett, and L. N. Ornston. 1989. Characterization of *Acinetobacter calcoaceticus catM*, a repressor gene homologous in sequence to transcriptional activator genes. J. Bacteriol. 171:5410–5421.
42. Neidle, E. L., M. K. Shapiro, and L. N. Ornston. 1987. Cloning and expression in *Escherichia coli* of *Acinetobacter calcoaceticus* genes for benzoate degradation. J. Bacteriol. 169:5496–5503.
43. Nishikimi, M., Y. Hosokawa, H. Toda, H. Suzuki, and T. Ozawa. 1989. Cloning and sequence analysis of a cDNA encoding the Rieske iron-sulfur protein of rat mitochondrial cytochrome *bc*-1 complex. Biochem. Biophys. Res. Commun. 159:19–25.
44. Normark, S., S. Bergstrom, T. Edlund, T. Grundstrom, B. Jaurin, F. P. Lindberg, and O. Olsson. 1983. Overlapping genes. Annu. Rev. Genet. 17:499–525.
45. Ornston, L. N., and E. L. Neidle. Evolution of genes for the β-ketoadipate pathway in *Acinetobacter calcoaceticus*. *In* K. J. Towner, E. Bergogne-Berezin, and C. A. Fewson (ed.), The biology of *Acinetobacter*. FEMS Symposium Series. Plenum Press, New York, in press.
46. Ostrowski, J., M. J. Barber, D. C. Rueger, B. E. Miller, L. M. Siegel, and N. M. Kredich. 1989. Characterization of the flavoprotein moieties of NADPH-sulfite reductase from *Salmonella typhimurium* and *Escherichia coli*. J. Biol. Chem. 264:15796–15808.
47. Ostrowski, J., G. Jagura-Burdzy, and N. M. Kredich. 1987. DNA sequences of the *cysB* regions of *Salmonella typhimurium* and *Escherichia coli*. J. Biol. Chem. 262:5999–6005.
48. Ostrowski, J., J.-Y. Wu, D. C. Ruegger, B. E. Miller, L. M. Siegel, and N. M. Kredich. 1989. Characterization of the *cysJIH* regions of *Salmonella typhimurium* and *Escherichia coli* B. J. Biol. Chem. 264:15726–15737.
49. Otaka, E., and T. Ooi. 1989. Examination of protein sequence homologies. V. New perspectives on evolution between bacterial and chloroplast-type ferredoxins inferred from sequence evidence. J. Mol. Evol. 29:246–254.
50. Porter, T. D., and C. B. Kasper. 1986. NADPH-cytochrome P-450 oxidoreductase: flavin mononucleotide and flavin adenine dinucleotide domains evolved from different flavoproteins. Biochemistry 25:1682–1687.
51. Reiner, A. M. 1971. Metabolism of benzoic acid by bacteria: 3,5-cyclohexadiene-1,2-diol-1-carboxylic acid is an intermediate in the formation of catechol. J. Bacteriol. 108:89–94.

52. **Reith, M. E., D. E. Laudenbach, and N. A. Sraus.** 1986. Isolation and nucleotide sequence analysis of the ferredoxin I gene from the cyanobacterium *Anacystis nidulans* R2. J. Bacteriol. **168:** 1319–1324.
53. **Rieske, J. S., D. H. MacLennan, and R. Coleman.** 1964. Isolation and properties of an iron-protein from the (reduced coenzyme Q)-cytochrome C reductase complex of the respiratory chain. Biochem. Biophys. Res. Commun. **15:**338–344.
54. **Ross, C. M., J. B. Kaplan, M. E. Winkler, and B. P. Nichols.** 1990. An evolutionary comparison of *Acinetobacter calcoaceticus trpF* with *trpF* genes of several organisms. Mol. Biol. Evol. **7:**74–81.
55. **Rossman, M. G., D. Moras, and K. W. Olsen.** 1974. Chemical and biological evolution of a nucleotide-binding protein. Nature (London) **250:**194–199.
56. **Sanger, F., S. Nicklen, and A. R. Coulson.** 1977. Nucleotide sequencing with chain-terminating inhibitors. Proc. Natl. Acad. Sci. USA **74:**5463–5467.
57. **Shepherd, J. C.** 1981. Method to determine the reading frame of a protein from the purine/pyrimidine genome sequence and its possible evolutionary justification. Proc. Natl. Acad. Sci. USA **78:**1596–1600.
58. **Shine, J., and L. Dalgarno.** 1975. Determination of cistron specificity in bacterial ribosomes. Nature (London) **254:**34–38.
59. **Stanier, R. Y., and L. N. Ornston.** 1973. The beta-ketoadipate pathway. Adv. Microb. Physiol. **9:**89–151.
60. **Subramanian, V., T.-N. Liu, W.-K. Yeh, M. Narro, and D. T. Gibson.** 1981. Purification and properties of NADH-ferredoxin TOL reductase. A component of toluene dioxygenase from *Pseudomonas putida*. J. Biol. Chem. **256:**2723–2730.
61. **Subramanian, V., T.-N. Liu, W.-K. Yeh, C. M. Serdar, L. P. Wackett, and D. T. Gibson.** 1985. Purification and properties of ferredoxin$_{TOL}$. J. Biol. Chem. **260:**2355–2363.
62. **Suzuki, M., T. Hayakawa, J. P. Shaw, M. Rekik, and S. Harayama.** 1991. Primary structure of xylene monooxygenase: similarity to and difference from the alkane hydroxylation system. J. Bacteriol. **173:**1690–1695.
63. **Takahashi, Y., T. Hase, H. Matsubara, G. N. Hutbur, and L. J. Rogers.** 1982. Amino acid sequence of *Chlorogloepsis fritschii* ferredoxin: taxonomic and evolutionary aspects. J. Biochem. **92:**1363–1368.
64. **Takruri, I. A. H., B. G. Haslett, D. Boulter, P. W. Andrew, and L. J. Rogers.** 1978. The amino acid sequence of ferredoxin from the red alga *Porphyra umbilicalis*. Biochem. J. **173:**459–466.
65. **Tanaka, M., M. Haniu, K. T. Yasunoba, K. K. Rao, and D. O. Hall.** 1975. Modification of the automated sequence determination as applied to the sequence determination of the *Spirulina maxima* ferredoxin. Biochemistry **14:**5535–5540.
66. **Thoeny-Meyer, L., D. Stax, and H. Hennecke.** 1989. An unusual gene cluster for the cytochrome bc_1 complex in *Bradyrhizobium japonicum* and its requirement for effective root nodule symbiosis. Cell **57:**683–697.
67. **Trumpower, B.** 1981. Function of the iron-sulfur protein of the cytochrome b-c_1 segment in electron-transfer and energy conserving reactions of the mitochondrial respiratory chain. Biochim. Biophys. Acta **639:**129–155.
68. **van der Plas, J., R. P. Groot, P. J. Weisbeek, and G. A. van Arkel.** 1986. Coding sequence of a ferredoxin gene from *Anabaena variabilis* ATCC 29413. Nucleic Acids Res. **14:**7803–7806.
69. **Vieira, J., and J. Messing.** 1982. The pUC plasmids, an M13mp7-derived system for insertion mutagenesis and sequencing with synthetic universal primers. Gene **19:**259–268.
70. **Wendoloski, J. J., J. B. Mathew, P. C. Weber, and F. R. Salemme.** 1987. Molecular dynamics of a cytochrome c-cytochrome b_5 electron transfer complex. Science **238:**794–797.
71. **Wierenga, R. K., P. Terpstra, and W. G. J. Hol.** 1986. Prediction of the occurrence of the ADP-binding βαβ-fold in proteins, using an amino acid sequence fingerprint. J. Mol. Biol. **187:**101–107.
72. **Yabusaki, Y., H. Murakami, and H. Ohkawa.** 1988. Primary structure of *Saccharomyces cerevisiae* NADPH-cytochrome P450 reductase deduced from nucleotide sequence of its cloned gene. J. Biochem. **103:**1004–1010.
73. **Yamaguchi, M., and H. Fujisawa.** 1978. Characterization of NADH-cytochrome c reductase, a component of benzoate 1,2-dioxygenase system from *Pseudomonas arvilla* C-1. J. Biol. Chem. **253:**8848–8853.
74. **Yamaguchi, M., and H. Fujisawa.** 1981. Reconstitution of iron-sulfur cluster of NADH-cytochrome *c* reductase, a component of benzoate 1,2-dioxygenase system from *Pseudomonas arvilla* C-1. J. Biol. Chem. **256:**6783–6787.
75. **Yamaguchi, M., and H. Fujisawa.** 1982. Subunit structure of oxygenase component in benzoate 1,2-dioxygenase system from *Pseudomonas arvilla* C-1. J. Biol. Chem. **257:**12497–12502.
76. **Yanisch-Perron, C., J. Vieira, and J. Messing.** 1985. Improved M13 cloning vectors and host strains: nucleotide sequences of the M13mp18 and pUC19 vectors. Gene **33:**103–119.
77. **Yao, Y., T. Tamura, K. Wada, H. Matsubara, and K. Kodo.** 1984. *Spirulina* ferredoxin-NADP$^+$ reductase. The complete amino acid sequence. J. Biochem. **95:**1513–1516.
78. **Zeyer, J., P. R. Lehrbach, and K. N. Timmis.** 1985. Use of cloned genes of *Pseudomonas* TOL plasmid to effect biotransformation of benzoates to *cis*-dihydrodiols and catechols by *Escherichia coli* cells. Appl. Environ. Microbiol. **50:**1409–1413.
79. **Zylstra, G. J., and D. T. Gibson.** 1989. Toluene degradation by *Pseudomonas putida* F1. J. Biol. Chem. **264:**14940–14946.

JOURNAL OF BACTERIOLOGY, Feb. 1997, p. 919–927
0021-9193/97/$04.00+0

Vol. 179, No. 3

Characterization of the *p*-Toluenesulfonate Operon *tsaMBCD* and *tsaR* in *Comamonas testosteroni* T-2

FRANK JUNKER,[1] ROLAND KIEWITZ,[2] AND ALASDAIR M. COOK[1,2]*

Institute of Microbiology, Swiss Federal Institute of Technology, ETH-Zentrum, CH-8092 Zürich, Switzerland,[1] and Faculty of Biology, The University, D-78434 Konstanz, Germany[2]

Received 3 September 1996/Accepted 18 November 1996

***Comamonas testosteroni* T-2 uses a standard, if seldom examined, attack on an aromatic compound and oxygenates the side chain of *p*-toluenesulfonate (TS) (or *p*-toluenecarboxylate) to *p*-sulfobenzoate (or terephthalate) prior to complete oxidation. The expression of the first three catabolic enzymes in the pathway, the TS methyl-monooxygenase system (comprising reductase B and oxygenase M; TsaMB), *p*-sulfobenzyl alcohol dehydrogenase (TsaC), and *p*-sulfobenzaldehyde dehydrogenase (TsaD), is coregulated as regulatory unit R1 (H. R. Schläfli Oppenberg, G. Chen, T. Leisinger, and A. M. Cook, Microbiology [Reading] 141:1891–1899, 1995). The components of the oxygenase system were repurified, and the N-terminal amino acid sequences were confirmed and extended. An internal sequence of TsaM was obtained, and the identity of the [2Fe-2S] Rieske center was confirmed by electron paramagnetic resonance spectroscopy. We purified both dehydrogenases (TsaC and TsaD) and determined their molecular weights and N-terminal amino acid sequences. Oligonucleotides derived from the partial sequences of TsaM were used to identify cloned DNA from strain T-2, and about 6 kb of contiguous cloned DNA was sequenced. Regulatory unit R1 was presumed to represent a four-gene operon (*tsaMBCD*) which was regulated by the LysR-type regulator, TsaR, encoded by a deduced one-gene transcriptional unit. The genes for the inducible TS transport system were not at this locus. The oxygenase system was confirmed to be a class IA mononuclear iron oxygenase, and class IA can now be seen to have two evolutionary groups, the monooxygenases and the dioxygenases, though the divergence is limited to the oxygenase components. The alcohol dehydrogenase TsaC was confirmed to belong to the short-chain, zinc-independent dehydrogenases, and the aldehyde dehydrogenase TsaD was found to resemble several other aldehyde dehydrogenases. The operon and its putative regulator are compared with units of the TOL plasmid.**

Aromatic sulfonates are produced in the multimillion tonne range annually and dispersed in the environment as detergents, dyestuffs, and additives to products as diverse as ink and engine oil (24). These charged compounds are now readily found in the environment (see, e.g., reference 38); defined, naturally occurring sulfonates, usually aliphatic compounds, are also known (64; see also reference 76). At least five different mechanisms for the desulfonation of the aromatic compounds in aerobes are known (17, 21, 34, 39, 84; see also reference 16), and different organisms can have different strategies to attack, e.g., *p*-toluenesulfonate as a carbon source (21, 34, 61). There is no information on the genetics of these pathways, and in only one case is an extensive understanding of the enzymology and physiological controls available, the degradation of *p*-toluenesulfonate by *Comamonas testosteroni* T-2 (35, 42, 61).

C. testosteroni T-2, grown with toluenesulfonate as the sole source of carbon and energy, synthesizes an inducible, specific, secondary proton symport system (42) and inducible enzymes that convert toluenesulfonate (or toluenecarboxylate) to sulfobenzoate (or terephthalate) in three steps (Fig. 1) (41). These reactions require four enzymes, now termed TsaMB (*p*-toluenesulfonate methyl-monooxygenase system, comprising reductase B and oxygenase M), TsaC (*p*-sulfobenzyl alcohol dehydrogenase) and TsaD (*p*-sulfobenzaldehyde dehydrogenase), which are synthesized in one regulatory unit, termed R1 (61).

* Corresponding author. Mailing address: Faculty of Biology, The University, Universitätstr. 10, D-78434 Konstanz, Germany. Phone: 7531 88 4247. Fax: 7531 88 2966. E-mail: Alasdair.Cook@uni-konstanz.de.

The pathway (Fig. 1) bears superficial comparison with the upper pathway of the TOL plasmid (see, e.g., reference 3) and is thus representative of a major mode of attack on aromatic compounds: degradation initiated at the alkyl side chain (41). The superficiality is immediately visible at the enzyme level. Oxygenase TsaMB (strain T-2) has been attributed to the class IA multicomponent, mononuclear iron oxygenases (5, 44, 51), whereas oxygenase XylMA (TOL plasmid) belongs to a class of multicomponent, di-iron monooxygenases (65, 70); the alcohol dehydrogenases seem to belong to different classes (41, 66), and the same was believed to be true for the aldehyde dehydrogenases (41).

Whereas it is reasonable to hypothesize that regulatory unit R1 (Fig. 1) (61) represents an operon (see, e.g., references 74 and 83), it is impossible to anticipate the type of regulation involved, e.g., LysR-, XylS/AraC-, or XylR-type (33, 53, 59). In addition, the (presumptive) genes encoding the inducible transport system for toluenesulfonate may be an integral part of an operon encoding degradative enzymes (49, 80) located close to the degradative operon (52) or found at another locus (48). The transport system for toluenesulfonate does not transport toluenecarboxylate (42).

We now report more information, including two enzyme purifications (TsaC and TsaD), on the four enzymes of regulatory unit R1 in *C. testosteroni* T-2 (Fig. 1) (61), and we report that R1 is indeed an operon comprising *tsaMBCD*, which is presumably under the control of a putative transcriptional LysR-type regulator, TsaR. The genes encoding the transport system(s) are distant from this structure. This is the first report characterizing both the enzymes and the nucleotide sequence encoding the attack on the side chain of an aromatic compound.

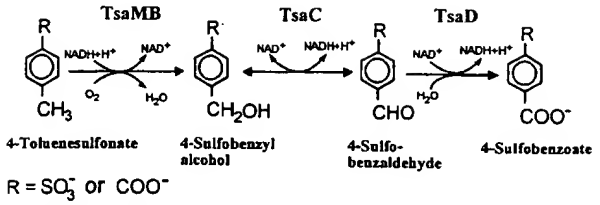

FIG. 1. The reactions catalyzed by the monooxygenase system TsaMB, the alcohol dehydrogenase TsaC, and the aldehyde dehydrogenase TsaD of regulatory unit R1 (61) of *C. testosteroni* T-2.

MATERIALS AND METHODS

Bacteria, growth conditions and plasmids. *C. testosteroni* T-2 (DSM 6577) was grown in batch culture at 30°C in mineral salts medium, pH 7.2, containing 6 mM toluenesulfonate (40). Most cells for enzyme purifications were grown in a 12.5-liter fermentor with an 8- to 10-liter working volume (Biostat V; Braun, Melsungen, Germany), harvested early (60 mg of protein/liter, to avoid problems with foaming and clumping) in a Pellikon cassette filtration system (Millipore, Neu-Isenburg, Germany), washed by centrifugation, and stored frozen, as in our earlier work (39). When vanillate or *p*-methoxybenzoate (6 mM) was used as the carbon source, the pH was adjusted to 7.0.

Escherichia coli DH5α was used as the host for pBluescript-KSII constructs and was routinely grown in Luria broth containing 100 μg of ampicillin per ml at 37°C.

Preparation of cell extracts, enzyme assays, and enzyme purifications. Cells were disrupted in a French pressure cell, and the crude extract, in 20 mM phosphate buffer (pH 7.0) with or without 1 mM dithiothreitol, was prepared as described elsewhere (39). Reductase TsaB was assayed at 25°C by the reduction of cytochrome *c* (39). Monooxygenase TsaM was assayed by oxygen uptake in a coupled assay with the reductase (40). Each component (TsaB and TsaM) was purified in two chromatographic steps, anion exchange and hydrophobic interaction (40).

Cell extract for the purification of alcohol dehydrogenase TsaC and aldehyde dehydrogenase TsaD was prepared without dithiothreitol. Activities were assayed at room temperature (21°C) by oxidation (TsaD) or reduction (TsaC) of *p*-carboxybenzaldehyde as described elsewhere (41). TsaC was purified in two chromatographic steps (anion exchange and hydrophobic interaction), essentially as described elsewhere (41). A new purification scheme for TsaD was developed, involving an anion exchange and subsequent gel filtration. The anion-exchange column (Mono Q HR 10/10; Pharmacia, Uppsala, Sweden) was equilibrated with 20 mM phosphate buffer, pH 6.8 (buffer A), and proteins were eluted with an increasing gradient of sodium sulfate (to 1 M, buffer B) at a flow rate of 4 ml/min as follows: from 0 to 40 min, 100% buffer A; from 40 to 68 min, 0 to 3% buffer B; from 68 to 130 min, 3 to 6% buffer B; from 130 to 200 min, 6 to 20% buffer B. Four-milliliter fractions were collected, and fraction 17 was worked up. In the second purification step the gel filtration column (Superose 12 HR 10/30; Pharmacia) was equilibrated with 150 mM sodium sulfate in 50 mM phosphate buffer, pH 6.8, at a flow rate of 0.5 ml/min and a sample volume of 300 μl was used.

Only the fraction of TsaC or TsaD with the highest specific activity was used for further work. Purifications were monitored by sodium dodecyl sulfate-polyacrylamide gel electrophoresis (SDS-PAGE) with Coomassie staining (37, 40). Purified protein bands were blotted to a polyvinylidenefluoride membrane (Immobilon-P; Millipore, Bedford, Mass.) and subjected to Edman degradation (39, 40).

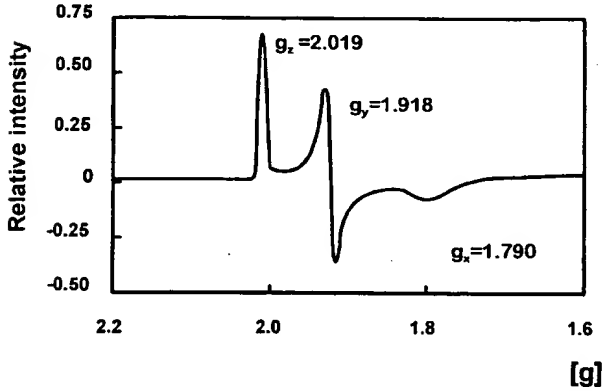

FIG. 2. EPR spectrum of the oxygenase component TsaM of monooxygenase system TsaMB from *C. testosteroni* T-2.

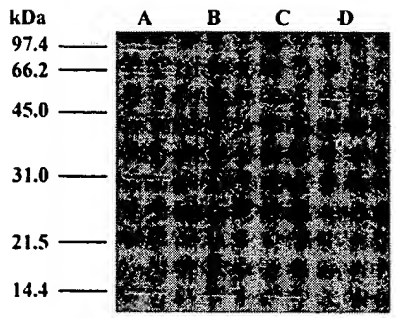

FIG. 3. SDS-PAGE, with Coomassie blue staining, of the products of purification of *p*-sulfobenzaldehyde dehydrogenase (TsaD) from *C. testosteroni* T-2. Lane A, molecular weight markers; lane B, crude extract (40 μg of protein); lane C, fraction from the anion exchanger (7 μg of protein); lane D, fraction from the gel filtration column (1 μg of protein).

Protein samples were concentrated by membrane filtration (Centricon-10; Amicon, Danvers, Mass.). The hydrophobic TsaD bound extensively to the filter unit unless the unit was first incubated overnight in 5% aqueous Tween 20 solution and then rinsed thoroughly with water.

Determinations of the molecular weights under native conditions were done with the gel filtration column. The sample volume for molecular weight markers (40) and samples was 300 μl.

EPR. Electron paramagnetic resonance (EPR) spectra of monooxygenase TsaM (about 2 mg in 0.3 ml) in the X band were recorded with an EPR 300 spectrometer (Bruker, Rheinstetten, Germany) at 10 K as described elsewhere (55).

Cyanogen bromide cleavage. Purified TsaM was separated on an SDS–12% PAGE gel, visualized by the Zn^{2+} reverse-staining method (18), and cut from the gel. The gel chip was minced, suspended in 500 μl of 0.1% CNBr, flushed with nitrogen, and allowed to react in the dark for 20 h. The reaction mixture was incubated for 2 h at 37°C with extraction solution (50% formic acid, 25% acetonitrile, 15% propanol, 10% H_2O) and then centrifuged (12,000 × *g*, 10 min). The supernatant fluid was taken to dryness in a vacuum centrifuge. The digest was dissolved in water, and protein fragments were separated by reversed-phase chromatography (ProRPC HR 10/10; Pharmacia). The column was equilibrated with 0.1% trifluoroacetic acid (0.5 ml/min), and the sample was eluted with an increasing gradient of methanol (0 to 100% in 50 min). The fragments eluted in two major peaks. All protein fragments of peak two were pooled and dried in a vacuum centrifuge. The pellet was dissolved in loading buffer and separated by SDS-PAGE in a 15% gel. Peptides were then stained with Coomassie brilliant blue. Three bands (14, 11.5, and 9.0 kDa) were identified, blotted onto a polyvinylidenefluoride membrane, and subjected to Edman degradation (see above). The N-terminal amino acids of the 9.0-kDa fragment were used to deduce an oligonucleotide probe.

Enzymes and reagents. All restriction enzymes, Klenow fragments, T4 DNA ligases, and polynucleotide kinases were obtained from Fermentas, Vilnius, Lithuania. [α-^{35}S]dATP for sequencing and [γ-^{32}P]dATP for oligonucleotide labeling were obtained from Dupont (Regensdorf, Switzerland).

All reagents for growth media and protein purification were purchased from Fluka (Buchs, Switzerland).

Preparation of total DNA and plasmid DNA. Total DNA from a 100-ml batch culture (200 mg of protein/liter of culture) of toluenesulfonate-grown *C. testosteroni* T-2 was prepared by the cetyltrimethylammonium bromide precipitation method (4). Plasmid DNA from *E. coli* was isolated with Nucleobond AX-100 columns (Macherey-Nagel, Oensingen, Switzerland).

DNA cloning, screening, sequencing, and analysis. Total DNA from strain T-2 was digested with restriction enzymes and separated in a 1% agarose gel. The DNA was blotted onto a Hybond-N nylon membrane (Amersham International, Amersham, United Kingdom). Degenerate oligonucleotide probes were 5′ labeled with [γ-^{32}P]dATP, and DNA fragments were labeled with [α-^{35}S]dATP by random oligonucleotide primers (4). Both probes were used for screening. DNA fragments were cut from the agarose gel and eluted by phenol-chloroform extraction (4). The eluted fragments were ligated into pBluescript-KSII and introduced via electroporation (4) into *E. coli* DH5α. All cloning was done with pBluescriptII.

Nucleotide sequencing of both strands was performed by the modified dideoxy chain termination method (57, 63) from double-stranded DNA templates with Sequenase (U.S. Biochemical Corp., Cleveland, Ohio), and PCR-based sequencing was performed with fluorescence-labeled nucleotides (Microsynth, Balgach, Switzerland). Nucleic acid and amino acid sequences were analyzed by using the

TABLE 1. Purification of *p*-sulfobenzyl alcohol dehydrogenase TsaC from *C. testosteroni* T-2

Purification step	Vol (ml)	Protein (μg)	Activity (nkat)	Sp act (kat/kg)	Yield (%)	Purification (fold)
Crude extract	2	45,000	6.5	0.15	100	1
Anion exchanger	4	1,300	1.8	1.4	27	9.8
Hydrophobic interaction	0.5	20	0.26	13.3	4	92

TABLE 2. Purification of *p*-sulfobenzaldehyde dehydrogenase TsaD from *C. testosteroni* T-2

Purification step	Vol (ml)	Protein (μg)	Activity (μkat)	Sp act (mkat/kg)	Yield (%)	Purification (fold)
Crude extract	2	70,700	140	2	100	1
Anion exchanger	4	648	124	192	88	96
Gel filtration	0.5	12.5	6	501	4	250

Genetics Computer Group program package (University of Wisconsin, Madison, Wis.). The evolutionary tree was generated with the CLUSTAL W program (71).

Nucleotide sequence accession number. The sequence data are available in the NCBI GenBank library under accession number U32622.

RESULTS

Biochemical characterizations and development of oligonucleotide probes for *tsaMB*. Both components of oxygenase TsaMB were repurified, and the molecular weights of the denatured proteins (43,000 and 36,000) were confirmed (40). The N-terminal amino acid sequences were confirmed and extended as follows: TsaM, MFIRNXWYVAAWDTEIPAEGL FHR; TsaB, ADVPVTVAAVRAVARDVLALELRHANGQ. The sequence of TsaM contained a suitable sequence of amino acids with low degeneracy of coding. The sequence of TsaB did not, and the amino acid composition (39), largely amino acids with high degeneracy of coding, implied that no such sequence could be expected. We therefore sequenced an internal fragment of TsaM to be able to derive a second oligonucleotide probe: $TsaM_{int}$, KPGYIHYQANYKLIVDNLLDFTHLAXV HPT.

The flavin content of the reductase component, TsaB, was consistent with the yellow color of the protein, and the ability of the protein to reduce cytochrome *c* indicated its [2Fe-2S] ferredoxin component (see reference 39). The nature of the [2Fe-2S] center in monooxygenase TsaM was presumed from its UV spectrum to be a Rieske center. We have now used EPR spectroscopy (Fig. 2; Table 4) to confirm the presence of the Rieske [2Fe-2S] center (see reference 40).

Monooxygenase TsaMB has a broad substrate range which includes *p*-methoxybenzoate (40). The monooxygenase systems vanillate-demethylase (VanAB) and *p*-methoxybenzoate-demethylase (MbdAB) reported in the literature (6, 9) are closely related to TsaMB (see below), and *C. testosteroni* T-2 utilized both *p*-methoxybenzoate and vanillate as sole sources of carbon for growth. Extracts of toluenesulfonate-grown cells of strain T-2, however, could not oxygenate vanillate, so monooxygenase system TsaMB is not identical with the vanillate-demethylase synthesized by this organism. Similarly, extracts of *p*-methoxybenzoate-grown cells of strain T-2 could not convert toluenesulfonate to sulfobenzoate, so, because TsaMB is expressed concomitantly with the dehydrogenases yielding the latter compound (61), monooxygenase system TsaMB is not identical with the *p*-methoxybenzoate-demethylase in this organism.

Purification of alcohol dehydrogenase TsaC to give identification tags. TsaC was purified to apparent homogeneity in a two-step procedure which gave a 92-fold purification (Table 1). The N terminus was unambiguously determined to be MN LNKQVAIV. SDS gel electrophoresis and gel filtration chromatography confirmed earlier data indicative of a dimeric native protein with a subunit molecular weight of 29,000 (see reference 41).

Purification of aldehyde dehydrogenase TsaD to give identification tags. TsaD was extensively purified (Fig. 3) in a two-step procedure which gave a 250-fold purification (Table 2). The keys to this purification were treatment of the concentration membranes to eliminate extensive protein losses due to binding (see Materials and Methods), the avoidance of pooled samples which introduced massive impurities, and a brisk routine to obtain data before the enzyme lost activity. We thus avoided pitfalls which led to separation of the wrong protein (41).

The subunit molecular weight determined by SDS-gel electrophoresis was 56,000. The protein smeared on gel filtration chromatography, presumably due to interaction of the extremely hydrophobic protein with the stationary phase, and we assume a homodimeric native protein (Table 2). The N-terminal amino acids were determined to be XSTVLYRXPEL.

Cloning, sequencing, and identification of the *tsaMBCD* and *tsaR* genes. We made a restriction digest map of the *tsaM* locus (Fig. 4) with the aid of an oligonucleotide probe representing the N terminus of TsaM (as indicated in Fig. 5) and confirmed the map with a probe representing the internal amino acid sequence (see above). Total DNA was subjected to digestion with *Sal*I and *Bgl*II, and fragments in the 4-kb region, localized in a Southern blot with a probe for *tsaM*, were ligated into pBluescript-KSII. Clones (250) were screened with the probe for *tsaM*, and a single clone was identified. Both DNA strands of the 4-kb *Sal*I-*Bgl*II insert were partially sequenced. One complete (*tsaR*, see below) and one incomplete open reading frame (ORF) were detected. The incomplete ORF included the N-terminal and internal sequences from the monooxygenase component, TsaM. To complete this sequence, a 6-kb *Kpn*I fragment (Fig. 4), which overlaps the 4-kb *Sal*I-*Bgl*II fragment, was cloned and partially sequenced. The 6-kb fragment was identified with a 0.3-kb *Kpn*I-*Bgl*II probe derived from the 4-kb *Sal*I-*Bgl*II clone. Downstream of *tsaM* we located a complete ORF, whose deduced sequence includes a section identical to the N-terminal sequence of reductase TsaB. In total, 6,040 bp were sequenced and five ORFs were found and analyzed (Fig. 4 and 5).

Sequence and characterization of monooxygenase TsaMB. The start codon (ATG) of monooxygenase *tsaM* was found at position 1477 (Fig. 5); the stop codon (TGA) was found at position 2518. We located a putative Shine-Dalgarno sequence (AAGGAG, position 1464) upstream of this gene (68). The start codon of reductase *tsaB* was found at position 2517, the stop codon was found at position 3468, and a putative Shine-Dalgarno sequence (CGGGA) was found at nucleotide 2505. The stop codon of *tsaM* (TGA) and the start codon of *tsaB* (ATG) overlap (Fig. 5). Gene *tsaM* has a coding capacity for 347 amino acids, giving a calculated molecular weight ($M_{r,calc}$) of 39,557, and gene *tsaB* has a coding capacity for 317 amino acids ($M_{r,calc}$ = 34,186); these molecular weights corresponded to the values (43,000 and 36,000, respectively) obtained with SDS-PAGE.

A sequence analysis of TsaM confirmed the presence of motifs attributed to a Rieske [2Fe-2S] center (e.g., Cys-48,

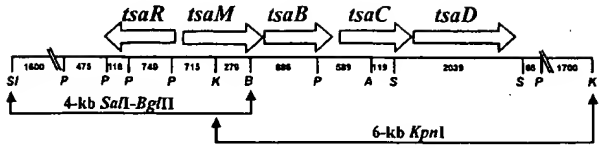

FIG. 4. Restriction digest map of the region containing operon *tsaMBCD* and *tsaR*. The two clones (*SalI-BglII* and *KpnI*) used for sequencing are shown. Only the restriction sites used for subcloning are shown. Distances between two restriction sites are marked in base pairs. The orientation and location of *tsaM*, *tsaB*, *tsaC*, *tsaD*, and *tsaR* are shown with arrows. *SI*, *SalI*; *P*, *PstI*; *K*, *KpnI*; *B*, *BglII*; *A*, *AccI*; *S*, *SacI*.

Cys-67, His-50, and His-70) and a mononuclear iron center (Asp-155, His-158, and His-163) (Fig. 5) (see also references 44 and 46) and confirmed the enzyme as a member of the class IA oxygenases (Table 3).

Similarly, TsaB was confirmed as a typical class IA reductase (Table 3) with presumed sites for *proR* NADH binding (60) (Gly-117, Gly-118, Ile-119, Gly-120, Thr-122, Pro-123, Met-127, Arg-145, Pro-195, Phe-232), flavin mononucleotide binding (Arg-51, Tyr-53, Ser-54, Leu-55), and a ferredoxin [2Fe-2S] center (Cys-266, Cys-271, Cys-274, Cys-304) (Fig. 5; see also references 44 and 46).

Sequencing and characterization of *p*-sulfobenzyl alcohol dehydrogenase TsaC. Downstream of reductase gene *tsaB* (Fig. 4 and 5) we located an ORF (759 bp) termed *tsaC*. The stop codon of reductase *tsaB* and the start codon of *tsaC* were 13 bp apart. The start codon of *tsaC* (ATG) was found at position 3484, the stop codon (TGA) was found at position 4240, and a potential Shine-Dalgarno sequence (AACCA) was found at position 3473. The deduced amino acid sequence (Fig. 5) includes the N-terminal sequence determined for the *p*-sulfobenzyl alcohol dehydrogenase (Fig. 1), and the $M_{r,calc}$ (26,438) corresponds to the observed value (29,000); *tsaC* thus encodes the alcohol dehydrogenase. TsaC has a high degree of sequence similarity (Table 3) with group II, short-chain, NAD(P)-dependent, zinc-independent alcohol dehydrogenases (54) for which a crystal structure is available (25). The conserved residues Asp-62 (Fig. 5), Ser-142, Tyr-155, and Lys-159 may be involved in the catalytic mechanism, whereas the pattern Gly-12–XXX–Gly-16–X–Gly-18 (part of the αβα motif) and Thr-11 of the N terminus presumably represent conserved amino acids in the coenzyme binding domain. These data confirm the assumption (41) of the classification of this enzyme.

Sequencing and characterization of *p*-sulfobenzaldehyde dehydrogenase TsaD. The stop codon of *tsaC* was found to overlap the start codon (ATG, position 4239) of a 1,427-bp ORF, termed *tsaD*, with a potential Shine-Dalgarno sequence (ACGGG) at position 4223 and a stop codon (TGA) at position 5667. The deduced amino acid sequence (Fig. 5) includes the N-terminal sequence determined for the aldehyde dehydrogenase (Fig. 1), and $M_{r,calc}$ (51,010) corresponds to the observed value (56,000); *tsaD* thus encodes the *p*-sulfobenzaldehyde dehydrogenase. A data bank analysis showed high levels of similarity to a wide varicty of aldehyde dehydrogenases (Table 3). The N-terminal region is poorly conserved, but a number of strictly conserved amino acids were found, especially Gly residues which are distributed throughout the protein. The residues Cys-286 (Fig. 5) and Gly-230 to Gly-235 (αβα motif) may be part of the NAD binding fold and Glu-252 is thought to be part of the active site (32). However, this interpretation conflicts with another (30), and no crystal structure is available to resolve the disagreement.

The region downstream of *tsaMBCD*. No ORF was found downstream (370 bp) of *tsaMBCD*. A putative transcription stop signal [stem-loop and poly(T) sequence] in the region from 5688 to 5718 and the functionality of the upstream region (see below) indicate that this gene cluster represents an operon.

Sequencing of the putative LysR-type transcriptional regulator, *tsaR*. At 114 bp upstream of *tsaM* an ORF, termed *tsaR*, was found in the reverse orientation to *tsaMBCD*. The putative start codon (GTG) of *tsaR* was attributed to position 1362, the stop codon (TGA) was attributed to position 468, and a potential Shine-Dalgarno sequence (CGGGA) was attributed to position 1374. A sequence analysis showed that *tsaR* would encode a protein containing 298 amino acids ($M_{r,calc}$ = 32,630) with similarities, largely at the N terminus (where the helix-turn-helix motif for DNA binding was located), to LysR-type transcriptional regulators (Table 3; Fig. 5 [where only highly conserved residues of the αβα structure are marked]) (59).

The region downstream of *tsaR*. No ORF was found downstream (465 bp in the direction of transcription) of *tsaR*. A putative transcription stop signal [stem-loop and poly(T) sequence] in the region from 387 to 407 and the location of the *tsaMBCD* operon indicate that this single gene constitutes a separate transcriptional unit.

Structure of the region between *tsaMBCD* and *tsaR*. The intergenic region between *tsaR* and *tsaM*, 114 bp, was found to have a GC content of 48%, much lower than the 70% observed in the coding regions. A low GC content of the intergenic region has been observed previously between a LysR-type regulator gene and the neighboring gene(s) it regulates (77). One putative recognition site for a LysR-type regulator was found, position 1376 (TTC-8 bp-GAA), which corresponds to Schell's model (59). A putative sigma^{70} "housekeeping" promoter of operon *tsaMBCD* is located upstream from *tsaM*, though the Pribnow box TAGCAT at position 1442 and the −35 region (1418; TTGTTG) show only weak homologies with the consensus sequences (45). Another potential promoter, which could be recognized by a sigma^{70} factor, lies upstream of *tsaR*: the Pribnow box (position 1401; TATAA; reverse strand) is identical to the consensus, whereas the −35 region (position 1424; ACAACA; reverse strand) has poor homology with the consensus sequence.

DISCUSSION

Each of the genes in the cluster *tsaMBCD* has been identified from the deduced N-terminal amino acid sequence (Fig. 5) and by its size. This cluster thus encodes the inducible enzymes which catalyze the reactions (Fig. 1) of the physiologically defined regulatory unit R1 involved in the degradation of toluenesulfonate in *C. testosteroni* T-2 (61). The evidence that the cluster represents a four-gene operon lies in the absence of neighboring genes (in the direction of transcription (Fig. 5), in the putative stop signal (Fig. 5), and in the detection of a 4.5-kb mRNA (33a), i.e., a polycistronic messenger of the correct length.

We presume that the putative LysR-type regulatory gene, *tsaR*, is expressed as a one-gene transcriptional unit and that its product is involved in both autoregulation and regulation of expression of the neighboring *tsa* catabolic operon. *tsaR* is typical of the supergene family, both from its structure and from the nature of the intergenic region with which it would have to interact (59), but only experiments will confirm this hypothesis. The induction of operons controlled by LysR-type regulators takes place through the binding to that protein of a substrate or an intermediate of the pathway, so toluenesulfon-

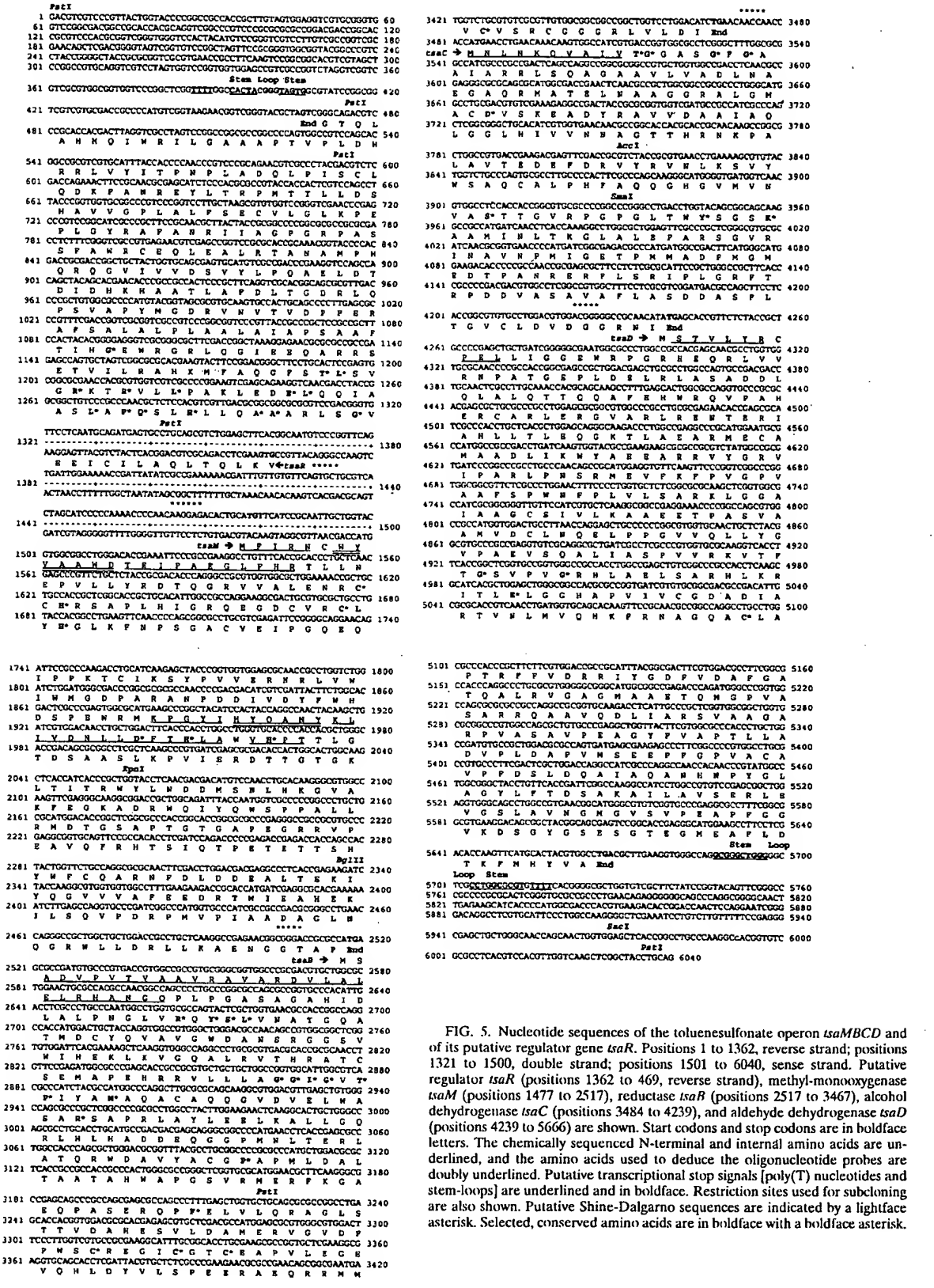

FIG. 5. Nucleotide sequences of the toluenesulfonate operon *tsaMBCD* and of its putative regulator gene *tsaR*. Positions 1 to 1362, reverse strand; positions 1321 to 1500, double strand; positions 1501 to 6040, sense strand. Putative regulator *tsaR* (positions 1362 to 469, reverse strand), methyl-monooxygenase *tsaM* (positions 1477 to 2517), reductase *tsaB* (positions 2517 to 3467), alcohol dehydrogenase *tsaC* (positions 3484 to 4239), and aldehyde dehydrogenase *tsaD* (positions 4239 to 5666) are shown. Start codons and stop codons are in boldface letters. The chemically sequenced N-terminal and internal amino acids are underlined, and the amino acids used to deduce the oligonucleotide probes are doubly underlined. Putative transcriptional stop signals [poly(T) nucleotides and stem-loops] are underlined and in boldface. Restriction sites used for subcloning are also shown. Putative Shine-Dalgarno sequences are indicated by a lightface asterisk. Selected, conserved amino acids are in boldface with a boldface asterisk.

TABLE 3. Comparison of TsaMBCD and TsaR with related proteins

Protein	$M_{r,calc}$[a]	Structure	Position		GC content (%)	Related proteins[b]					
			SD[c]	Gene		Name	% Identity	$M_{r,calc}$	Structure	GC content (%)	Accession no.
TsaR	32,630 (298)	ND[d]	1374	1362–469	70	Nac	27.8	32,754 (305)	ND	62	Q08597
						ClcR	27.2	32,527 (294)	ND	56	L06464
						SdsB	27.1	32,955 (306)	ND	74	M86744
						CynR	26.9	32,961 (299)	ND	55	P27111
						TfdR	25.9	32,070 (295)	ND	67	P10086
TsaM	39,557 (347)	Tetramer	1464	1477–2517	66	VanA	32.7	36,578 (329)	ND	69	P12609
						Pht3	23.8	49,297 (439)	Tetramer	59	D13229
						CbaA	23.7	48,927 (432)	ND	59	U00692
						PobA	21.0	46,258 (409)	ND	67	X78823
TsaB	34,186 (317)	Monomer	2505	2517–3467	71	VanB	41.2	33,706 (314)	ND	73	P12580
						PobB	38.9	33,558 (319)	ND	73	X78823
						Pht2	34.1	35,999 (324)	Monomer	57	D13229
						CbaB	30.9	31,699 (288)	ND	59	U00692
TsaC	26,438 (252)	Dimer	3473	3484–4239	69	Xan	38.9	26,143 (250)	ND	69	S47054
						BudC	37.4	25,313 (241)	Tetramer	63	Q04520
						3Bhd	37.4	26,848 (253)	ND	59	P19871
						LinX	36.8	25,492 (250)	ND	59	D23722
						Dhk1	36.1	28,393 (272)	ND	72	P16542
TsaD	51,010 (476)	Dimer?	4223	4239–5666	71	GabD	38.7	51,719 (482)	ND	58	P25526
						AldH	34.7	54,158 (497)	ND	54	X95396
						Ald	34.0	52,142 (478)	Tetramer	51	P25553
						DhaC	33.7	54,743 (500)	Dimer	ND	P15437
						AldH6	33.3	56,009 (512)	ND	55	A55684

[a] $M_{r,calc}$, molecular weight calculated from amino acid composition. The total number of amino acids is in parentheses.
[b] LysR-type regulators: Nac, nitrogen assimilation control regulator; CynR, cyanate operon regulator; SdsB, sodium dodecyl sulfatase regulator; ClcR, chlorocatechol operon regulator; TfdR, 2,4-dichlorophenoxyacetate operon regulator. Oxygenases and reductases: VanAB, Pht23, CbaAB, and PobAB (see legend for Fig. 6). Group II dehydrogenases (DH): Xan, hypothetical protein; BudC, acetoin (diacetyl) DH; 3Bhd, 3-β-hydroxysteroid DH; LinX, γ-hexachlorocyclohexane dehydrochlorinase; Dhk1, putative ketoacyl reductase (granaticin polyketide synthase). Aldehyde DHs: GabD, succinate-semialdehyde DH; AldH, aldehyde DH; Ald, lactaldehyde DH; DhaC, horse cytosol aldehyde DII; AldH6, human cytosol aldehyde DII.
[c] SD, Shine-Dalgarno sequence.
[d] ND, not determined.

ate or toluenecarboxylate or the intermediates in the pathway (Fig. 1) could interact with TsaR. The LysR-type autoregulatory transcriptional regulators are widespread and regulate many target genes, which include catabolic operons for xenobiotics (13, 75). A subfamily of regulators for chlorocatechol degradation has been described (62) that shows homologies to TsaR (see Table 3). LysR-type regulators are often plasmid encoded and involved in the positive regulation of catabolic operons. TfdR (Table 3) is located on plasmid pJP4, which belongs to the same incompatibility group, IncP1β, as plasmid pTSA (see below) and has a similar GC content.

The genes we have sequenced (Fig. 5) encode regulatory and catalytic functions. We know that transport is essential to the metabolism of sulfonates, both theoretically, because these charged compounds would otherwise not come in contact with the soluble cytoplasmic enzymes catalyzing their degradation, and from direct observation of a toluenesulfonate transport system in strain T-2 (42). The inducible transport system must thus be encoded at another locus, and it will be interesting to discover whether TsaR also regulates its expression. The enzymes encoded by the *tsa* catabolic operon also convert *p*-toluenecarboxylate to terephthalate when the organism utilizes toluate (41). It is unclear whether a toluenecarboxylate transport system is required for growth by strain T-2, but when at least porins are required for the metabolism of xylene (XylN) and benzene (27a, 79), it seems likely that some membrane structure will be required by the organism to utilize toluenecarboxylate.

The GC content of total DNA of *C. testosteroni* T-2 is 61.8% ± 0.5%, typical of the species (10). Chromosomally located genes in *C. testosteroni* have a GC content of 61% ± 1% with 73% for the third base (1, 2, 8, 11, 20, 36, 50). In contrast, our ORFs show a high GC content (70%) and an extremely high GC content in the third base (91%). The codon usage among the genes in both the *tsa* operon and *tsaR* is the same but different from that of the chromosomal genes. We have now shown that the *tsa* operon and *tsaR* are located on plasmid pTSA, and we conclude that these genes were recruited from another organism (33b).

Aerobic metabolism of inert aromatic compounds typically starts by oxygenation at the ring or at the (methyl) side chain (see reference 41 and citations therein). Although many ring oxygenations have been studied, our understanding of oxygenation of the methyl side chain is limited largely to work related to the TOL plasmids, and even there, the oxygenase XylM has not been purified (70). The work with *C. testosteroni* T-2 thus presents the first set of data in which all catabolic enzymes involved in side chain manipulation have been purified, characterized, and sequenced. By comparison of the TOL and TSA systems, we see clearly that nature has used very different detailed solutions for oxidizing a methyl group by the "same" pathway. The TOL upper pathway has a different gene order

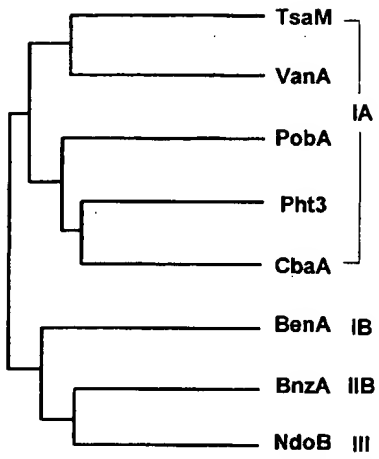

FIG. 6. Rooted evolutionary tree of class IA multicomponent oxygenases with representatives from classes IB, IIB, and III based on the amino acid composition of the oxygenases. VanA, vanillate demethylase (9); CbaA, 3-chlorobenzoate 2,3-dioxygenase (46); Pht3, phthalate 4,5-dioxygenase (49); PobA, phenoxybenzoate dioxygenase (15); BenA, benzoate dioxygenase (accession number [AC.] P07767); BnzA, benzene dioxygenase (AC. P08084); NdoB, naphthalene dioxygenase (AC. P23094). The N-terminal amino acid sequence of *p*-sulfobenzoate dioxygenase PsbA (another dioxygenase system in the degradative pathway of toluenesulfonate) (39) displays a high sequence identity value of 48% with CbaA over the available 35-amino-acid sequence, indicating that the oxygenases are closely related (46) and that PsbAC is another class IA dioxygenase system. *p*-Methoxybenzoate demethylase system MbdAB (no sequence data available) apparently shares substrates with vanillate-demethylase system VanAB (3-methoxybenzoate and 3,4-dimethoxybenzoate) and monooxygenase system TsaMB (4-methylbenzoate and 4-methoxybenzoate), whereas TsaMB does not share any common substrate with VanAB. We expect high levels of sequence similarity between monooxygenase MbdAB and the other two monooxygenases.

than the *tsa* catabolic operon and includes a transport function (XylN); different regulatory systems are used (sigma^{54} promoter, integration host factor, and the NtrC-like regulator XylR in the TOL system contrasted with putative sigma^{70} promoters and LysR-type regulation) and different types of monooxygenases and different gene families of alcohol dehydrogenases (class I in TOL [67] and class II in *tsa* [Table 3]) are involved. Only the aldehyde dehydrogenases (Table 3) (see the introduction) belong to the same family, with 29% sequence identity between TsaD and XylC being determined. When two types of attack on a methyl side chain differ so markedly (see also reference 31), we may expect yet more diversity when further pathways of oxidation of aromatic methyl groups are examined.

The short-chain alcohol dehydrogenases have been found frequently in aromatic metabolism, but usually as diene-diol dehydrogenases (e.g., XylL) (47), which represent a very different reaction type (regeneration of the aromatic ring structure) from that of TsaC (Fig. 1). Sequence comparisons similar to those in Table 3 show that the diene-diol dehydrogenases have identities with TsaC lower than 32% (Table 3).

As anticipated from biochemical data (44); monooxygenase system TsaMB has a high level of homology to class IA oxygenase systems, the reductases showing a higher level of identity than the oxygenases (Table 3). We generated an evolutionary tree for oxygenase components of oxygenase systems with an arbitrarily set root (Fig. 6). It was apparent that, despite the similarities in class IA, there are two separate evolutionary lines in this group of oxygenase components. The subdivision of the class IA oxygenase components into monooxygenases and dioxygenases, considered with the similarity of the Rieske centers (Table 4) (27), presumably indicates differences due to the binding site for the aromatic substrate and oxygen. In contrast, no subgroups were apparent in trees obtained from alignments of sequences from reductase components (not shown). It is well known that the domain structure of the reductases in class IA differs from those in other classes. Thus, we rationalize the homogeneity in the class IA reductases in the common property of supplying electrons to the oxygenase components.

Whereas there is considerable understanding of the function of the reductases of the mononuclear iron oxygenase systems (14, 22, 44) and a steady increase in our understanding of the [2Fe-2S] Rieske center in the oxygenase (27, 28, 44), there is still very little information on the mononuclear iron itself. The long-standing data from Bernhardt's group (7), from which no sequence data are available, are only now being expanded (72). The close biochemical similarity of monooxygenase TsaMB and *p*-methoxybenzoate demethylase (M_r, redox centers, amino acid composition, and overlapping substrate ranges [e.g., 4-methoxybenzoate and 4-methylbenzoate]) (40) serves to link the biophysical work (7) with the biochemical and/or sequencing work done with several dioxygenase systems (Table 3).

The catalytic enzymes (TsaM, TsaC, and TsaD) encoded by the *tsa* operon do not discriminate between the sulfonate and the carboxyl substituents, whereas the subsequent enzymes do (61). Despite the similarities of both aromatic substituents, it seems that their different physical and chemical properties sometimes require specialized enzymes. Each class IA oxygenase requires an aromatic carboxyl or, as in this case, an aromatic sulfonate substituent in its substrate. As monooxygenase TsaM can accommodate a sulfonate substituent, the question of whether other class IA oxygenases can tolerate a sulfonate substituent and still oxygenate the compound arises.

The high degree of similarity of monooxygenase and dioxygenase systems seen in Fig. 6 (51), in the face of old strictures

TABLE 4. Data from EPR spectra of the [2Fe-2S] centers in the oxygenase components of some multicomponent oxygenase systems

Enzyme	Class	g_z	g_y	g_x	Center	Source or reference
4-Toluenesulfonate methyl-monooxygenase	IA	2.019	1.918	1.790	Rieske	This paper
4-Sulfobenzoate DOS[a]	IA	2.025	1.921	1.745	Rieske	35
4-Methoxybenzoate demethylase	IA	2.008	1.913	1.72	Rieske	73
Phthalate DOS	IA	2.016	1.914	1.763	Rieske	12
4-Chlorophenylacetate DOS	IA	2.021	1.922	1.737	Rieske	43
2-Halobenzoate DOS	IB	2.025	1.912	1.788	Rieske	19
Pyrazon DOS	IIA	2.02	1.91	1.79	Rieske	58
Benzene DOS	IIB	2.018	1.917	1.754	Rieske	23
Naphthalene DOS	III	2.01	1.91	1.80	Rieske	69

[a] DOS, dioxygenase system.

from the Enzyme Commission (81), is not restricted to sequence comparisons. Not only can dioxygenase systems monooxygenate some substrates (26, 78), but a monooxygenase system (MbdAB) can dioxygenate at least one substrate (82). When promulgated, the wording of the Enzyme Commission rule was quite correct (29). It would seem appropriate to adjust the rules of nomenclature to the biochemical and molecular biological facts, especially as a monooxygenase system in class IB has also been detected (56).

ACKNOWLEDGMENTS

We are grateful to T. Leisinger for his ready advice and for making available laboratory space and apparatus. P. M. H. Kroneck kindly collected the EPR spectra. We are grateful for discussions with P. M. H. Kroneck, S. Vuilleumier, A. Riedel, V. Weiss-Rudolf, M. Schmid-Appert, and A. Wasserfallen and to S. Fetzner, who kindly made preprints available.

The work was supported by a grant from the Priority Programme Environment of the Swiss National Science Foundation and by funds made available by the University of Konstanz.

REFERENCES

1. **Abalain, J. H., S. Di Stefano, Y. Amet, E. Quemener, M. L. Abalain-Colloc, and H. H. Floch.** 1993. Cloning, DNA sequencing and expression of (3-17) beta hydroxysteroid dehydrogenase from *Pseudomonas testosteroni*. J. Steroid Biochem. Mol. Biol. **44**:133–139.
2. **Ahmad, D., J. Fraser, M. Sylvestre, A. Larose, A. Khan, J. Bergeron, M. J. Juteau, and M. Sondossi.** 1995. Sequence of the *bphD* gene encoding 2-hydroxy-6-oxo-(phenyl/chlorophenyl)hexa-2,4-dienoic acid (HOP/cPDA) hydrolase involved in the biphenyl/polychlorinated biphenyl degradation pathway in *Comamonas testosteroni*: evidence suggesting involvement of Ser^{112} in catalytic activity. Gene **156**:69–74.
3. **Assinder, S. J., and P. A. Williams.** 1990. The TOL plasmids: determinants of the catabolism of toluene and the xylenes. Adv. Microb. Physiol. **31**:1–69.
4. **Ausubel, F. M., R. Brent, R. E. Kingston, D. D. Moore, J. G. Seidman, J. A. Smith, and K. Struhl (ed.).** 1987. Current protocols in molecular biology. John Wiley & Sons, Inc., New York.
5. **Batie, C. J., D. P. Ballou, and C. C. Correll.** 1991. Phthalate dioxygenase reductase and related flavin-iron-sulfur containing electron transferases, p. 543–556. *In* F. Müller (ed.), Chemistry and biochemistry of flavoenzymes, vol. 3. CRC Press, Boca Raton, Fla.
6. **Bernhardt, F.-H., E. Bill, A. X. Trautwein, and H. Twilfer.** 1988. 4-Methoxybenzoate monooxygenase from *Pseudomonas putida*: isolation, biochemical properties, substrate specificity, and reaction mechanisms of the enzyme components. Methods Enzymol. **161**:281–294.
7. **Bernhardt, F.-H., K. Gersonde, H. Twilfer, P. Wende, E. Bill, A. X. Trautwein, and K. Pfleger.** 1982. Dioxygen activation by putidamonooxin: substrate-modulated reaction of activated dioxygen, p. 63–77. *In* M. Nozaki, S. Yamamoto, Y. Ishimura, M. J. Coon, L. Ernster, and R. R. Estabrook (ed.), Oxygenases and oxygen metabolism. Academic Press, New York.
8. **Bocco, J. L., G. Panzetta, L. A. Actis, and S. Genti-Raimondi.** 1993. *Pseudomonas testosteroni* beta-hydroxysteroid dehydrogenase gene, and translated products. EMBL data library accession number U08971.
9. **Brunel, F., and J. Davison.** 1988. Cloning and sequencing of *Pseudomonas* genes encoding vanillate demethylase. J. Bacteriol. **170**:4924–4930.
10. **Busse, H.-J., T. El-Banna, H. Oyaizu, and G. Auling.** 1992. Identification of xenobiotic-degrading isolates from the beta subclass of the *Proteobacteria* by a polyphasic approach including 16S rRNA partial sequencing. Int. J. Syst. Bacteriol. **42**:19–26.
11. **Choi, K. Y., and W. F. Benisek.** 1988. Nucleotide sequence of the gene for the Δ^5-3-ketosteroid isomerase of *Pseudomonas testosteroni*. Gene **69**:121–129.
12. **Cline, J. F., B. M. Hoffman, W. B. Mims, E. LaHaie, D. P. Ballou, and J. A. Fee.** 1985. Evidence for N coordination to Fe in the [2Fe-2S] clusters of *Thermes* Rieske protein and phthalate dioxygenase from *Pseudomonas*. J. Biol. Chem. **260**:3251–3254.
13. **Coco, W. M., R. K. Rothmel, S. Henikoff, and A. M. Chakrabarty.** 1993. Nucleotide sequence and initial functional characterization of the *clcR* gene encoding a LysR family activator of the *clcABD* chlorocatechol operon in *Pseudomonas putida*. J. Bacteriol. **175**:417–427.
14. **Correll, C. C., C. J. Batie, D. P. Ballou, and M. L. Ludwig.** 1992. Phthalate dioxygenase reductase: a modular structure for electron transfer from pyridine nucleotides to [2Fe-2S]. Science **258**:1604–1610.
15. **Dehmel, U., K.-H. Engesser, K. N. Timmis, and D. F. Dwyer.** 1995. Cloning, nucleotide sequence, and expression of the gene encoding a novel dioxygenase involved in metabolism of carboxydiphenyl ethers in *Pseudomonas pseudoalcaligenes* POB310. Arch. Microbiol. **163**:35–41.
16. **Denger, K., M. A. Kertesz, E. H. Vock, R. Schön, A. Mägli, and A. M. Cook.** 1996. Anaerobic desulfonation of 4-tolylsulfonate and 2-(4-sulfophenyl)butyrate by a *Clostridium* sp. Appl. Environ. Microbiol. **62**:1526–1530.
17. **Feigel, B. J., and H.-J. Knackmuss.** 1993. Syntrophic interactions during degradation of 4-aminobenzenesulfonic acid by a two species bacterial culture. Arch. Microbiol. **159**:124–130.
18. **Ferreras, M., J. G. Gavilanes, and J. M. García-Segura.** 1993. A permanent Zn^{2+} reverse staining method for the detection and quantification of proteins in polyacrylamide gels. Anal. Biochem. **213**:206–212.
19. **Fetzner, S., R. Müller, and F. Lingens.** 1992. Purification and some properties of 2-halobenzoate 1,2-dioxygenase, a two-component enzyme system from *Pseudomonas cepacia* 2CBS. J. Bacteriol. **174**:279–290.
20. **Florin, C., T. Köhler, M. Grandguilliot, and P. Plesiat.** 1996. *Comamonas testosteroni* 3-ketosteroid-Δ^4(5α)-dehydrogenase: gene and protein characterization. J. Bacteriol. **178**:3322–3330.
21. **Focht, D. D., and F. D. Williams.** 1970. The degradation of *p*-toluenesulphonate by a *Pseudomonas*. Can. J. Microbiol. **16**:309–316.
22. **Gassner, G. T., M. L. Ludwig, D. L. Gatti, C. C. Correll, and D. P. Ballou.** 1995. Structure and mechanism of the iron-sulfur flavoprotein phthalate dioxygenase reductase. FASEB J. **9**:1411–1418.
23. **Geary, P. J., F. Saboowalla, D. Patil, and R. Cammack.** 1984. An investigation of the iron-sulphur proteins of benzene dioxygenase from *Pseudomonas putida* by electron-spin-resonance spectroscopy. Biochem. J. **217**:667–673.
24. **Gerhartz, W. (ed.).** 1995. Ullmann's encyclopedia of industrial chemistry, 5th ed. VCH Verlagsgesellschaft, Weinheim, Germany.
25. **Ghosh, D., C. M. Weeks, P. Grochulski, W. L. Duax, M. Erman, R. L. Rimsay, and J. C. Orr.** 1991. Three-dimensional structure of holo 3α,20β-hydroxysteroiddehydrogenase: a member of short-chain dehydrogenase family. Proc. Natl. Acad. Sci. USA **88**:10064–10068.
26. **Gibson, D. T., S. M. Resnick, K. Lee, J. M. Brand, D. S. Torok, L. P. Wackett, M. J. Schocken, and B. E. Haigler.** 1995. Desaturation, dioxygenation, and monooxygenation reactions catalyzed by naphthalene dioxygenase from *Pseudomonas* sp. strain 9816-4. J. Bacteriol. **177**:2615–2621.
27. **Gurbiel, R. J., P. E. Doan, G. T. Gassner, T. J. Macke, D. A. Case, T. Ohnishi, J. A. Fee, D. P. Ballou, and B. M. Hoffman.** 1996. Active site structure of Rieske-type proteins: electron nuclear double resonance studies of isotopically labeled phthalate dioxygenase from *Pseudomonas cepacia* and Rieske protein from *Rhodobacter capsulatus* and molecular modeling studies of a Rieske center. Biochemistry **35**:7834–7845.

27a. **Harayama, S.** Lecture at ETH. Zurich, Switzerland.

28. **Harayama, S., M. Kok, and E. L. Neidle.** 1992. Functional and evolutionary relationships among diverse oxygenases. Annu. Rev. Microbiol. **46**:565–601.
29. **Hayaishi, O.** 1974. General properties and biological function of oxygenases, p. 1–28. *In* O. Hayaishi (ed.), Molecular mechanisms of oxygen activation. Academic Press, New York.
30. **Hidalgo, E., Y. M. Chen, E. C. C. Lin, and J. Aguilar.** 1991. Molecular cloning and DNA sequencing of the *Escherichia coli* K-12 *ald* gene encoding aldehyde dehydrogenase. J. Bacteriol. **173**:6118–6123.
31. **Hopper, D. J.** 1988. Properties of *p*-cresol methylhydroxylases, p. 247–258. *In* S. R. Hagedorn, R. S. Hanson, and D. A. Kunz (ed.), Microbial catabolism and the carbon cycle. Harwood Academic Publishers, New York.
32. **Horn, J. M., S. Harayama, and K. N. Timmis.** 1991. DNA sequence determination of the TOL plasmid (pWWO) *xylGFJ* genes of *Pseudomonas putida*: implications for the evolution of aromatic catabolism. Mol. Microbiol. **5**:2459–2474.
33. **Inouye, S., A. Nakazawa, and T. Nakazawa.** 1988. Nucleotide sequence of the regulatory gene xylR of the TOL plasmid from *Pseudomonas putida*. Gene **66**:301–306.

33a. **Junker, F.** Unpublished data.

33b. **Junker, F., and A. M. Cook.** Submitted for publication.

34. **Junker, F., T. Leisinger, and A. M. Cook.** 1994. 3-Sulphocatechol 2,3-dioxygenase and other dioxygenases (EC 1.13.11.2 and EC 1.14.12.-) in the degradative pathways of 2-aminobenzenesulphonic, benzenesulphonic and 4-toluenesulphonic acids in *Alcaligenes* sp. strain O-1. Microbiology (Reading) **140**:1713–1722.
35. **Junker, F., E. Saller, H. R. Schläfli Oppenberg, P. M. H. Kroneck, T. Leisinger, and A. M. Cook.** 1996. Degradative pathways for *p*-toluenecarboxylate and *p*-toluenesulfonate and their multicomponent oxygenases in *Comamonas testosteroni* strains PSB-4 and T-2. Microbiology (Reading) **142**: 2419–2427.
36. **Kuliopulos, A., D. Shortle, and P. Talalay.** 1987. Isolation and sequencing of the gene encoding Δ^5-3-ketosteroid isomerase of *Pseudomonas testosteroni*: overexpression of the protein. Proc. Natl. Acad. Sci. USA **84**:8893–8897.
37. **Laemmli, U. K.** 1970. Cleavage of structural proteins during the assembly of the head of bacteriophage T4. Nature (London) **227**:680–685.
38. **Lange, F. T., M. Wenz, and H.-J. Brauch.** 1995. Trace-level determination of aromatic sulfonates in water by on-line ion-pair extraction/ion-pair chromatography and their behaviour in the aquatic environment. J. High Resolut. Chromatogr. **18**:243–252.
39. **Locher, H. H., T. Leisinger, and A. M. Cook.** 1991. 4-Sulpholbenzoate 3,4-dioxygenase: purification and properties of a desulphonative two-component

enzyme system from *Comamonas testosteroni* T-2. Biochem. J. 274:833–842.
40. **Locher, H. H., T. Leisinger, and A. M. Cook.** 1991. 4-Toluene sulfonate methyl-monooxygenase from *Comamonas testosteroni* T-2: purification and some properties of the oxygenase component. J. Bacteriol. 173:3741–3748.
41. **Locher, H. H., C. Malli, S. Hooper, T. Vorherr, T. Leisinger, and A. M. Cook.** 1991. Degradation of *p*-toluic acid (*p*-toluenecarboxylic acid) and *p*-toluene sulphonic acid via oxygenation of the methyl sidechain is initiated by the same set of enzymes in *Comamonas testosteroni* T-2. J. Gen. Microbiol. 137:2201–2208.
42. **Locher, H. H., B. Poolman, A. M. Cook, and W. N. Konings.** 1993. Uptake of 4-toluene sulfonate by *Comamonas testosteroni* T-2. J. Bacteriol. 175:1075–1080.
43. **Markus, A., D. Krekel, and F. Lingens.** 1986. Purification and some properties of component A of the 4-chlorophenylacetate 3,4-dioxygenase from *Pseudomonas* species strain CBS. J. Biol. Chem. 261:12883–12888.
44. **Mason, J. R., and R. Cammack.** 1992. The electron-transport proteins of hydroxylating bacterial dioxygenases. Annu. Rev. Microbiol. 46:277–305.
45. **Moran, C. P. J., N. Lang, S. F. J. Legrice, G. Lee, M. Stephens, A. L. Sonenshein, J. Pero, and R. Losick.** 1982. Nucleotide sequences that signal the initiation of transcription and translation in *Bacillus subtilis*. Mol. Gen. Genet. 186:339–346.
46. **Nakatsu, C. H., N. A. Straus, and R. C. Wyndham.** 1995. The nucleotide sequence of the Tn*5271* 3-chlorobenzoate 3,4-dioxygenase genes (*cbaAB*) unites the class IA oxygenases in a single lineage. Microbiology (Reading) 141:485–495.
47. **Neidle, E. L., C. Hartnett, L. N. Ornston, A. Bairoch, M. Rekik, and S. Harayama.** 1992. *Cis*-diol-dehydrogenase encoded by the TOL pWW0 plasmid *xylL* gene and the *Acinobacter calcoaceticus* chromosomal *benD* gene are members of the short chain alcohol dehydrogenase superfamily. Eur. J. Biochem. 204:113–120.
48. **Nichols, N. N., and C. S. Harwood.** 1995. Repression of 4-hydroxybenzoate transport and degradation by benzoate: a new layer of regulatory control in the *Pseudomonas putida* β-ketoadipate pathway. J. Bacteriol. 177:7033–7040.
49. **Nomura, Y., M. Nakagawa, N. Ogawa, S. Harashima, and Y. Oshima.** 1992. Genes in PHT encoding the initial degradation pathway of phthalate in *Pseudomonas putida*. J. Ferment. Bioeng. 74:333–344.
50. **Plesiat, P., M. Grandguillot, S. Harayama, S. Vragar, and Y. Michel-Briand.** 1991. Cloning, sequencing, and expression of the *Pseudomonas testosteroni* gene encoding 3-oxosteroid Δ^1-dehydrogenase. J. Bacteriol. 173:7219–7227.
51. **Powlowski, P., and V. Shingler.** 1994. Genetics and biochemistry of phenol degradation by *Pseudomonas* sp. CF600. Biodegradation 5:219–236.
52. **Prieto, M. A., E. Díaz, and J. L. García.** 1996. Molecular characterization of the 4-hydroxyphenylacetate catabolic pathway of *Escherichia coli* W: engineering a mobile aromatic degradative cluster. J. Bacteriol. 178:111–120.
53. **Ramos, J. L., F. Rojo, L. Zhou, and K. N. Timmis.** 1990. A family of positive regulators related to the *Pseudomonas putida* TOL plasmid XylS and the *Escherichia coli* AraC activators. Nucleic Acids Res. 18:2149–2152.
54. **Reid, M. F., and C. A. Fewson.** 1994. Molecular characterization of microbial alcohol dehydrogenases. Crit. Rev. Microbiol. 20:13–56.
55. **Riester, J., W. G. Zumft, and P. M. H. Kroneck.** 1989. Nitrous oxide reductase from *Pseudomonas stutzeri*: redox properties and spectroscopic characterization of different forms of the multicopper enzyme. Eur. J. Biochem. 178:751–762.
56. **Rosche, B., B. Tshisuaka, S. Fetzner, and F. Lingens.** 1995. 2-Oxo-1,2-dihydroquinoline-8-monooxygenase, a two-component enzyme system from *Pseudomonas putida* 86. J. Biol. Chem. 270:17836–17842.
57. **Sanger, F., S. Nicklen, and A. R. Coulson.** 1977. DNA sequencing with chain-terminating inhibitors. Proc. Natl. Acad. Sci. USA 74:5463–5467.
58. **Sauber, K., C. Fröhner, G. Rosenberg, J. Eberspächer, and F. Lingens.** 1977. Purification and properties of pyrazon dioxygenase from pyrazon-degrading bacteria. Eur. J. Biochem. 74:89–97.
59. **Schell, M. A.** 1993. Molecular biology of the LysR family of transcriptional regulators. Annu. Rev. Microbiol. 47:597–626.
60. **Schläfli, H. R., D. P. Baker, T. Leisinger, and A. M. Cook.** 1995. Stereospecificity of hydride removal from NADH by reductases of multicomponent nonheme iron oxygenase systems. J. Bacteriol. 177:831–834.
61. **Schläfli Oppenberg, H. R., G. Chen, T. Leisinger, and A. M. Cook.** 1995. Regulation of the degradative pathways from 4-toluenesulfonate and 4-toluenecarboxylate to protocatechuate in *Comamonas testosteroni* T-2. Microbiology (Reading) 141:1891–1899.
62. **Schlaman, H. R. M., R. J. H. Okker, and B. J. J. Lugtenberg.** 1992. Regulation of nodulation gene expression by NodD in rhizobia. J. Bacteriol. 174:5177–5182.
63. **Schuurman, R., and W. Keulen.** 1991. Modified protocol for DNA sequence analysis using sequenase 2.0. BioTechniques 10:185.
64. **Seitz, A. P., and E. R. Leadbetter.** 1995. Microbial assimilation and dissimilation of sulfonate sulfur. ACS Symp. Ser. 612:365–375.
65. **Shanklin, J., E. Whittle, and B. G. Fox.** 1994. Eight histidine residues are catalytically essential in a membrane-associated iron enzyme, stearoyl-CoA desaturase, and are conserved in alkane hydroxylase and xylene monooxygenase. Biochemistry 33:12787–12794.
66. **Shaw, J. P., and S. Harayama.** 1990. Purification and characterization of TOL plasmid-encoded benzyl alcohol dehydrogenase and benzaldehyde dehydrogenase of *Pseudomonas putida*. Eur. J. Biochem. 191:705–714.
67. **Shaw, J. P., F. Schwager, and S. Harayama.** 1992. Substrate specificity of benzyl alcohol and benzaldehyde dehydrogenases encoded by TOL plasmid pWW0. Biochem. J. 273:789–794.
68. **Shine, J., and L. Dalgarno.** 1975. Determinant of cistron specificity in bacterial ribosomes. Nature (London) 254:34–38.
69. **Suen, W.-C., and D. T. Gibson.** 1993. Isolation and preliminary characterization of the subunits of the terminal component of naphthalene dioxygenase from *Pseudomonas putida* NCIB 9816-4. J. Bacteriol. 175:5877–5881.
70. **Suzuki, M., T. Hayakawa, P. J. Shaw, M. Rekik, and S. Harayama.** 1991. Primary structure of xylene monooxygenase: similarities to and differences from the alkane hydroxylation system. J. Bacteriol. 173:1690–1695.
71. **Thompson, J. D., D. G. Higgins, and T. J. Gibson.** 1994. CLUSTAL W: improving the sensitivity of progressive multiple alignment through sequence weighting, position specific gap penalties and weight matrix choice. Nucleic Acids Res. 22:4673–4680.
72. **Tsang, H.-T., C. J. Batie, D. P. Ballou, and J. E. Penner-Hahn.** 1996. Structural characterization of the mononuclear iron site in *Pseudomonas cepacia* phthalate DBO1 dioxygenase using X-ray absorption spectroscopy. J. Biol. Inorg. Chem. 1:24–33.
73. **Twilfer, H., F.-H. Bernhardt, and K. Gersonde.** 1981. An electron-spin-resonance study on the redox-active centers of the 4-methoxybenzoate monooxygenase from *Pseudomonas putida*. Eur. J. Biochem. 119:595–602.
74. **van der Meer, J. R., W. M. de Vos, S. Harayama, and A. J. B. Zehnder.** 1992. Molecular mechanisms of genetic adaptation to xenobiotic compounds. Microbiol. Rev. 56:677–694.
75. **van der Meer, J. R., A. C. J. Frijters, J. H. J. Leveau, R. I. L. Eggen, A. J. B. Zehnder, and W. M. de Vos.** 1991. Characterization of the *Pseudomonas* sp. strain P51 gene *tchR*, a LysR-type transcriptional activator of the *tchCDEF* chlorocatechol oxidative operon, and analysis of the regulatory region. J. Bacteriol. 173:3700–3708.
76. **van Loon, W. M. G. M., J. J. Boon, and B. de Groot.** 1993. Quantitative analysis of sulfonic acid groups in macromolecular lignosulfonic acids and aquatic humic substances by temperature-resolved pyrolysis-mass spectrometry. Environ. Sci. Technol. 27:2387–2396.
77. **Viale, A. M., H. Kobayashi, T. Akazawa, and S. Henikoff.** 1991. *rbcR*, a gene coding for a member of the LysR family of transcriptional regulators, is located upstream of the expressed set of ribulose 1,5-bisphosphate carboxylase/oxygenase genes in the photosynthetic bacterium *Chromatium vinosum*. J. Bacteriol. 173:5224–5229.
78. **Wackett, L. P., L. D. Kwart, and D. T. Gibson.** 1988. Benzylic monooxygenation catalyzed by toluene dioxygenase from *Pseudomonas putida*. Biochemistry 27:1360–1367.
79. **Wang, Y., M. Rawlings, D. T. Gibson, D. Labbè, H. Bergeron, R. Brousseau, and P. C. K. Lau.** 1995. Identification of a membrane protein and a truncated LysR-type regulator associated with the toluene degradation pathway in *Pseudomonas putida* F1. Mol. Gen. Genet. 246:570–579.
80. **Wang, Y. Z., Y. Zhou, and G. J. Zylstra.** 1995. Molecular analysis of isophthalate and terephthalate degradation by *Comamonas testosteroni* YZW-D. Environ. Health Perspect. 130:9–12.
81. **Webb, E. C.** 1992. Enzyme nomenclature. Academic Press, San Diego, Calif.
82. **Wende, P., F.-H. Bernhardt, and K. Pfleger.** 1989. Substrate-modulated reactions of putidamonooxin: the nature of the active oxygen species found and its reaction mechanism. Eur. J. Biochem. 181:189–197.
83. **Wyndham, R. C., A. E. Cashore, C. H. Nakatsu, and M. C. Peel.** 1994. Catabolic transposons. Biodegradation 5:323–342.
84. **Zürrer, D., A. M. Cook, and T. Leisinger.** 1987. Microbial desulfonation of substituted naphthalenesulfonic acids and benzenesulfonic acids. Appl. Environ. Microbiol. 53:1459–1463.

1: Biochemistry. 1996 Jun 18;35(24):7834-45.

Active site structure of Rieske-type proteins: electron nuclear double resonance studies of isotopically labeled phthalate dioxygenase from Pseudomonas cepacia and Rieske protein from Rhodobacter capsulatus and molecular modeling studies of a Rieske center.

Gurbiel RJ, Doan PE, Gassner GT, Macke TJ, Case DA, Ohnishi T, Fee JA, Ballou DP, Hoffman BM.

Department of Chemistry, Northwestern University, Evanston, Illinois 60208, USA.

Continuous wave electron nuclear double resonance (CW ENDOR) spectra of [delta-15N,epsilon(-14)N]histidine-labeled phthalate dioxygenase (PDO) from Pseudomonas cepacia were recorded and found to be virtually identical to those previously recorded from [delta,epsilon-15N2]histidine-labeled protein [Gurbiel, R. J., Batie, C. J., Sivaraja, M., True, A. E., Fee, J. A., Hoffman, B. M., & Ballou, D. P. (1989) Biochemistry 28, 4861-4871]. Thus, the two histidine residues, previously shown to ligate one of the irons in the cluster [cf. Gurbiel et al. 1989)], both coordinate the metal at the N(delta) position of their imidazole rings. Pulsed ENDOR studies showed that the "remote", noncoordinating nitrogen of the histidine imidazole ring could be observed from the Rieske protein in a sample of Rhodobacter capsulatus cytochrome bc1 complex uniformly labeled with 15N but not in a sample of PDO labeled with [delta-15N,epsilon-14N]histidine, but this atom was easily observed with a sample of Rh. capsulatus cytochrome bc1 complex that had been uniformly labeled with 15N; this confirmed the conclusion from the CW ENDOR studies that ligation is exclusively via N(delta) for both ligands in the PDO center. Modifications in the algorithms previously used to simulate 14N ENDOR spectra permitted us to

compute spectra without any constraints on the relative orientation of hyperfine and quadrupole tensors. This new algorithm was used to analyze current and previously published spectra, and slightly different values for the N-Fe-N angle and imidazole ring rotation angles are presented [cf. Gurbiel et al. (1989) Gurbiel, R. J., Ohnishi, T., Robertson, D. E., Daldal, F., and Hoffman, B. M. (1991) Biochemistry 30, 11579-11584]. This analysis has permitted us to refine the proposed structure of the [2Fe-2S] Rieske-type cluster and rationalize some of the properties of these novel centers. Although the spectra of cytochrome bc1 complex from Rh. capsulatus are of somewhat lower resolution than those obtained with samples of PDO, our analysis nevertheless permits the conclusion that the geometry of the cluster is essentially the same for all Rieske and Rieske-type proteins. Structural constraints inferred from the spectroscopic results permitted us to apply the principles of distance geometry to arrive at possible three-dimensional models of the active site structure of Rieske protein from Rh. capsulatus. Results from this test case indicate that similar procedures should be generally useful in metalloprotein systems. We also recorded the pulsed and CW ENDOR spectra of 57Fe-labeled PDO, and the resulting data were used to derive the full hyperfine tensors for both Fe(III) and Fe(II) ions, including their orientations relative to the g tensor. The A tensor of the ferric ion is nominally isotropic, while the A tensor of the ferrous ion is axial, having A(parallel) > A(perpendicular); both tensors are coincident with the observed g tensor, with A(parallel) of the ferrous ion lying along the maximum g-value, g1. These results were examined using refinements of existing theories of spin-coupling in [2Fe-2S]+ clusters, and it is concluded that current theories are not adequate to fully describe the experimental results.

PMID: 8672484 [PubMed - indexed for MEDLINE]

1: Annu Rev Microbiol. 1992;46:565-601.

Functional and evolutionary relationships among diverse oxygenases.

Harayama S, Kok M, Neidle EL.

Department of Medical Biochemistry, University of Geneva, Switzerland.

Oxygenases that incorporate one or two atoms of dioxygen into substrates are found in many metabolic pathways. In this article, representative oxygenases, principally those found in bacterial pathways for the degradation of hydrocarbons, are reviewed. Monooxygenases, discussed in this chapter, incorporate one hydroxyl group into substrates. In this reaction, two atoms of dioxygen are reduced to one hydroxyl group and one H2O molecule by the concomitant oxidation of NAD(P)H. Dioxygenases catalyze the incorporation of two atoms of dioxygen into substrates. Two types of dioxygenases, aromatic-ring dioxygenases and aromatic-ring-cleavage dioxygenases, are discussed. The aromatic-ring dioxygenases incorporate two hydroxyl groups into aromatic substrates, and cis-diols are formed. This reaction also requires NAD(P)H as an electron donor. Aromatic-ring-cleavage dioxygenases incorporate two atoms of dioxygen into aromatic substrates, and the aromatic ring is cleaved. This reaction does not require an external reductant. All the oxygenases possess a cofactor, a transition metal, flavin or pteridine, that interacts with dioxygen. The concerted reactions between dioxygen and carbon in organic compounds are spin forbidden. The cofactor is used to overcome this restriction. For the oxygenases that require the NAD(P)H cofactor, the enzyme reaction is separated into two steps, the oxidation of NAD(P)H to generate two reducing equivalents, and the hydroxylation of substrates. Flavoprotein hydroxylases that catalyze the monohydroxylation of the aromatic ring carry out these two reactions on a single

polypeptide chain. In other oxygenases, the NAD(P)H oxidation and a hydroxylation reaction are catalyzed by two separate polypeptides that are linked by a short electron-transport chain. Two reducing equivalents generated by the oxidation of NAD(P)H are transferred through the electron-transport chain to the cofactor on a hydroxylase component that they reduce. Dioxygen couples with the reduced cofactor and subsequently hydroxylates substrates. The electron-transport chains associated with oxygenases contain at least two redox centers. The first redox center is usually a flavin, while the second is an iron-sulfur cluster. The electron transport is initiated by a single two-electron transfer from NAD(P)H to a flavin, followed by two single-electron transfers from the flavin to an iron-sulfur cluster. The primary sequences of many oxygenases have been determined, and according to their sequence similarities, the oxygenases can be grouped into several protein families. Among proteins of the same family, the sequences in regions involved in cofactor binding are strongly conserved. Local sequence similarities are also observed among oxygenases from different families, primarily in regions involved in cofactor binding.

Publication Types:

Review

Review, Academic

PMID: 1444267 [PubMed - indexed for MEDLINE]